

---

A

Presented to  
the faculty of the School of Engineering and Applied Science  
University of Virginia

---

in partial fulfillment  
of the requirements for the degree

by

# APPROVAL SHEET

This

is submitted in partial fulfillment of the requirements  
for the degree of

Author:

Advisor:

Advisor:

Committee Member:

Committee Member:

Committee Member:

Committee Member:

Committee Member:

Committee Member:

Accepted for the School of Engineering and Applied Science:

A handwritten signature in black ink that reads "Jennifer L. West". The signature is written in a cursive, flowing style.

Jennifer L. West, School of Engineering and Applied Science

# **B Cells and Humoral Immunity in Atherosclerosis From Mice to Human**

Tanyaporn (Oom) Pattarabanjird  
Bangkok, Thailand

B.Sc. Biology and Chemistry, Massachusetts Institute of Technology, 2016

A Dissertation presented to the Graduate Faculty of the University of Virginia in Candidacy for  
the Degree of Doctor of Philosophy

Department of Biomedical Engineering

University of Virginia  
October, 2021

---

Coleen McNamara, MD

---

Mete Civelek, PhD

---

Sepideh Dolatshahi, PhD

---

Eli Zunder, PhD

---

Stefan Bekarinov, PhD

---

Loren Erickson, PhD

## Abstract

Atherosclerotic cardiovascular disease is a chronic inflammatory disease and a number one cause of death in the United States. It is characterized by accumulation of oxidized low-density lipoprotein (OxLDL) in the artery wall initiating a cascade of inflammatory responses as well as macrophage uptake of OxLDL leading to formation of foam cells, a hallmark of atherosclerotic plaque formation. Despite the ubiquitous use of lipid lowering medications as a standard care to treat hyperlipidemia and cardiovascular diseases, the prevalence of cardiovascular disease still remains high indicating that lipid modification is not sufficient as a stand-alone treatment for cardiovascular diseases. The completion of the Canakinumab anti-inflammatory thrombosis outcome study (CANTOS) is the first evidence proving that inhibiting inflammation in the absence of lipid modifications can also improve atherosclerotic outcomes. This finding highlights the importance of immune-modulatory therapy in managing atherosclerosis.

B cells have emerged as important immune cells in modulating atherosclerosis through subtype dependent mechanisms. In murine, B1 cells are atheroprotective, while B2 cells are pro-atherogenic. B1 cells can be further subtyped into B1a and B1b cells based on CD5 expression. B1 cells are self-renewed and produce anti-inflammatory antibody IgM that recognizes and helps clear oxidation specific epitopes (OSEs), such as malondialdehyde LDL (MDA-LDL), which ameliorates atherosclerosis. Therefore, understanding of factors regulating self-renewal of B1 cells, IgM production can help identify targets for atherosclerosis immunotherapy. Additionally, identification of human B cells equivalent to murine B1 cells is also crucial as the discovery will facilitate translating findings from mice to humans.

In this dissertation, I present the evidences that p62, an autophagy and cell proliferative adaptor protein, regulates self-renewal of murine B1b cells. Lentiviral-mediated overexpression of p62 in murine B1 cells leads to an increase in B1b cell number, higher IgM production, and reduction of atherosclerotic plaque. More importantly, expression of p62 can be promoted through activation of E2A transcription factor or loss of inhibitor of differentiation 3 (Id3), an inhibitory binding partner of E2A.

To allow translation of this discovery to human, I seek to identify IgM producing human B cells. Through utilizing mass cytometry, I identified human IgM producing B cells to be marked by CD27+/IgM+. Additionally, CD24 is shown to promote IgM production in these cells through interacting with CCR6 to reduce ligand induced CCR6 internalization. This allows higher level of CCR6 to be on the surface to mediate trafficking to the spleen where these CD27+/IgM+ B cells produce IgM antibody. Use of CD24 blocking monoclonal antibody also leads to an increase in vascular inflammation in hyperlipidemic humanized mice model. This second discovery does not only allow identification of human equivalent murine B1 cells, but also suggests that CD24 and CCR6 might also be promising targets for B cell targeted therapy for atherosclerosis.

## Acknowledgement and Dedication

A graduate study at the University of Virginia has been a remarkable journey. It has not only taught me science, engineering or medicine, but also taught me tremendous amount of life skills. First and foremost, I would like to thank Coleen McNamara for her dedication, guidance, and support. Coleen taught me to become a critical and passionate scientist and along the way she also taught me how to be a good presenter, a decent writer, a fair team player, and a nice collaborator for others. In addition to science, she also taught me to be kind, optimist, compassionate and forgiving. Thank you so much Coleen for taking me in and allowing me to follow the science despite all the challenges we both faced and new directions we have taken in the past few years.

In the past 3 years, McNamara Lab has not only been my lab but also my home. Melissa Marshall has been essential to my success. She taught me to work with mice since the day that I never touched these furry test tubes once in my life till the day that I performed splenectomy on them. Chantel McSkimming has been helping me tremendously and provides me great insights on many experiments. Fabrizio Drago is not only my colleague but also my great friend that provides me help with both science and life. Prasad Srikakulapu, Vineela Bonsai, Jeff Sturek, and Hema Kothari all help bounce ideas with me and provide crucial feedbacks on my projects. Jim Garmey always helps keep the lab running through tough time both during COVID-19 lockdown as well as our move allowing me to focus on my experiments. Tori Osinski and Aditi Upadhye gave me guidance, mental support, taught me necessarily lab skills and provided me feedbacks especially when I first joined the lab and had no clues what I was doing.

I am also very thankful for all our collaborators inside and outside of UVA. Stefan Bekarinov, my great co-mentor, taught me bioinformatics and computational biology since the first day when I had no background in computation. He is also very good at asking me to reflect

the basis and punchline of my project which allows me to emphasize significance and importance of my project in talks, grant application, as well as paper writing. The technical assistance from UVA flow cytometry especially from Claude Chew, Mike Solga, Alex Wendling, and Taylor Harper was essential to my success. I would also like to thank our collaborators at La Jolla Institute of Technology including Drs. Yury Miller, Catherine Hedrick, Huy Dinh, Klaus Ley and Rishab Gultali for their scientific assistance and insights.

I would like to extend my thanks to my previous mentor, Dr. Wenjing Wang, who built my foundation of science, taught me how to critically criticize scientific works, and all the essential lab techniques. My MSTP friends, Thai community at UVA, my MIT friends, especially Sarah, Heejin, Nutta, Pumidech, Narisara, Chawit, Jinny, Thipok, Ekapob, Kamphol, and Pichaya have helped me through thick and thin and provide me great mental support.

Finally, my family is the core to all my success and accomplishment. My mom, Dangnoi Pattarabanjird, and my dad, Narongchai Pattarabanjird, taught me all the life skills and provided me with all the resources and opportunities that allow me to focus on my study and become who I am today. Lastly, I would like to thank Anson Chen, my boyfriend, who always lend extra ears, watch my cry, try to help solve my problems, and calm me down. I genuinely appreciate all of them from the bottom of my heart.

## Table of Contents

<b>Abstract.....</b>	<b>ii</b>
<b>Acknowledgments and Dedication.....</b>	<b>iv</b>
<b>Table of Contents.....</b>	<b>vi</b>
<b>List of Figures.....</b>	<b>ix</b>
<b>List of Tables.....</b>	<b>xii</b>
<b>List of Abbreviations.....</b>	<b>xiii</b>
 <b>Chapter 1: Introduction</b>	
Pathogenesis of atherosclerosis.....	2
Brief overview of B cell biology.....	3
Murine B cells and atherosclerosis.....	4
Human B cells and atherosclerosis.....	8
Roles of Id3 in B cell mediated atherosclerosis.....	12
Roles of p62 in cell proliferation and atherosclerosis.....	13
Roles of CD24 in cardiovascular diseases.....	13
Project Rationales.....	15
 <b>Chapter 2: Materials and Methods.....</b>	
 <b>Chapter 3: B-1b cells possess unique bHLH-driven p62-dependent self-renewal and atheroprotection .....</b>	
<b>Abstract.....</b>	<b>32</b>
Abstract.....	33
Introduction.....	34
Results.....	36

Discussion.....	49
<b>Chapter 4: CD24 promotes human B cell CCR6-mediated splenic trafficking and IgM production, limiting vascular inflammation and coronary artery disease severity.....</b>	<b>54</b>
Abstract.....	55
Introduction.....	56
Results.....	57
Discussion.....	81
<b>Chapter 5: Discussion and Future Directions.....</b>	<b>85</b>
TCF3 smutations associates with reduced p62 expression in human IgM producing B cells and an increase in CAD severity.....	87
p62, autophagy and B cell survival.....	92
Roles of p62 in B2 B cells.....	93
p62 as a target for modulatory therapy to treat atherosclerosis.....	95
IgM to oxidation specific epitopes and atheroprotection.....	95
CD24 and Siglec10.....	97
CD24, B cell proliferation, and antibody/cytokine production.....	99
<b>Literature Cited.....</b>	<b>100</b>

## List of figures

### **Chapter 1**

Figure 1: Murine B cells can be divided into B cell subsets based on established cell surface markers.....7

### **Chapter 2**

None.

### **Chapter 3**

Figure 2: Loss of Id3 promoted BAFF-p62-NFKB expression and proliferation in B1b but not B1a cells.....37

Figure 3: Loss of p62 significantly reduces B1b cell proliferation *in vitro* and *in vivo*.....40

Figure 4: E-box sequences (CANNTG) located in p62 promoter region.....41

Figure 5: Loss of Id3 and increased expression of E12 and E47 promote p62 promoter activation. ....42

Figure 6: BAFF induced binding of p62 to TRAF6 in B-1b, but not B-1a cells, leading to NFKB activation and upregulation of c-myc driven cell proliferation. ....45

Figure 7: Overexpression of p62 increased B-1b cell number and plasma IgM levels and reduced diet induced atherosclerosis. ....47

Figure 8: Plasma total IgM level two weeks post transfer measured by ELISA obtained from AT of Id3KO (grey) and Id3KO p62KO (white) B1 cells into C57BL/6 host mice.....48

Figure 9: Human B1 cells from subjects with an ID3 SNP at rs11574, known to attenuate Id3 function, have increased p62 expression; a finding associated with B1 frequency and plasma IgM to MDA-LDL levels.....49

## **Chapter 4**

Figure 10: Unsupervised metalouvain clustering of CD19 <sup>+</sup> B cells obtained from 28 subjects with high and low plasma levels of IgM to MDA-LDL.....	58
Figure 11: Clusters 1 and cluster 8 uniquely express CD27 <sup>+</sup> IgM <sup>+</sup> (B <sup>27+</sup> IgM <sup>+</sup> ) and their frequency as a percentage of total B cells was higher in subjects with high levels of IgM specific to MDA-LDL.....	60
Figure 12: Plasma level of IgM <sup>MDA-LDL</sup> strongly associates with Plasma level of IgM <sup>PC-BSA</sup> and IgM <sup>OxCE</sup> .....	61
Figure 13: Subjects with high plasma IgM <sup>MDA-LDL</sup> levels have higher frequencies of CD43 <sup>+</sup> cluster 1 compared to subjects with low plasma IgM <sup>MDA-LDL</sup> levels.....	62
Figure 14: B <sup>27+</sup> IgM <sup>+</sup> with high CD24 expression produced IgM and IgM <sup>MDA-LDL</sup> upon stimulation and has high expression of chemokine receptors.....	63
Figure 15: GM of CD24 on clusters 1 and 8 does not associate with IgG to MDA-LDL.....	64
Figure 16: Sorting strategy for clusters 1 and 8.....	66
Figure 17: Pathway analysis to identify upregulated pathways in sort purified B <sup>27+</sup> IgM <sup>+</sup> CD24 <sup>hi</sup> .....	67
Figure 18: B <sup>27+</sup> IgM <sup>+</sup> CD24 <sup>hi</sup> cells have characteristics of circulating MZ B cells.....	68
Figure 19: CD24 reduces CCL20-induced CCR6 internalization and promotes B <sup>27+</sup> IgM <sup>+</sup> CD24 <sup>hi</sup> migration. ....	70
Figure 20: GM of CD24 on B <sup>27+</sup> IgM <sup>+</sup> CD24 <sup>hi</sup> does not associate with GM of CCR7, CXCR3, CXCR4, CXCR5 chemokine receptors. ....	71
Figure 21: CD24 inhibition reduces surface CCR6 expression, splenic trafficking, IgM production and increased diet induced vascular inflammation <i>in vivo</i> . ....	74
Figure 22: Schematics demonstrating Gensini scoring system to evaluate CAD severity...76	

Figure 23: CITEseq demonstrated increased in Cluster 6 (a surrogate of B<sup>27+IgM+CD24hi</sup>) frequency and CD24 expression as well as enhanced CCR6 signaling, BCR signaling, and IgM production in low CAD severity subjects.....77

Figure 24: Differential gene expression and pathway analysis of cluster 9 (surrogate of B<sup>27+IgM+CD24lo</sup>). .....80

## **Chapter 5:**

Figure 25: Presence of TCF3 mutations associates with higher coronary artery disease.....89

Figure 26: TCF3 somatic mutations are potentially enriched in subjects with high CAD severity and in CD27+IgM+ B cells.....90

Figure 27: Subjects with TCF3 somatic mutations have decreased frequency of B<sup>27+IgM+CD24hi</sup> and B<sup>27+IgM+CD24lo/-</sup> .....91

Figure 28: Subjects with TCF3 somatic mutations have decreased mTOR, NFKB activation and p62 expression.....91

Figure 29: Loss of Id3 in both B1a and B1b lead to an increase in NRF2 expression.....93

Figure 30: Higher expression of p62 but lower BAFF induced cell proliferation in B2 cells than B1b cells.....94

Figure 31: Humanized mice model for in vivo macrophage engulfment of B cells.....98

## List of tables

### Chapter 1:

None.

### Chapter 2:

Table 1: Flow cytometry antibodies used for sorting, analyzing B cells from <i>in vitro</i> culture and tissue harvest.....	19
Table 2: CyTOF antibodies.....	24
Table 3: FACS sorting antibodies.....	25
Table 4: Flow cytometry antibodies for tissue samples following humanized mice harvest.....	26
Table 5: List of 26 titrated oligonucleotide-tagged monoclonal antibodies used in CITEseq experiment to subtype B cells. ....	30

### Chapter 3:

None.

### Chapter 4:

Table 6: Differences in IgM and IgG to OSEs between high and low IgM <sup>MDA-LDL</sup> groups.....	59
Table 7: DE genes compared between B <sup>27+IgM+CD24hi</sup> and B <sup>27+IgM+CD24lo/-</sup> cells.....	65
Table 8: <b>DE genes compared between high- versus low-CAD subjects obtained from B<sup>27+IgM+CD24hi</sup> cells.....</b>	79
Table 9: <b>DE genes compared between high- versus low-CAD subjects obtained from B<sup>27+IgM+CD24lo/-</sup> cells.....</b>	79

### Chapter 5:

None.

## List of Abbreviations

OSE	Oxidation Specific Epitopes
MDA	Malondialdehyde
LDL	Low density lipoprotein
DAMPs	Danger-associated molecular patterns
TLR	Toll-like receptors
PRR	Pattern recognition receptors
PVAT	Perivascular adipose tissue
ATLO	Adventitial tertiary lymphoid organ
CVD	Cardiovascular disease
CAD	Coronary artery disease
CRF	Cardiac risk factor
BM	Bone marrow
PerC	Peritoneal cavity
MZB	Marginal zone B cells
FOB	Follicular B cells
Id3	Inhibitor of differentiation 3
SQSTM1	Sequestome 1
HLH	Helix-loop-helix
BAFF	B cell activating factor
BAFF-R	B cell activating factor receptor
SNP	Single nucleotide polymorphism
CytoF	Cytometry by time of flight
UMAP	Uniform manifold approximation and projection

B <sup>27+</sup> IgM <sup>+</sup>	CD27 <sup>+</sup> IgM <sup>+</sup> B cells
B <sup>27+</sup> IgM <sup>+</sup> CD24 <sup>hi</sup>	CD24 high CD27 <sup>+</sup> IgM <sup>+</sup> B cells
B <sup>27+</sup> IgM <sup>+</sup> CD24 <sup>lo</sup>	CD24 low CD27 <sup>+</sup> IgM <sup>+</sup> B cells
CCR6	Chemokine receptor 6
CCL20	Chemokine ligand 20
<b>NSG</b>	NOD <i>scid</i> gamma
IP	Intraperitoneal
mAb	Monoclonal antibody
PLA	Proximity ligation assay
QCA	Quantitative coronary angiography
CITEseq	Single cell multi-omics sequencing
ELISA	Enzyme linked immunosorbent assay
FACS	Fluorescence activated cell sorting
Ig	Immunoglobulin
PBMC	Peripheral blood mononuclear cells
PC	Phosphorylcholine
OxCE	Oxidation cholesterol ester
RLU	Relative light units
WD	Western diet
FDG	Fluorodeoxyglucose
PET	Positron emission tomography
DEGs	Differentially expressed genes
GM	Geometric mean
MFI	Mean fluorescent intensity

**Chapter 1**  
**Introduction**

## **Pathogenesis of atherosclerosis**

A wealth of data has implicated smoking, hypertension, diabetes, hyperlipidemia, and lifestyle in the risk of developing atherosclerotic CVD and interventions to modify these factors are effective and are the mainstay of current CVD prevention approaches<sup>1</sup>. Yet, despite these important interventions, CVD remains the leading cause of death worldwide<sup>2</sup>, underscoring the need for a deeper understanding of the underpinnings of atherosclerotic lesion formation. Nearly fifty years ago, Ross and Glomset published a seminal paper in the NEJM on the pathogenesis of atherosclerosis, defining it as a “response to injury” with the injurious stimuli including the risk factors mentioned above<sup>3</sup>. Gerlis and Schwartz reported the presence of immune cells within atherosclerotic plaques and the adventitia of arteries in 1956 and 1962 respectively<sup>4,5</sup>. These important observations accompanied by the biomedical research advances of many over the ensuing decades lead to our current understanding of atherosclerosis as a chronic inflammatory disease<sup>6-9</sup>.

A major initiating event in atherosclerosis is deposition of lipids in the arterial wall. These lipids are acted upon by oxidative enzymes produced by vessel wall cells creating oxidation-specific epitopes (OSE)<sup>8</sup>. These OSE in turn stimulate vascular cells such as smooth muscle cells, endothelial cells to produce adhesion molecules, cytokines and chemokines that attract additional leukocytes, such as circulating monocytes and T cells, to the vessel wall. Monocytes that enter the arterial wall differentiate into macrophages. The mechanisms whereby T cells and macrophages contribute to atherosclerosis has been extensively reviewed elsewhere<sup>10,11</sup>. In brief, macrophages can take up oxidized lipids to become foam cells. In addition, OSE and other lesion-derived neoantigens function as danger-associated molecular patterns (DAMPs). These DAMPs can engage toll-like receptors (TLRs) and other pattern recognition receptors (PRR)<sup>12</sup>, further stimulating inflammatory pathways in macrophages and T cells. T cells can

also encounter local antigen and cytokines also contributing to lesion progression through amplification of the inflammatory response<sup>10,13</sup>.

Recent use of cutting edge high dimensional analysis of murine and human atherosclerotic lesions confirm and extend prior studies that T cells and macrophages are predominant cell types in the atherosclerotic lesion itself<sup>14,15</sup>. B cells, on the contrary, are not a predominant immune cell type identified within the atherosclerotic lesions<sup>14,15</sup>. However, they are in abundance in perivascular adipose tissue (PVAT), which in addition to the spleen and bone marrow, serves as a niche for immunoglobulin production<sup>16</sup>. Like other tissues with chronic inflammation, atherosclerotic vessels also harbor tertiary lymphoid organs or ATLOs which contain immunoglobulin and cytokine-producing B cells<sup>17</sup>. Cytokines and immunoglobulins produced by B cells at these sites are felt to be important regulators of inflammation in atherosclerosis lesion formation.

### **Brief overview of B cell biology**

B cells are lymphocytes that play major roles in both innate and adaptive immunity mainly through production of antibodies and cytokines<sup>18</sup>. Murine B cells are broadly divided into B1 and B2 cells, that have distinct characteristics and cell surface markers reviewed in detail elsewhere<sup>19</sup>. In brief, B1 cells develop mostly in the fetal liver and undergo self-renewal in the periphery. They reside predominantly in serosal cavities, but can traffic to spleen and bone marrow where they produce predominantly IgM antibodies in a T cell-independent manner<sup>19</sup>. Murine B1 cells can be subdivided into B1a and B1b cells, which are distinguished based on CD5 expression—B1a is CD5<sup>+</sup> and B1b is CD5<sup>-</sup><sup>20</sup>. On the other hand, B2 cells are known as conventional B cells and participate in adaptive immunity. They arise from lymphoid progenitors in bone marrow (BM), and differentiate into immature B cells through Ig heavy and light chain

rearrangement<sup>21</sup>. These immature B cells leave BM to travel to secondary lymphoid organs (SLOs), undergoing transitional stages to become mature B cells, which further differentiate into marginal zone (MZ) B cells and follicular (Fol) B cells<sup>22,23</sup>. Fol-B cells comprise a majority of B2 cells which participate in adaptive immune responses as they become activated by antigens stimulation via T cell help in germinal center (GC)<sup>22,23</sup>. These activated B cells in GC then undergo affinity maturation, class switching, somatic hypermutation to produce highly antigen specific predominantly IgG antibodies. These GC B cells then further differentiate into plasma cells or memory B cells<sup>23</sup>. Additionally, certain B cell subtype regulates inflammatory reactions through cytokine production. Regulatory B cells (Breg) is known to produce anti-inflammatory IL-10 cytokine, which suppresses T helper cells, inhibits macrophage Ag presentation and pro-inflammatory cytokine production<sup>23</sup>.

### **Murine B cells and atherosclerosis**

An important role for B cells in murine atherosclerosis has been clearly demonstrated over the last several years. Roles of murine B cells in atherosclerosis is subset specific as depicted in Figure 1. B1 cells protect against atherosclerosis development through secreting IgM that binds OSE on LDL, preventing lipid uptake and inflammatory cytokine production by macrophages, thus reducing formation of foam cells and limiting inflammation<sup>24</sup>. In addition, B-1-derived IgM binds epitopes on apoptotic cells and enhances clearance of these cells, further contributing to limiting inflammation. In contrast, B2 cells are largely considered atherogenic via production of pathogenic IgG, activation of T cells, and induction of pro-inflammatory cytokines such as interferon- $\gamma$  (IFN- $\gamma$ )<sup>25</sup>. The evidence supporting these B cell subset-specific effects goes back nearly 20 years. In 2002, Caligiuri et al. showed that, removal of the spleen in apolipoprotein E gene knockout (ApoE<sup>-/-</sup>) mice exacerbated atherosclerosis, while adoptive transfer of B cells to these splenectomized mice attenuated disease development<sup>26</sup>. In the same year, Major et al.

demonstrated that low density lipoprotein (LDL) receptor-deficient (LDLR<sup>-/-</sup>) mice with < 1.0% of their normal B cell population in the bone marrow had a 30-40% increase in atherosclerotic lesion area<sup>27</sup>. These two studies provided novel evidence that B cells protect against atherosclerosis development. Follow on studies supported data implicating loss of anti-oxidized LDL antibodies as mice unable to secrete IgM had increased atherosclerotic disease. Interestingly, studies utilizing a CD20 monoclonal antibody (mAb) or B-cell activating factor receptor deletion (BAFFR<sup>-/-</sup>) to deplete B cells in hyperlipidemic mice resulted in decreased atherosclerosis compared to control mice despite comparable serum cholesterol levels<sup>28</sup>. B2 depletion increased IL17 production, suppresses T cell production of IFN- $\gamma$ , decreased proliferation of CD4 T cells in the spleen, lessened production of other pro-inflammatory cytokines such as TNF- $\alpha$  and IL1- $\beta$  and chemokines such as MCP-1 and and reduced atherosclerosis<sup>28</sup>. Furthermore, murine B2 B cells produce IgG antibodies that bind OSEs and stimulate inflammation, at least in part through the Fc- $\gamma$  receptor. These data countered the notion that B cells were atheroprotective. Notably, in these studies, the predominant B cell subtype depleted with anti-CD20 or BAFFR deficiency was the B2 cell. Follow-on studies, utilizing adoptive transfer of specific B cell subsets confirmed that B cell effects on atherosclerosis were subset-specific with B-1 cells inhibiting<sup>29</sup> and B-2 cells promoting atherosclerosis<sup>30</sup>.

Extrapolation of murine B cell subtypes into human has been challenging due to differences in surface markers defining subtypes<sup>31</sup>. However, emerging evidence has demonstrated common surface markers on human and murine B-1 cells (eg. CXCR4) that associate with plasma levels of atheroprotective IgM to OSE. Mechanistic gain and loss of function studies in mice confirmed a causal relationship for CXCR4 on B-1a cells and bone marrow production of IgM to OSE<sup>32</sup>. That CXCR4 expression on B-1 cells results in increased IgM to OSE in mice and

humans and is inversely associated with coronary artery plaque volume as measured by intravascular ultrasound in humans<sup>32</sup> underscores that parallels between mice and human can exist and that combining both preclinical mechanistic studies and studies in humans may be the best approach to understanding B cell-mediated regulation of atherosclerosis. The identification of the putative human equivalents of the murine B-1 cells that produces IgM to OSE and the abundance of evidence, albeit largely associative, that B cells are important in human disease and that IgM to OSE is inversely associated with CAD.

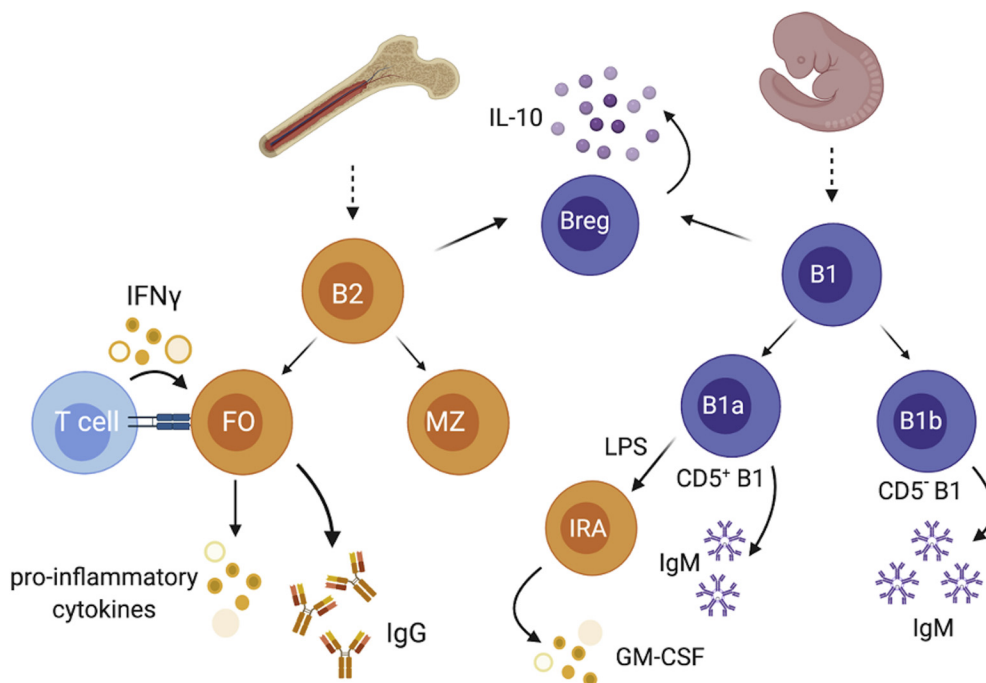


Figure 1: Murine B cells can be divided into B cell subsets based on established cell surface markers. The B1 B cells are atheroprotective and can be divided into B1a and B1b based on CD5 expression with B1a being CD5<sup>+</sup> and B1b being CD5<sup>-</sup>. B1a and B1b have unique capability to produce atheroprotective IgM in a T cell independent manner. In response to LPS, B1a cells can migrate to spleen and produce GM-CSF, promoting extramedullary hematopoiesis and atherogenesis (IRA B cells). Both B1 and B2 cells can give rise to IL-10 producing regulatory B cells (Breg). Breg is defined by its capability to produce anti-inflammatory cytokines like IL-10. B2, on the other hand, promotes atherosclerosis through production of atherogenic IgG, activation of T cells, and induced production of inflammatory cytokines (eg, IFN). GM-CSF 1/4 granulocyte- macrophage colony-stimulating factor; IgG 1/4 immunoglobulin G; IgM 1/4 immunoglobulin M; IL 1/4 interleukin; IFN 1/4 interferon; LPS 1/4 lipopolysaccharide.

## Human B cells and atherosclerosis

Key data implicating B cells in human atherosclerosis comes from important studies in patient cohorts that reported on the relationship between coronary artery disease (CAD) and antibodies to OSE. Consistent with the data in mice demonstrating B-1 cell-derived IgM attenuated atherosclerosis and B-2-derived IgG promoted atherosclerosis, in a cohort of 504 patients undergoing medically indicated coronary angiography, univariate analysis revealed that IgM to OSE was inversely and IgG to OSE was positively associated with coronary stenoses >50%<sup>33</sup>. Analysis of 748 cases and 1723 controls in the EPIC-Norfolk study, suggested that IgM and IgG autoantibodies and immune complexes could modify risk prediction for CVD<sup>34</sup>. Indeed, a subsequent report analyzing incident CVD (ischemic stroke, myocardial infarction, new-onset unstable angina, acute coronary interventions, and vascular death) over 15 years of follow up in the Bruneck Study revealed that subjects with high IgG to OSE had higher risk of CVD, while those with high IgM to OSE had lower risk<sup>33</sup>. Using these biomarkers as variables, improved CVD risk prediction, enabling reclassification of subjects into more correct risk categories. In the Dallas Heart Study, autoantibodies to MDA-LDL were measured in 3509 subjects that were followed for 10.5 years<sup>35</sup>. Multivariable-adjusted Cox regression analysis demonstrated that IgG to MDA-LDL was independently associated with time to incident MACE. Analysis of subjects with CAD development and respective controls in the Nordic Diltiazem Study (NORDIL) supported the hypothesis that lower IgM to MDA-LDL was associated with CAD development and further showed that there was also an inverse relationship with IgM to MDA-LDL and necrotic core volume as measured by intravascular ultrasound (IVUS)<sup>36</sup>. A few studies have implicated low levels of IgG to a specific ApoB100 peptide (p210) and CAD events along with the association of low IgM to native and MDA-modified versions of p210 and p45. Other studies demonstrated that low levels of IgG to native p210 but not IgM to MDA-modified p210 were inversely associated with severity of CAD and MI risk, raising the interesting possibility that

isotype responses may be idiotype-specific. In addition, these studies highlight the complexity and controversy related to IgG autoantibodies and CVD. As in murine models, evidence for a protective role for IgM to OSE in human atherosclerosis is more consistent than the evidence for IgG.

In addition to this wealth of evidence that antibodies, produced exclusively by B cells, are associated with CVD, additional data support an important role for B cells in human atherosclerosis. Huan et.al. performed a network-driven analysis incorporating whole blood gene expression profiles and coronary artery disease (CAD) single nucleotide polymorphism (SNP) analysis constructed from 188 coronary heart disease cases and 188 age- and sex-matched controls from the Framingham Heart Study (FHS) with Bayesian networks. Results clearly identified B cell-centered immune function to be related to CAD pathogenesis. Gene ontology enrichment (GEO) analysis identified B-cell activation, B-cell differentiation and B-cell receptor signaling pathways as significantly enriched in CAD. Of the top 20 CAD key driver genes, B cell genes predominated supporting a critical role for B cells in human atherosclerosis and suggesting that B cell-targeted therapies may be useful to prevent or treat atherosclerosis. Yet, while much is known about murine B cell subtypes in atherosclerosis, much less is known about B cell subtypes in human disease.

It is not possible to directly extrapolate murine B cell subtypes to humans. One major issue that contributes to this limitation includes fundamental differences in immune cells between mice and human. Multiple studies completed by the Inflammation and Host Response to Injury, Large Scale Collaborative Research Program demonstrate that immune responses in mice often do not predict immune responses in humans. Until recently, there has been a paucity of robust assays that allow comprehensive immune profiling in humans. Prior standards set by the

Human Immunophenotyping Consortium relied on the use of 5 markers to define human B cell subtypes. However, these still lack the capacity to identify the human equivalent of murine IgM-producing B-1 cells which seems particularly relevant in CVD as IgM to MDA-LDL (produced by B-1 cells) is implicated in reducing inflammation and atherosclerosis. The recent publication of an integrated multi-omic single cell atlas of human B cells provides unprecedented high dimensional data and identified 12 unique human B cell clusters. It is likely that the human B-1 cell is part of the the CD45RB+ CD27+CD73- memory cluster, but this was not further explored.

Due to the difficulty with using murine marker strategies to identify the human equivalent of IgM-producing B-1 cells, Griffin et al. identified a putative human B-1 cells by sort-purifying B cell fractions and testing for three fundamental murine B-1 cell functions (spontaneous IgM secretion, efficient T cell stimulations, and tonic intracellular signaling). They found that CD20+CD27+CD43+ identified the human B cell subset that fulfilled these criteria. While some controversies have surrounded the identification of surface markers that define these cells, it is clear that cells within this subset produce IgM to modified phospholipids linked to atherosclerosis and are inversely associated with CAD. Similar to mice, these B-1 cells comprise < 5-10% of circulating B cells. Griffin went on to show that these B-1 cells can be further subdivided into orchestrator B1 cells (CD11b<sup>+</sup>) and secretor B1 cells (CD11b<sup>-</sup>). Secretor B1 cells secrete large amounts of IgM, while orchestrator B1 cells produce both IgM and anti-inflammatory cytokine interleukin (IL10) to suppress T cell activation. In support of a role for human B-1 cells in protecting from atherosclerosis, Meeuwssen demonstrated higher numbers of unswitched memory B cells (CD27<sup>+</sup>CD43<sup>+</sup> B1-like) associated with fewer secondary cardiovascular events, defined as anyone or combination of cardiovascular death, stroke, MI, coronary intervention, and peripheral intervention following carotid endarterectomy. Apart from an association between B-1 cell frequency and cardiovascular incidents, recent studies

demonstrated that the amount of the chemokine receptor, CXCR4, on human CD20<sup>+</sup>CD27<sup>+</sup>CD43<sup>+</sup> B-1 cells significantly associated with circulating levels of IgM antibodies specific for malondialdehyde (MDA)-modified LDL (31) suggesting that CXCR4 is a crucial marker for identifying IgM to MDA-LDL-producing B-1 cells in humans. In support of this associative finding, gain and loss of function studies in mice demonstrated that CXCR4 expression on B1a cells induced migration to bone marrow, and enhanced production of IgM to MDA-LDL. Moreover, CXCR4 expression on circulating human CD20<sup>+</sup>CD27<sup>+</sup>CD43<sup>+</sup> B-1 cells inversely correlated with coronary artery plaque burden and necrosis as measured by intravascular ultrasound with virtual histology (IVUS-VH) and female mice lacking B cell CXCR4 had increased atherosclerosis. While confirming the causal link between CXCR4 expression on B-1a cells and production of IgM to MDA-LDL via regulation of trafficking to the bone marrow is not possible in humans, the common associative data in mice and humans strengthens the likelihood for a common or related mechanism and provides rationale for pursuing strategies that may augment CXCR4 on human B-1 cells primed to produce IgM to OSE.

B2 cells develop in the bone marrow and travel to secondary lymphoid organs where they can transition into mature naïve B cells in follicular regions, or differentiate to become memory B cells or antibody producing plasma cells. In the early antibody response, plasmablasts are rapidly produced but are short lived. In humans, increased plasmablasts are associated with atherosclerosis. The plasmablasts then further develop into plasma cells, which secrete much higher levels of antibodies, including high-affinity IgG. This IgG as mentioned earlier has been shown to correlate with coronary artery stenosis in some human studies.

Regulatory B cells (Bregs) are a group of B cells that suppress the immune system and control inflammation, often through the secretion of IL10. Thus far, cell surface markers for murine Bregs have been identified, but markers to identify human Bregs remain unclear. Due to their anti-inflammatory nature, it has been hypothesized that IL10-producing Bregs suppress plaque development. Decreased serum levels of IL10 have long been associated with human cardiovascular disease. IL-10 is produced by many cells and it is unclear whether IL10 produced specifically by B cells is sufficient to attenuate atherosclerosis, although patients with a history of atherosclerotic events had lower levels of IL10<sup>+</sup> B cells.

### **Roles of Id3 in B cell mediated atherosclerosis**

The *ID3* gene encodes the protein Inhibitor of Differentiation 3 (Id3). Id3 is a member of the helix-loop-helix (HLH) transcription factor family and functions as a dominant negative inhibitor of bHLH factor-induced gene regulation. Id3 dimerizes with broadly expressed E-proteins such as E12 and E47 preventing dimerization of these E proteins with each other or other tissue-specific bHLH factors, inhibiting subsequent DNA binding and gene activation by these dimers<sup>37–39</sup>. Preclinical studies have clearly shown that atherosclerosis prone mice with global deletion of the ID3 gene have significantly more atherosclerosis at all time points studied in LDLR<sup>-/-</sup> or Apoe<sup>-/-</sup> mice, whether Chow or Western diet-fed and by en face or cross-sectional analysis<sup>40–42</sup>. Intriguingly, the human ID3 variant at rs11574 that is associated with CAD results in attenuated ability of Id3 to dimerize with E12 and antagonize E12-mediated gene regulation<sup>8</sup>.

In B cells, Id3 is a regulator of B cell development, function, and antibody production<sup>43–45</sup>. Initial studies in Id3 global deletion demonstrated equivalent numbers of total B cells compared to WT but decreased in proliferation in response to BCR cross-linking<sup>44</sup>. Years later, Rosenfeld et al showed that roles of Id3 in regulating B cell number and antibody production might be subtype

dependent<sup>46</sup>. His findings indicated that loss of Id3 in B cells led to an increase in B1b but not B1a cell number in peritoneal cavity, spleen, and bone marrow, resulting in higher production of atheroprotective IgM to OSE and reduction in atherosclerotic plaque formation<sup>46</sup>. However, the underlying mechanism of this selective regulation of B1b cell number still remain unexplored.

### **Roles of p62 in cell proliferation and atherosclerosis**

P62/SQSTM1, an adaptor protein, is well-known to regulate cell proliferation and autophagy in various cell types, such as prostate cancer cells<sup>47</sup>, neurons<sup>48</sup>, osteoclasts<sup>49</sup>, and macrophages<sup>50</sup>. It can directly bind to MEKK3 and activate mTORC1 pathway to drive Myc expression leading to cell proliferation<sup>51</sup> or can interact with TRAF6 to induce NFKB activation which is a known driver of cell proliferation<sup>52</sup>. In addition, p62 is also subject to positive transcriptional regulation and NFKB can stimulate transcription of p62<sup>53</sup>. This feedback loop is crucial for aberrant cell proliferation in cancers. However, whether p62 regulates B cell self-renewal and proliferation still remains unknown.

Role of p62 in atherosclerosis was investigated in macrophages<sup>50</sup>. p62 was shown to exert atheroprotective effect through facilitating clearance of polyubiquitinated inclusion body resulting in stabilization of plaque formation<sup>50,54</sup>. Additionally, TFEB, a bHLH zipper transcription factor, can drive p62 transcription<sup>55</sup> and a disaccharide trehalose can increase TFEB expression. Despite a wealth of data showing roles of p62 in both cell proliferation and atherosclerosis, impact of p62 in B cells on atherosclerosis has never been investigated.

### **Roles of CD24 and cardiovascular diseases**

CD24, a GPI-anchored sialoglycoprotein, is a membrane protein composed of a short peptide backbone with no trans-membrane domain. Overexpression of CD24 was found in many B cell

malignancy such as non-Hodgkin B cell lymphomas, and acute lymphoblastic leukemia (ALL)<sup>56</sup>. Even though CD24 has been extensively studied in cancers, various studies demonstrated roles of CD24 in cardiovascular disease.

CD24 was found to express on immature cardiomyocytes and located near infarct regions post myocardial infarction. Ischemic injury also induces expansion of this CD24+ cardiomyocytes demonstrating that this rare cardiomyocyte population pertains regenerative capacity<sup>57</sup>. In addition to importance of CD24 on cardiomyocytes, CD24 also plays a major role in immune cells mediating inflammation which is a pathogenesis of cardiovascular diseases. Chen et al discovered that CD24 inhibits tissue injury through binding with Siglec-G/10 to counter danger associated molecular patterns (DAMPs) induced TLR activation and downstream NF $\kappa$ B<sup>58</sup> on dendritic cells, which is also a known process driving macrophage differentiation to foam cells<sup>59</sup>. In B cells, CD24 is a common marker expressing on most of immature B cells to regulate their differentiation and proliferation. Jiao et al identified CD24<sup>high</sup> CD27<sup>+</sup> B cells to pertain regulatory B cells characteristics and produce anti-inflammatory IL-10. The same study also discovered that lower frequency of CD24<sup>high</sup> CD27<sup>+</sup> B cells associate with dilated cardiomyopathy and chronic vasculitis<sup>60</sup>. However, roles of CD24 on B cells in regulating IgM production and effects on atherosclerosis has never been investigated.

It is crucial to evaluate the effect of CD24 in mediating inflammation and cardiovascular disease now rather than before as CD24 was discovered as a target for both cancer and COVID-19 therapies. Therefore, their long-term side effects on cardiovascular diseases should also be investigated.

## Project Rationales

Prior to investigation through these projects, B1 was known as atheroprotective B cells and B1b cells were more modulatory than B1a cells *in vivo*. Previous work from Dr. Sam Rosenfeld demonstrated that B1b cells but not B1a cells can be stimulated by pneumococcal polysaccharide vaccine (PPSV) to produce IgM to OSEs in Rag<sup>-/-</sup> mice (unpublished). Additionally, B1b was also shown to increase in number of B cells lacking Id3 transcription factor<sup>46</sup>. Therefore, understanding protein factor(s) that might regulate B1b cell number leading to an increase in atheroprotective IgM and reduction of atherosclerotic plaque development might be a potential immunotherapy for atherosclerosis. However, as previously mentioned, translating discovery in murine B1 cells to humans is difficult due to the differences in surface markers used to mark B cells in human and murine. This problem led us to identify and investigate IgM producing B cells in human.

In Chapter 3, we present the evidence that Id3 regulates B1b cell number through inhibiting E2A driven p62 expression. P62 is an adaptor protein known to mediate cancer cell proliferation and autophagy. Our study suggests that BAFF stimulates binding between p62 and TRAF6 which further activates NF $\kappa$ B signaling, drives c-myc expression, resulting in proliferation of B cells. Additionally, double knockout of p62 and Id3 yields significantly lower B1b *in vivo* cell proliferation than when Id3 was knocked out alone suggesting that p62 is crucial in Id3 dependent B1b cell proliferation. An adoptive transfer study of p62 overexpressed B1 cells into C57BL/6J mice following with AAV-PCSK9 gain of function injection and 8 weeks western diet fed also leads to higher number of B1b cells, higher IgM production, and reduced atherosclerosis. These results indicate that p62 can be a potential target for atherosclerosis.

immunotherapy. To be able to translate this discovery into human, we pursue identification of human IgM producing B cells in Chapter 4.

In Chapter 4, we utilize an unbiased approach to identify B cell subtype that associates with IgM-MDA-LDL level and develop an *in vivo* humanized model to validate IgM production of these B cells. Our results indicate that CD27 and IgM mark B cell subtype that produces IgM-MDA-LDL and CD24 augments IgM production. Through bulk RNA sequencing and series of *in vitro* and *in vivo* studies, we demonstrate that CD24 interacts with CCR6 to lower internalization of CCR6 allowing CCR6 to mediate splenic trafficking, and IgM production. Additionally, we also found that CD24 protects against diet-induced vascular inflammation in hyperlipidemic humanized mice. Lastly, we investigate roles of CD24<sup>high</sup> CD27<sup>+</sup>IgM<sup>+</sup> B cells in human coronary artery disease by applying single cell multi-omics to B cells obtained from high and low severity coronary artery disease patients. We show that high level of CD24<sup>high</sup> CD27<sup>+</sup>IgM<sup>+</sup> B cells associate with low CAD severity and enrichment of CCR6 as well as IgM production were detected in low CAD severity subjects.

## **Chapter 2**

### **Material and Methods**

### **Human Coronary Artery Disease Subjects**

All human subjects were recruited for study through the Cardiac Catheterization laboratory at the University of Virginia. All participants provided written informed consent before enrollment, and the study was approved by the Human Institutional Review Board. Peripheral blood were obtained from these participants prior to catheterization.

### **Healthy Human Volunteers**

Peripheral blood from healthy volunteers were obtained after provided with written informed consent. The study was approved by the Human Institutional Review Board at University of Virginia.

### **Mice**

All animal protocols were approved by the Animal Care and Use Committee at the University of Virginia. Mice were purchased from Jackson Laboratory as described in detailed methods. Mice were fed a standard chow diet or a Western diet.

### **Quantitative Coronary Angiography (QCA)**

Patients underwent standard cardiac catheterization with two orthogonal views of the right coronary artery and four of the left coronary artery according to accepted standards. QCA was performed using automatic edge detection at an end diastolic frame. For each lesion, the frame was selected based on the most severe stenosis with minimal foreshortening and branch overlap. Computer software was used to calculate the minimum lumen diameter, reference diameter, percent diameter stenosis and stenosis length. Analysis was performed by blinded, experienced investigators. The Gensini score was used to determine disease burden for each patient. Briefly, each artery segment was assigned a score of 0-32 based on stenosis

percentage. The severity score for each segment was multiplied by 0.5 – 5, depending on stenosis location. Scores for all segments were then added together to give a final score of angiographic disease burden. Score adjustment for collateral was not performed for this study.

### Cell Preparations for Murine and Human flow cytometry

Peritoneal cavity cells were processed for flow cytometry or fluorescence activated cell (FAC) sorting as previously described (Rosenfeld et al). Isolation of human PBMCs was performed as previously described (Rosenfeld et al). Clone and fluorophore information for flow cytometry antibodies are given in Table 1.

Table 1: Flow cytometry antibodies used for sorting, analyzing B cells from *in vitro* culture and tissue harvest.

Fluorophore	Clone	Manufacturer	Antigen
PE-CF594	1D3	BD Bioscience	CD19
AF700	O323	Biolegend	CD3
BV421	52-7.3	BD Bioscience	CD5
APC	RA3-6B2	Invitrogen	B220
AF488	EPR4844	Abcam	p62
AF647	EP591Y	Abcam	TRAF6
PE	MFRDTRK	Invitrogen	IKBa
AF555	Y69	Abcam	c-myc
PE	7H22-E16	Biolegend	BAFFR
PE	16A8	Biolegend	Ki-67

### Samples preparation of Bulk RNA sequencing

Sort-purified peritoneal B1a and B1b obtained from Id3KO and Id3WT C57BL/6 mice were RNA extracted by using Qiagen RNeasy Plus kit. The purified RNAs were stored at -80°C and sent to third party vendor to perform sequencing.

### **Differentially expressed genes and pathway analysis**

RNA sequences in raw FASTQ data files were obtained from third party vendor. Sequencing reads were aligned to reference genome (GRCm38/mm10) using HISAT2. The annotated sequences were then quantified and assembled by using StringTie, and differentially expressed genes were analyzed using R Ballgown package. Volcano plots of differentially expressed genes were visualized by using python bioinfokit package. Ingenuity Pathway Analysis was performed on all the annotated RNA to analyze for differentially regulated cellular processes, canonical pathways and network analysis.

### ***In Vitro* and *In Vivo* Cell Proliferation Assay**

Peritoneal cavity cells were enriched for B cells using EasySep Mouse Pan-B cell enrichment kit, incubated with Celltrace-violet for 20 minutes at 37°C, and then washed with FACS buffer (1% FBS, 0.1%NaN<sub>3</sub> in PBS). Labeled cells were cultured in B cell culture media (RPMI + 10%FBS + 10mM HEPES, 1mM Na-pyruvate + 10ug/mL Gentamycin + non-essential amino acid) for 3 days with 20ng/mL recombinant BAFF or PBS control to measure *in vitro* proliferation. For *in vivo* proliferation, Celltrace-violet labelled cells were intraperitoneally transferred into C57BL/6 mice.

### **Lentiviral Production and P62 Overexpression on mouse B cells.**

P62-eGFP lentivirus was generated using pLV-eGFP vector (purchased from addgene) and mouse p62 was subcloned into the vector. The eGFP or P62-eGFP lentiviruses were generated using four plasmid system by co-transfecting pLV-eGFP or pLV-P62-eGFP plasmid along with pLP1(Gag-Pol vector), pLP2 (Rev vector), and pVSV-G (VSV-G vector) plasmids into 293T cells. The eGFP ctrl and P62-eGFP lentiviruses were used to transduce enriched peritoneal mouse B cells by using 5ug/mL polybrene and spinning at 1000g for 60 mins. Transduced

murine B cells were harvested 48 hrs post transduction and FAC-sorted for GFP+ B1 cells to be used for adoptive transfer. Approximately 25-30% of B-1 cells were successfully transduced by this method.

### **P62 CRISPR/sgRNA Knockout and Pp62-GFP transfection on Mouse B cells.**

crRNA molecule-targeting exon of p62 (UUGUAGCGGGUCCUACCAC-PAM AGG) was purchased from IDT and conjugated with tracrRNA-ATTO. Pp62-GFP plasmid was generated by subcloning 1000bp of p62 promoter to replace CMV promoter in CMV-GFP plasmid purchased from Addgene. Murine peritoneal cells were enriched for B cells, cultured in B cell culture media, and stimulated with 50ng/mL LPS overnight. The stimulated B cells were then nucleotransfected with Cas9 ribonuclear protein and pre-conjugated p62 crRNA-tracrRNA ATTO, Pp62-GFP, or CMV-GFP ctrl plasmid using the P3 Primary cells Nucleofection Kit purchased from Lonza. B cells were collected for analysis and sorting 24 hrs after nucleofection.

### **Nucleofection of Engineered Plasmids into Human B cells.**

Cryopreserved PBMCs obtained from healthy donors were thawed and washed with warm complete media (RPMI supplemented with 5% FBS, 1 mM sodium pyruvate and Pen-Strep). Cells were then enriched for B cell using EasySep human pan-B cell enrichment kit (STEMCELL). CMV-E12-Flag, CMV-E47-Flag were generated using CMV-Flag plasmid to subclone human E12 and E47 into. These plasmids were nucleotransfected into unstimulated enriched human B cells using the P3 Primary cells Nucleofection Kit purchased from Lonza. B cells were collected for analysis and sorting 24 hrs after nucleofection.

### **Quantification of markers colocalization by using imaging flow cytometry**

Murine peritoneal cells obtained from Id3KO and Id3WT mice were enriched for B cells. The

enriched B cells were incubated with 20ng/mL murine recombinant BAFF or PBS control for 12 hrs in B cell media. Prior to running on Imagestream imaging flow cytometry machine, cells were stained with p62, TRAF6, B220, CD5, and CD19 antibodies. Images of 1000 Id3KO or Id3WT B1b cells from both unstimulated, BAFF stimulated conditions were collected, and quantitative co-localization analysis was performed using Amnis Imagestream colocalization software.

### **ELISA for Quantification of Total and Anti-OSE IgM or IgG Isotypes in Mice and Humans**

Total IgM subtypes in mouse plasma were measured using colorimetric ELISA as described previously (Rosenfeld et al, Circ Res, 2015). Levels of IgM against MDA-LDL in human plasma were measured by chemiluminescent ELISA as previously described (Rosenfeld et al, Circ Res, 2015).

### **Adoptive Transfer**

Celltrace violet+ or eGFP+ (eGFP-ctrl or p62-eGFP) B1 (CD3-CD19+B220-) cells were sort-purified. After sorting, these cells were adoptively transferred into C57BL/6 host mice intraperitoneally. Mice adoptively transferred with Celltrace-violet+ cells were fed with chow diet for 2 weeks, Mice adoptively transferred with eGFP-ctrl or p62-eGFP B1 cells were fed with Western diet for 8 weeks. After 2 weeks or 8 weeks period, mice were sacrificed and peritoneal cavity was processed for flow cytometry as previously described (Rosenfeld, CirC Res, 2015). For western diet fed mice, aortas were harvested and stained using Sudan IV as previously described (Rosenfeld, Cir Res, 2015). Flow cytometry was used to quantify for number of B1a and B1b cells as well as degradation of Celltrace-violet signal of harvested cells obtained from C57BL/6 mice.

### **CyTOF optimization and staining**

All metal-conjugated antibodies were purchased from Fluidigm and purified unlabeled antibodies from Biolegends. Unlabeled antibodies were conjugated in-house using the MaxPAR antibody labeling kit (Fluidigm) according to the manufacturer's protocol and stored at 4°C. Cryopreserved PBMCs obtained from healthy volunteers were used for antibody titration to determine optimal concentration.

Cryopreserved PBMCs obtained from 27 CAD subjects with high and low plasma IgM<sup>MDA-LDL</sup> were thawed and washed twice with warm complete media (RPMI supplemented with 5% FBS, 1 mM sodium pyruvate and Pen-Strep). All PBMC samples had 85-98% viability. PBMCs from each individual subject were barcoded using the palladium-based 20-Plex Pd Barcoding Kit (Fluidigm) according to the manufacturer's protocol. Barcoded cells were then combined into a single tube prior to Fc receptor blocking (BD Biosciences) and staining with a cocktail of metal-conjugated antibodies against cell-surface markers (Table 2) for 30 minutes at RT. Stained cells were washed with CSB buffer and chilled on ice for 5 minutes. After washing, cells were fixed with 2% PFA for 10 minutes at RT, washed again and stored overnight at 4°C. The next day, prior to running mass cytometry, cells were stained with iridium DNA intercalator (Fluidigm) in Maxpar Fix and Perm Buffer (Fluidigm) for 20 minutes at RT, washed once with CSB followed by two washes with the Maxpar Cell Acquisition Solution (Fluidigm) and filtered through a 40 µm membrane. Cells were then acquired on a Helios mass cytometer (Fluidigm).

**Table 2: CyTOF antibodies**

Metal Tag	Clone	Manufacturer	Antigen
89Y	HI30	Fluidigm	CD45
141Pr	G034E3	Fluidigm	CD196
142Nd	HIB19	Fluidigm	CD19
146Nd	IA62	Fluidigm	IgD
147Sm	2H7	Fluidigm	CD20
148Nd	3G8	Fluidigm	CD16
149Sm	2A3	Fluidigm	CD25
152Sm	BL13	Fluidigm	CD21
156Gd	IT2.2	Fluidigm	CD86
159Tb	G043H7	Fluidigm	CD197
167Er	HIT2	Fluidigm	CD38
169Er	ML5	Fluidigm	CD24
170Er	UCHT1	Fluidigm	CD3
172Yb	MHM88	Fluidigm	IgM
174Yb	EH12.2H7	Fluidigm	CD279
175Lu	M5E2	Fluidigm	CD14
209Bi	ICRF44	Fluidigm	CD11b
143Nd	CB3-1	Biolegend	CD79b
151Eu	DL-101	Biolegend	CD138
153Eu	HTF1	Biolegend	CD142
154Sm	MU5UBEE	Biolegend	CD185
155Gd	610015	Biolegend	CD284
158Gd	M-T271	Biolegend	CD27
162Dy	1C6/CXCR3	Biolegend	CD183
164Dy	2B11	Biolegend	CD184
165Er	IG10	Biolegend	CD43
171Yb	3F3	Biolegend	CD72
176Yb	11C1	Biolegend	CD268

### CyTOF data pre-processing and analysis

FCS data files were obtained from the Helios instrument. Data were normalized using the Nolan lab MATLAB normalizer (<http://github.com/nolanlab/bead-normalization/releases>) and debarcoded using Zunder's lab debarcoder 24 (<https://github.com/zunderlab/single-cell-debarcoder>). Normalized and debarcoded files were further gated based on barcode stringency parameters and iridium DNA intercalator to remove non-cell debris and cellular aggregates. B cells were identified by manual gating determined by CD19<sup>+</sup>CD3<sup>-</sup>CD14<sup>-</sup>. CyTOF data were analyzed using R framework (v3.5.0) and Bioconductor (v3.7). First, protein expression was normalized using arcsinh (cofactor=5) transformation. Then, we used the self-organizing map method<sup>61</sup> for clustering with the number of clusters from 2 to 30. Cluster robustness was

evaluated using the relative change in area under cumulative distribution function using consensus clustering<sup>62</sup> that identified 11 clusters. Heatmap of average expression for each cluster used a pheatmap R package with expression scale from 0 to 1.

### Sort-purifying B cells

Cryopreserved PBMCs were thawed and washed twice with warm complete media (RPMI supplemented with 5% FBS, 1 mM sodium pyruvate and Pen-Strep). Cells were then incubated with Fc receptor blocking (BD Biosciences) and stained with a cocktail of fluorophore-conjugated antibodies against cell-surface markers (Table 3) for 30 minutes at RT and then washed with FACS buffer (1% FBS, 0.1%NaN<sub>3</sub> in PBS). Prior to FACS sorting, cells were stained with 7AAD and filtered through a 40 µm membrane. Cells were sorted on Influx cell sorter into 2% FBS RPMI media.

**Table 3: FACS sorting antibodies**

Fluorophore	Clone	Manufacturer	Antigen
BV711	ML5	Biolegend	CD24
BV421	O323	Biolegend	CD27
APC	MHM88	Biolegend	IgM
APC-Cy7	2H7	Biolegend	CD20
PE-CF594	UCHT1	BD Bioscience	CD3
BUV737	M5E2	BD Bioscience	CD14

### Using imaging flow cytometry to quantify marker co-localization

Cryopreserved PBMCs were thawed and washed with warm complete media (RPMI supplemented with 5% FBS, 1 mM sodium pyruvate and Pen-Strep). Cells were then enriched for B cells using EasySep human pan-B cell enrichment kit (STEMCELL). The enriched B cells were incubated with 20µg/mL IgG isotype control or 20µg/mL CD24 monoclonal antibody (ThermoFisher, SN3 clone) for 12 hrs in 20% FBS RPMI media. The next day, the cells were blocked with Fc-receptor blocker and stained with a cocktail of fluorophore-conjugated

antibodies (Table 4) and then washed with FACS buffer. Prior to processing on an Imagestream imaging flow cytometer, cells were stained with live-dead marker, washed once with FACS buffer and filtered through a 40  $\mu\text{m}$  membrane. Images of 1000  $\text{B}^{27+\text{IgM}+\text{CD24}^{\text{hi}}}$  cells from both pre-incubated IgG isotype and CD24 mAb were collected, and quantitative co-localization analysis was performed using Amnis Imagestream co-localization software.

### ***In vitro* transwell migration assay**

Cryopreserved PBMCs were sort-purified for  $\text{B}^{27+\text{IgM}+\text{CD24}^{\text{hi}}}$  and  $\text{B}^{27+\text{IgM}+\text{CD24}^{\text{lo/-}}}$ . These cells were

**Table 4: Flow cytometry antibodies for tissue samples following humanized mice harvest**

Fluorophore	Clone	Manufacturer	Antigen
BV711	ML5	Biolegend	CD24
BV421	O323	Biolegend	CD27
APC	MHM88	Biolegend	IgM
APC-Cy7	2H7	Biolegend	CD20
PerCP	H130	ThermoFisher	CD45
PE	11A9	BDBiosciences	CD196

combined with 20% FBS RPMI media at 50,000 cells/mL, incubated with either 20 $\mu\text{g}/\text{mL}$  IgG isotype control or 20 $\mu\text{g}/\text{mL}$  CD24 mAb and seeded into the upper wells of the transwell plate. 20% FBS RPMI media was mixed with DMSO or 1  $\mu\text{g}/\text{mL}$  human recombinant CCL20 and added to the lower wells of the transwell plate. Migrated cells were collected after culturing for 24 hrs and stained with 7AAD to quantify the live migrated cells using flow cytometry.

### ***In vitro* internalization assay**

Sort-purified  $\text{B}^{27+\text{IgM}+\text{CD24}^{\text{hi}}}$  and  $\text{B}^{27+\text{IgM}+\text{CD24}^{\text{lo/-}}}$  were seeded at 50,000 cells/mL and incubated with either 20 $\mu\text{g}/\text{mL}$  IgG isotype control or 20 $\mu\text{g}/\text{mL}$  CD24 mAb with or without 1 $\mu\text{g}/\text{mL}$  human recombinant CCL20. Cell suspension samples (100  $\mu\text{l}$ ) were harvested at 0, 2, 5 and 10 min and incubated in a dry ice/ethanol bath for 3–5s to stop the reaction. Cells were washed with ice-

cold FACS buffer, blocked with Fc-receptor blocker, stained with live-dead aqua and then stained with PE-conjugated CCR6 antibody. Following a wash with FACS buffer, cells were intracellularly stained with BV421-conjugated CCR6 antibody, following the BD Cytotfix/Cytoperm Fixation/Permeabilization kit, and fixed again with 2% PFA at RT for 10 min. Flow cytometry was used to evaluate the GM of surface PE-CCR6 and the GM of intracellular BV421-CCR6.

### ***In vitro* Filipin-induced lipid raft disintegration treatment and migration assay**

Sort-purified B<sup>27</sup>+IgM+CD24<sup>hi</sup> cells were incubated with either 10ug/mL Filipin or PBS control for 5 min and vigorously washed twice with FACS buffer. Following Filipin treatment, B<sup>27</sup>+IgM+CD24<sup>hi</sup> /- cells were seeded at 50,000 cells/mL in the upper well of the transwell in 20% FBS RPMI media. 20% FBS RPMI media was mixed with 1 μg/mL human recombinant CCL20 and added to the lower wells of the transwell plate. Migrated cells were collected after culturing for 24 hrs and stained with 7AAD to quantify the live migrated cells using flow cytometry.

### **Adoptive Transfer to Humanized Mice**

B<sup>27</sup>+IgM+CD24<sup>hi</sup> and B<sup>27</sup>+IgM+CD24<sup>lo</sup>/- were sort-purified. After sorting, these cells were either rested in 20% FBS RPMI, incubated with either 20μg/mL IgG isotype control or 20μg/mL CD24 mAb or stimulated with 100ug/mL MDA peptide mimotope (Amir et al., *J Lipid Res*, 2012) for 1 hr at 37C. Following *in vitro* stimulation/treatment, 200,000 of these cells were adoptively transferred intraperitoneally into NOD.Cg-Prkdc<sup>scid</sup> Il2rg<sup>tm1Wjl</sup>/SzJ (NSG) mice. These NSG mice are on the NOD/ShiLtJ genetic background and carry mutations in the severe combined immune deficiency (*scid*) and a complete null allele of the IL2 receptor common gamma chain (*IL2rg<sup>null</sup>*). The *scid* mutation renders the mice B and T cell deficient. The *IL2rg<sup>null</sup>* mutation prevents cytokine signaling through multiple receptors, leading to a deficiency in functional NK cells.

Such severe immunodeficiency allows the mice to be humanized by engrafting human peripheral blood mononuclear cells (PBMC)<sup>63</sup>. One week post adoptive transfer, mice were sacrificed and the peritoneal cavity, bone marrow and spleen were processed for flow cytometry as previously described (Rosenfeld, *Cir Res*, 2015). Harvested cells were blocked with Fc-receptor blocker and stained with a cocktail of fluorophore-conjugated antibodies (Table 4) and then washed with FACS buffer. Flow cytometry was used to quantify human B<sup>27+IgM+CD24hi</sup> and B<sup>27+IgM+CD24lo/-</sup> in each compartment of humanized mice.

### **Human PBMC CCR6 Knockout**

gRNA molecule-targeting exon 1 of CCR6 (sequence GAGUCAUGCCACCGGUGCGU) was purchased from IDT and conjugated with tracrRNA ATTO. Total human PBMCs were enriched for B cells using the EasySep Human Pan-B cell Enrichment Kit purchased from Stemcell and stimulated with 1ug/mL human IL-4 for 2 hrs. The enriched B cells were then nucleotransfected with Cas9 ribonuclear protein and pre-conjugated CCR6 gRNA-tracrRNA ATTO using the P2 Primary cells Nucleofection Kit purchased from Lonza. B cells were collected for analysis and sorting 24 hrs after nucleofection.

### **Generation of Hyperlipidemic Humanized Mice**

NSG mice were engrafted with  $1 \times 10^7$  human PBMCs obtained from healthy donors via tail vein injection. A day after PBMCs engraftment, mice were intravitreally injected with  $1 \times 10^{12}$  AAV8 (D377Y) PCSK9 to induce gain of function PCSK9 allowing induction of hyperlipidemia. Humanized mice were then fed a Western Diet (WD) beginning at the time of AAV8-PCSK9 delivery for 10 weeks. Blood was drawn after 10 weeks WD fed to measure total cholesterol using Infinity cholesterol colorimetric kit.

### **In vivo CD24mAb Treatment and <sup>18</sup>F-FDG-PET/CT Imaging**

Hyperlipidemic humanized mice after 10 weeks WD feeding were treated with 200ug CD24mAb or IgG isotype control 2 times a week for 3 weeks via intravitreal injection. At the end of 3 weeks treatment, <sup>18</sup>F-FDG-PET/CT images were acquired on a Bruker Albira Si scanner. The mice were fasted overnight before the scan. During anesthesia with isoflurane, 10 MBq of <sup>18</sup>F-FDG was tail vein injected to the mice. A static PET scan was obtained 30 mins post <sup>18</sup>F-FDG injection. FDG uptake was quantified using average standardized uptake volume (SUV) performed by PMOD 3.9 software. The region of interest (ROI) for the aorta area was determined using the CT images. The ROI was then transferred to the co-registered PET images in order to measure SUV.

### **CITEseq Optimization and Staining**

A detailed protocol can be found in Vallejo et al.<sup>64</sup>. In brief, PBMC tubes were thawed at 37° C and washed with complete RPMI-1640 solution. Cells were aliquoted at 1 million cells per aliquot, incubated on ice with Fc Block (BD) at 1:20 dilution in staining buffer (SB) and transferred to sample multiplexing kit tubes (BD) to incubate for 20 mins at RT. Cells were then washed three times and centrifuged at 400 xg for 5 minutes. DRAQ7 and Calcein AM were used for viability count. Tube contents were pooled in equal proportions with total cell counts not to exceed 1 million cells and then resuspended in a cocktail of 26 CITEseq (Table 5) antibodies (2 μL each and 20 μL of SB) on ice for 30-60 min per the manufacturer's recommendations. The tubes were then washed with 2 mL of SB followed by centrifugation at 400 xg for 5 min. This

was repeated two more times for a total of three washes. Library preparation for RNA sequencing was prepared according to BD's protocol.

**Table 5: List of 26 titrated oligonucleotide-tagged monoclonal antibodies used in CITEseq experiment to subtype B cells.**

Antigen	Clone
CD11c	B-LY6
CD123 (IL-3RA)	7G3
CD126 (IL-6R)	M5
CD137	4B4-1
CD142	HTF-1
CD183 (CXCR3)	1C6/CXCR3
CD184 (CXCR4)	12G5
CD185 (CXCR5)	RF8B2
CD19	SJ25C1
CD196 (CCR6)	11A9
CD197 (CCR7)	3D12
CD20	2H7
CD24	ML5
CD25	2A3
CD27	M-T271
CD273	MIH18
CD274	MIH1
CD279	MIH4
CD38	HIT2
CD43	1G10
CD69	FN50
CD86	2331(FUN-1)
IgD	IA6-2
IgM	G20-127
TLR4	TF901
SLAN	hSF6

### **CITEseq data pre-processing and analysis**

Out of total PBMCs, B cells were first identified by manual gating determined by CD19<sup>+</sup>CD3<sup>-</sup>. CSV files for all samples obtained from CAD subjects within the CAVA cohort contained measurements of all 26 surface antibodies and 488 genes expression. All measurements were normalized by dividing by total counts for each cell and scaling up to  $1 \times 10^5$  and then  $\text{Log}_2$  transformed. The pre-processed data were passed through python pipeline using scikit-learn

and Scanpy packages to perform UMAP dimensionality reduction and Louvain clustering to determine B cell subtypes in an unsupervised manner to identify potential B<sup>27+IgM+CD24<sup>hi</sup></sup> and B<sup>27+IgM+CD24<sup>lo</sup></sup> subtypes. Expression of 488 genes within these two subtypes were compared between low and high CAD severity subjects by performing a t-test with Bonferonni corrected p-values and calculating fold change in gene expression using R software. Differentially expressed genes were defined as genes with FDR < 0.05 and Log<sub>2</sub>FC < 1 or > 1. Volcano plots of differentially expressed genes were visualized using the python bioinfokit package. Ingenuity Pathway Analysis was performed on all annotated RNA to analyze for differentially regulated cellular processes and canonical pathways.

### **Statistics**

Statistics were calculated using GraphPad Prism Version 7.0a (GraphPad Software, Inc.), Python 3.0, R 3.6.1 or SAS 9.4. Results from all replicated experiments are displayed, and bar graphs display mean±SEM.

## **Chapter 3**

# **B-1b cells possess unique bHLH-driven p62-dependent self-renewal and atheroprotection**

## Abstract

**Background:** B1 cells produce IgM that inactivates oxidation-specific epitopes (OSEs) on low-density lipoprotein and protects against atherosclerosis. Loss of inhibitor of differentiation 3 (Id3) in B cells promotes B1b but not B1a cell number leading to higher IgM production and reduction in atherosclerotic plaque formation. Yet, the mechanism how Id3 selectively mediates B1b cell number remains unexplored.

**Methods:** Bulk RNA sequencing was utilized to identify differentially expressed genes (DEGs) in Id3KO B1b cells. CRISPR/Cas9 and lentiviral genome editing coupled with adoptive transfer were used understand how p62 regulated B1b cell proliferation and their effects on atherosclerosis. Human association study was performed to explore relationships among Id3, p62, B1, and IgM in coronary artery disease (CAD) subjects.

**Results:** Through RNA sequencing, p62 was identified as a DEG uniquely enriched in Id3KO B1b cells. BAFF stimulation on B1b cells induced binding between TRAF6 and p62 leading to activation of NF $\kappa$ B pathway, subsequent c-myc expression, and B1b cell proliferation. Double knockout of p62 and Id3 coupled with *in vivo* proliferation assay supported that Id3 suppressed B1b cell proliferation was p62 dependent. Promoter-reporter assays implicated that E2A, a binding partner of Id3, activated p62 promoter and Id3 inhibited the activation. Adoptive transfer of B1 cells with p62 overexpression, following with AAV-PCSK9 injection and Western diet fed in C57BL/6J mice resulted in an increase in B1b cell number, plasma IgM, and a reduction in atherosclerosis. Lastly, in a 58-CAD subject cohort, p62 expression in circulating B1 cells was higher in subjects with Id3 functionally reduced rs11574 SNP, and associated with higher frequency of B1 cells and plasma IgM to OSEs.

**Conclusions:** This study demonstrates that Id3 regulates B1b cell number through inhibiting E2A activated p62 expression, and p62 mediates BAFF induced B1b cell proliferation. This p62 promoted B1b cell proliferation also leads to an increase in IgM production and reduction in atherosclerotic plaque formation. The fact that p62 expression in circulating human B1 is higher in subjects with high atheroprotective IgM suggests that p62 can be a potential immune-modulatory target for atherosclerosis.

## Introduction

Cardiovascular disease (CVD) is the leading cause of death worldwide and atherosclerosis is the major underlying pathology of most CVD<sup>2</sup>. Atherosclerosis is characterized by accumulation and subsequent oxidative modification of lipoproteins within the artery wall, leading to inflammatory cell infiltration and lesion formation<sup>7</sup>. Innate and adaptive immunity contribute to atherosclerosis and B cells have emerged as important modulators of both pro- and anti-inflammatory effects in atherosclerosis. Murine B cells are divided into 2 subsets: B-2 cells, which include conventional follicular and marginal zone B cells; and B-1 cells, which are fetal liver derived and persist throughout life through self-renewal<sup>65</sup>. A wealth of evidence, both murine mechanistic and human associative studies, has implicated an atheroprotective role for B1 cells, mainly through T cell independent production of IgMs that inactivate oxidation specific epitope (OSE) on LDL, and prevent lipid uptake and inflammatory cytokine production by macrophages<sup>20,21,35,33</sup>. In mice, B1 cells can be subtyped into B1a and B1b subsets based on their expression of CD5<sup>66</sup>. Both B-1a and B-1b cells produce IgM *in vivo*, however, adoptive transfer studies in Apoe<sup>-/-</sup>Rag1<sup>-/-</sup> mice revealed that B1b cells produce significantly higher levels of IgM *in vivo* compared to B1a<sup>46</sup>. As such, identifying the molecular and cellular mechanisms

that promote increased B-1b cell numbers may have important implications for preventing atherosclerosis and its progression.

Id3 is a member of the helix-loop-helix (HLH) family of transcription factors. The HLH transcription factor family contains members with a basic DNA-binding domain (bHLH) such as E12 and E47<sup>40,39</sup> and those without the DNA-binding domain, such as the Id proteins, which can antagonize E12 and E47 function by dimerizing with them, inhibiting their DNA binding<sup>43,67</sup>. There are 4 Id proteins (Id1-4) that have both unique and redundant properties<sup>43</sup> (Engel et al). Id3 has emerged as an important factor in atherosclerosis<sup>40</sup>. Specific deletion of Id3 in B cells (Id3<sup>BKO</sup>) in ApoE<sup>-/-</sup> mice selectively increased B-1b cell numbers in the peritoneal cavity (PerC), bone marrow (BM) and spleen, increased plasma atheroprotective IgM levels and attenuated diet-induced atherosclerosis<sup>46</sup>. Yet, the molecular mechanisms mediating the selective increase in B1b cell number in Id3<sup>BKO</sup> mice are unknown.

The present study demonstrated that loss of Id3 increased proliferation in B-1b but not B-1a cells. Bulk RNA sequencing on sorted PerC B1a and B1b cells from Id3<sup>WT</sup> and Id3<sup>KO</sup> mice identified only 20 differentially expressed (DE) genes in B-1a cells compared to 1903 DE genes in B-1b cells. While genes involved in B cell proliferation were among the DE genes in B-1b cells from Id3<sup>KO</sup> mice, p62, a scaffold and ubiquitin binding protein, was found to be one of the most highly enriched genes. Further pathway analysis also suggested that p62 might regulate B1b cell proliferation through B cell activating factor (BAFF) and NFκB signaling. Imaging flow cytometry and proliferation assays provided evidence that BAFF stimulation recruited p62 to TRAF6 and further activated NFκB signaling to drive B1b proliferation. Promoter-reporter assays implicated a direct effect of Id3 on p62 transcription as Id3 and its partner proteins significantly regulated p62 promoter activity. Increased expression of p62 in B1b cells

enhanced proliferation, increased atheroprotective IgM in plasma and reduced atherosclerosis formation in mice. Moreover, humans harboring a SNP in ID3 at rs11574, shown to attenuate Id3 function<sup>39</sup> had higher expression of p62 expression on their B1 cells and higher p62 on human B1 cells was significantly associated with the % of B1 cells in circulation and plasma levels of IgM to MDA. This study provides insights into mechanisms that mediate Id3 effects on B-1b proliferation and is the first to identify a role for p62 in B1 cell-mediated atherosclerosis, both novel findings with important therapeutic implications.

## Results

### **Loss of Id3 promoted BAFF-p62- NFKB expression and proliferation in B1b but not B1a cells.**

To determine potential mechanisms mediating the selective increase in B-1b cell number in Id3<sup>BKO</sup> mice we measured Ki67 expression in B1a and B1b cells obtained from the peritoneal cavity of C57BL/6 mice null for Id3 (Id3KO) and littermate controls (Id3WT). Results showed an average of 3.59% of B-1a and 8.64% of B-1b cells in the PerC expressed Ki67 at homeostasis and that B-1b but not B-1a cells had a significant increase in the %Ki67 positivity with loss of Id3(Figure 2a+b). To identify genes and pathways whereby Id3 may regulate B1b cell number, bulk RNA sequencing was performed on PerC B-1a and B-1b cells from Id3KO and Id3WT mice. Differentially expressed gene (DEG) analysis revealed only 20 DEG (FDR  $\leq$  0.05) out of 14933 aligned genes in B1a cells between Id3WT and Id3KO. In contrast, there were 1903 DEG (FDR  $\leq$  0.05) out of 14399 aligned genes in B1b cells (Figure 2c-d). Notably, SQSTM1 or p62 was markedly overexpressed in Id3KO B1b cells compared to Id3WT B1b cells with a 90.8 folds increase and a p-value of  $8.7 \times 10^{-5}$ . SQSTM1/p62 was not differentially expressed in B1a cells.

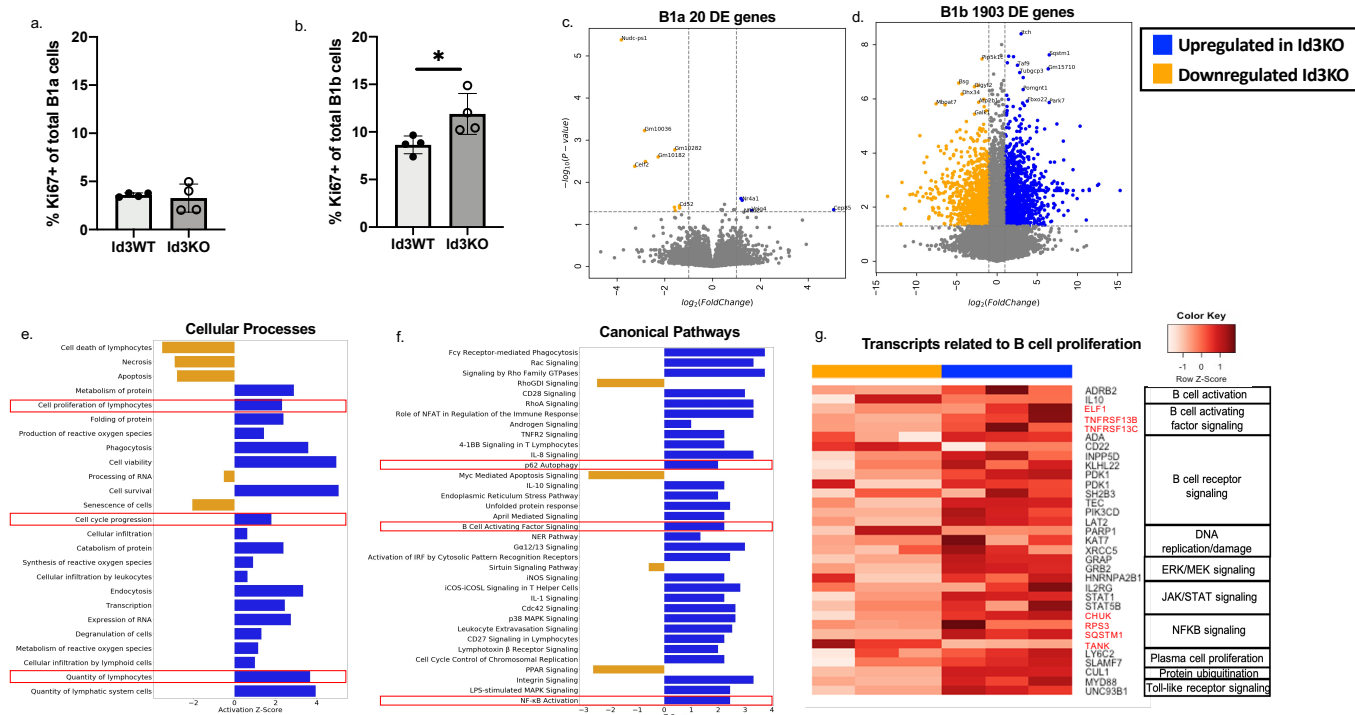


**Figure 2: Loss of Id3 promoted BAFF-p62-NFKB expression and proliferation in B1b but not B1a cells. (a-b)** Percentage of Ki67+ of total B1a (a) and B1b (b) obtained from Id3WT and Id3KO peritoneal cells (c-d) Volcano plots compared between Id3 WT (orange, n = 3) vs Id3 KO (blue, n = 3) B1a (c) and B1b (d) cells obtained from peritoneal cavity. (e-f) Cellular processes (e) and canonical (f) pathway analysis determining pathways downregulated in Id3 KO (orange) and upregulated in Id3 KO (blue) B1b cells. (g) Transcripts related to B cell proliferation categorized by canonical pathways downregulated in Id3 KO (orange) and upregulated in Id3 KO (blue) in B1b cells. Results are represented with Mean  $\pm$  SEM with unpaired Mann-Whitney t-test. \*p<0.05, \*\*p<0.01.

Consistent with the increase in the %Ki67+ B-1b cells in Id3KO mice, pathway analysis of cellular processes indicated upregulation of cell proliferation, cell cycle progression, as well as cell survival/viability in Id3KO B1b cells compared to Id3WT (Figure 2e). Canonical pathway

analysis demonstrated an enrichment of cell survival/proliferation related pathways such as p62 autophagy, B cell activating factor (BAFF), and NF $\kappa$ B signaling in Id3KO B1b cells compared to Id3WT (Figure 2f). Consistent with the increase in proliferation and survival pathways in Id3KO B1b cells, genes involving in B cell activation, BCR activation, DNA replication and repair, ERK/MEK, JAK/STAT, BAFF, NF $\kappa$ B, TLR signaling, plasma cell proliferation, and protein ubiquitination were enriched in Id3KO B-1b cells as shown in Fig. 1g. CD22 (a negative regulator of BCR activation), PARP1 (Poly ADP-ribose polymerase 1 which regulates DNA protein interaction during DNA repair), and TANK (a negative regulator of TRAF2 mediated NF $\kappa$ B activation) were downregulated.

### **Loss of Id3 increased BAFFR expression and BAFF-induced B-1b proliferation in a p62-dependent manner**

BAFF is a key factor that promotes B cell proliferation and survival<sup>68</sup> and DEG analysis from bulk RNAseq indicated an enrichment in BAFFR/TNFRSF13C gene in B-1b cells from Id3KO compared to Id3WT (Figure 2). We investigated BAFFR protein expression level on B-1a and B-1b cells from Id3KO and Id3WT mice by flow cytometry. Result indicated a significant increase in BAFFR expression in B1b cells but not in B1a cells from Id3KO compared to Id3WT mice (Figure 3a). Consistent with these findings, BAFF stimulation of B1a and B1b cells obtained from Id3WT and Id3KO mice revealed a significant increase in cell proliferation in B-1b but not B-1a cells that was further augmented in the Id3KO mice (Figure 3b).

As SQSTM1/p62 was one of the most highly enriched transcripts in Id3KO compared to Id3WT B1b cells, yet a role for p62 in B cell proliferation has not been reported, we sought to determine whether p62 was critical for B-1b proliferation. Nucleofection of Cas9 and p62 targeted gRNA

was utilized to knockout p62 in B cells (Figure 3c). Result demonstrated a significant reduction of BAFF-induced B1b cell proliferation with knockout of p62 in both Id3WT and Id3KO mice (Figure 3d).

To determine if p62 promoted B1b cell proliferation *in vivo*, p62 was knocked out in Id3KO B1 cells (Figure 3e). Equal numbers of B1 cells with double knockout of p62 and Id3 and B1 cells with only single knockout of Id3 was adoptive transferred (AT) through intraperitoneal injection into WT C57BL/6 mice. Mice were harvested 2 weeks post AT and cell trace violet was used to track the transferred cells as well as measured their proliferation using cell trace violet (Figure 3e). Results demonstrated that PerC Id3KO-p62KO B1b cells had significantly lower proliferation when compared to Id3KO B1b cells (Figure 3f).

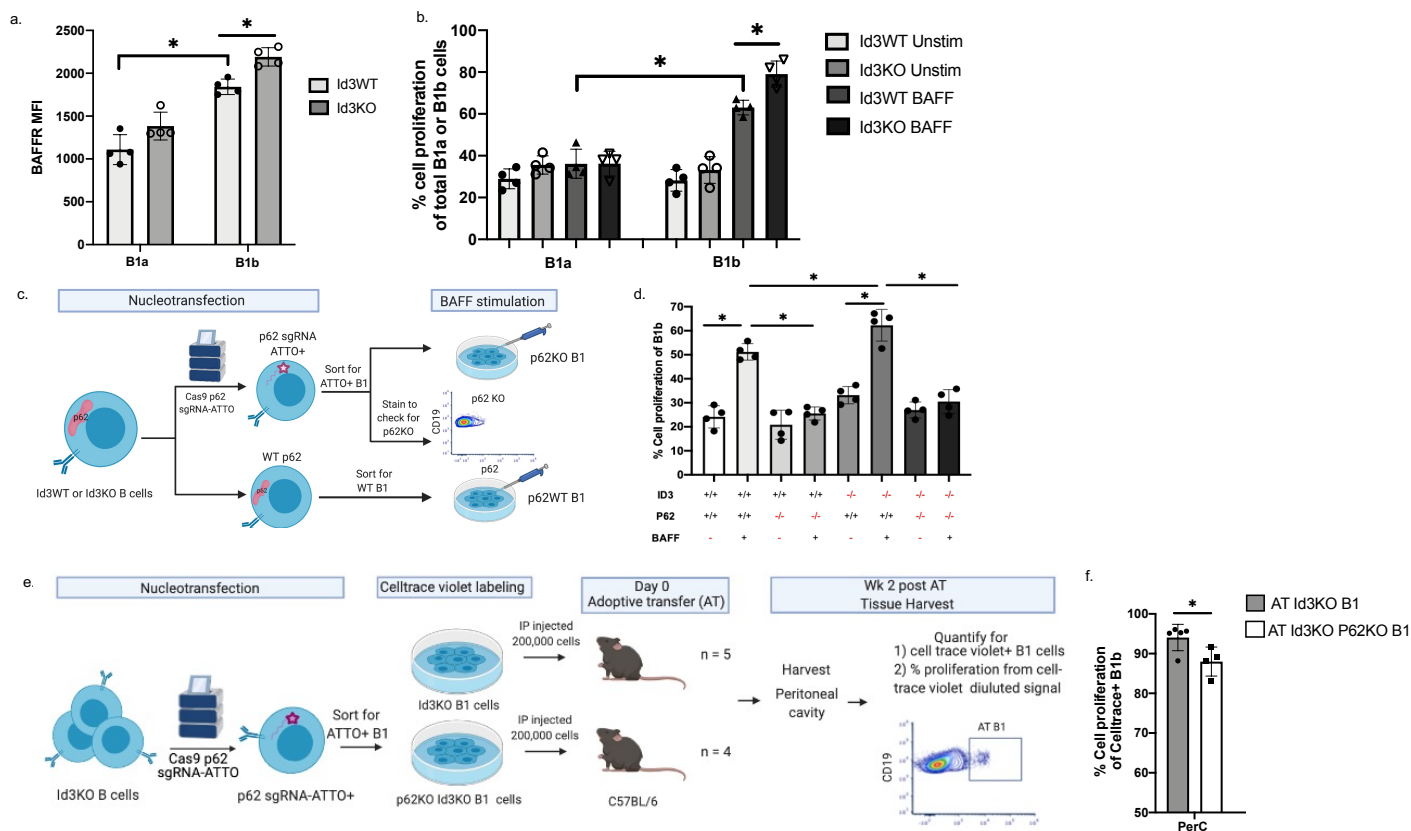


**Figure 3: Loss of p62 significantly reduces B1b cell proliferation *in vitro* and *in vivo*.**(a)

MFI of BAFFR in Id3WT and Id3KO B1a and B1b cells. (b) percentage of cell proliferation

measured by Celltrace-violet on Id3WT and Id3KO B1a and B1b cells under unstimulated and

BAFF stimulated conditions. (c) Schematics showing nucleofection of Cas9 p62 targeted gRNA

labeled with ATTO fluorophore ribonucleoprotein complex (p62-gRNA-RNP) into murine Id3WT

and Id3KO B cells following with sorting for ATTO+ B1 cells to select for p62KO B1 cells. (d)

Percentage of cell proliferation of Id3 WT and Id3KO B1b cells with conditional p62KO and

BAFF stimulation measured by Celltrace-violet. (e) Schematics showing nucleofection of p62-

gRNA-RNP into Id3KO B cells and sorting for ATTO+ B1 cells to select for p62KO B1 cells,

following with AT of Id3KO p62KO or Id3KO B1 cells into C57BL/6 to quantify proliferation of AT

cells in various tissue compartment 2 wks post AT. (f) Percentage of cell proliferation of AT



significantly greater p62 promoter activation compared to Id3WT (Figure 5b). To determine whether increased expression of E12 and E47 impact on p62 protein expression in human B cells, we cloned C-terminal flag-tagged E12 or E47 cDNA downstream of the CMV promoter in an expression plasmid and performed nucleofection with PBS or these constructs into sort-purified human B cells (Figure 5c). Flow cytometry of the flag + population for intracellular staining of p62 revealed significantly more p62 protein in the cells with E12 and E47 overexpressed compared to PBS control (Figure 5d).

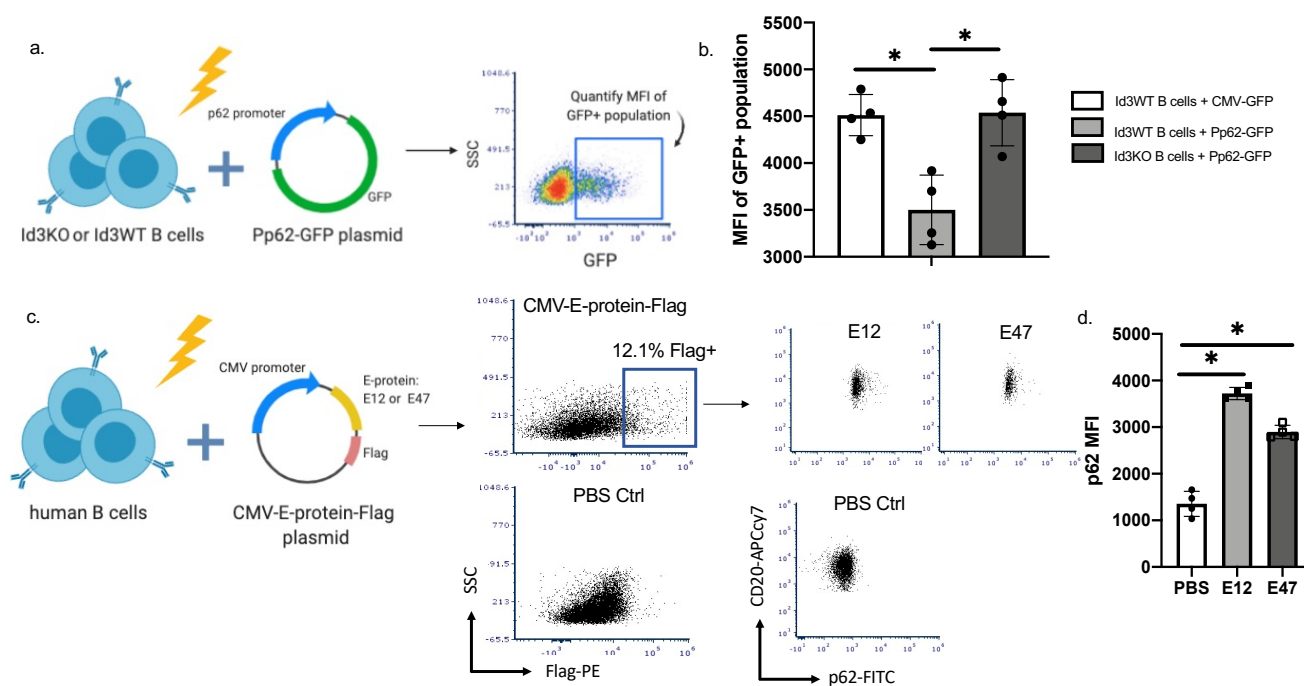


**Figure 5: Loss of Id3 and increased expression of E12 and E47 promote p62 promoter activation. (a)** Schematics showing nucleofection of p62 promoter GFP plasmid (Pp62-GFP) or CMV-GFP plasmid control in murine Id3 WT or Id3 KO B cells to quantify GFP expression. **(b)** MFI of GFP+ B cells to compare GFP expression between Id3WT B cells transfected with CMV-GFP control, Id3WT B cells transfected with Pp62-GFP and Id3KO B cells transfected with

Pp62-GFP. **(c)** Schematics demonstrating nucleo-transfection CMV-E12-Flag and CMV-E47-Flag plasmids into human B cells to measure p62 expression driven by overexpression of E-protein. **(d)** MFI of p62 compared across PBS control, CMV-E12-Flag and CMV-E47-Flag transfection in human B cells. \* $p < 0.05$  by Mann-Whitney test.

### **BAFF-induced binding of p62 to TRAF6 in B1b cells, but not B1a cells, led to NF $\kappa$ B activation, upregulation of c-myc expression and cell proliferation**

While SQSTM1/p62 has been implicated in cellular proliferation in cancer cells, its role in BAFF-induced B cell proliferation is unknown. To identify potential p62 interacting proteins in B cells that may mediate p62-dependent BAFF-induced proliferation, a protein-protein interaction network analysis using DEGs obtained from our RNAseq data was performed. Through interaction network analysis, SQSTM1 was shown to interact with TRAF and TANK which are proteins involving in NF $\kappa$ B activation and cell proliferation (Figure 6a).

Flow cytometry demonstrated increased p62 protein in response to BAFF stimulation in B-1b but not B-1a cells from Id3KO and Id3WT mice. Notably, the BAFF-stimulated p62 protein expression was significantly greater in B-1b cells from Id3KO compared to Id3WT mice (Figure 6b). Moreover, consistent with RNAseq result, no difference in TRAF6 expression was observed between Id3KO and Id3WT mice in either B1a or B1b cells under unstimulated condition (Figure 6c). However, BAFF stimulation increased TRAF6 expression in B-1b but not B-1a cells and this increase was further augmented in Id3KO B1b cells (Figure 6c), suggesting that TRAF6 is an important mediator of BAFF-induced proliferation in B-1b cells. To test this hypothesis, we measured cell proliferation of B1b cells stimulated with BAFF in the presence and absence of

the TRAF6 inhibitor (TRAF6i, C<sub>17</sub>H<sub>17</sub>NO)<sup>69</sup>. BAFF-induced B1b cell proliferation was significantly reduced by the TRAF6i (Figure 6d).

To determine if p62 and TRAF6 interact in B-1b cells and if BAFF stimulation promotes this interaction, imaging flow cytometry was performed (Figure 6e). Under unstimulated conditions, colocalization of p62 and TRAF6 was observed in Id3WT B1b cells (score =  $1.34 \pm 0.28$ ). Consistent with our flow cytometry findings (Figure 6b), higher p62 expression was observed in Id3KO B1b cells, however the co-localization score (score =  $1.28 \pm 0.29$ ) was unchanged. In contrast, BAFF stimulation increased p62-TRAF6 colocalization (score =  $1.65 \pm 0.57$ ) particularly in B-1b cells from Id3KO mice (score =  $2.48 \pm 0.24$ ). The addition of the TRAF6i to the BAFF-stimulated Id3KO B-1b cells resulted in abrogation of BAFF-induced increase in p62-TRAF6 co-localization (score =  $1.62 \pm 0.54$ ).

To determine if p62-TRAF6 interaction impacts downstream NF $\kappa$ B signaling, we measured the endogenous NF $\kappa$ B inhibitor, IKBa, in B-1b cells with low (pink, co-localization score < 1.5) and high (white, co-localization score > 2)(Figure 6f). IKBa was observed at higher level in cells with low p62-TRAF6 co-localization (Figure 6g). Consistent with this finding, IKBa levels in BAFF stimulated B-1b cells were significantly reduced compared to unstimulated B-1b cells, and Id3KO B-1b cells demonstrated a further decrease compared to Id3WT (Figure 6g). BAFF stimulation increased c-myc expression in B-1b cells, an effect further increased in Id3KO mice (Figure 6h).

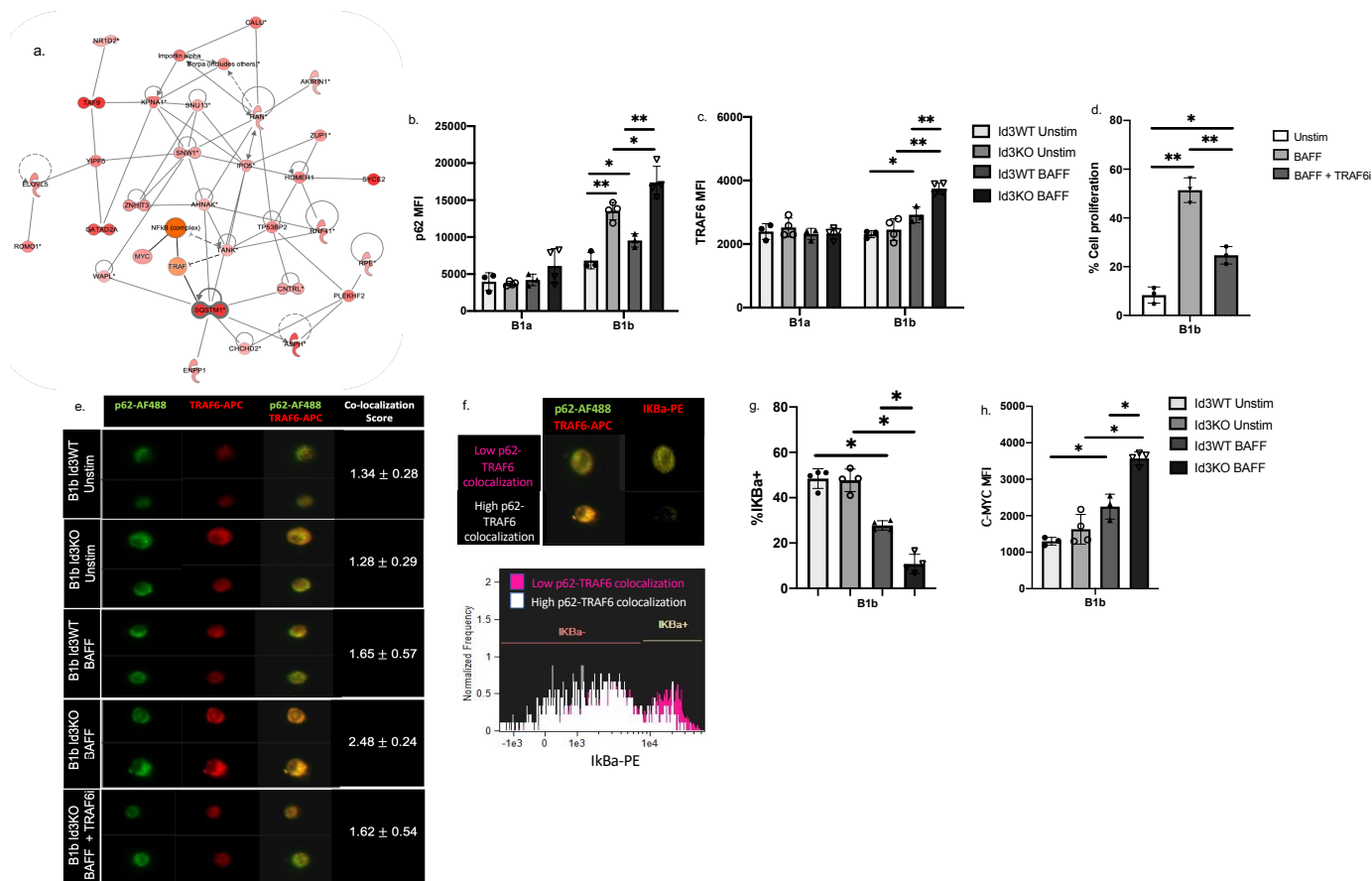


**Figure 6: BAFF induced binding of p62 to TRAF6 in B-1b, but not B-1a cells, leading to NFKB activation and upregulation of c-myc driven cell proliferation.** (a) protein interaction analysis indicated sqstm1/p62 interaction with proteins related to cell proliferation and cell cycle. (b-c) MFI of p62 (b) and TRAF6 (c) on Id3WT and Id3KO B1a and B1b cells under unstimulated and BAFF stimulated conditions. (d) percentage of *in vitro* cell proliferation of total B1b measured by Celltrace -violet under unstimulated, BAFF stimulated, and BAFF + TRAF6 inhibitor conditions. (e) Co-localization between p62 and TRAF6 on B1b cells under unstimulated, BAFF stimulated, and BAFF + TRAF6 inhibitor conditions quantified by imaging flow cytometry. (f) Representative images of IKBa degradation with low and high p62 and TRAF6 co-localization. (g) percentage of IKBa+ on Id3WT and Id3KO B1b cells under unstimulated and BAFF stimulated conditions. (h) MFI of c-myc on Id3WT and Id3KOB1b cells

under unstimulated and BAFF stimulated conditions. Results are represented with Mean  $\pm$  SEM with unpaired Mann-Whitney t-test. \* $p < 0.05$ , \*\* $p < 0.01$ .

### **Overexpression of p62 increased B-1b cell number and plasma IgM levels and reduced diet induced atherosclerosis**

We utilized a lentiviral system to overexpress GFP-p62 and GFP control in murine B1 cells. Equal numbers of the engineered cells were intraperitoneal injected into C57BL/6 WT mice. Hyperlipidemia was induced by tail vein injections of AAV8 D337Y PCSK9<sup>70</sup> and Western diet (WD) feeding (Figure 7a). After 8 weeks of WD, the number of GFP<sup>+</sup> B1b cells in the PerC of mice injected with GFP-p62-transduced cells was significantly higher than those injected with equal numbers of GFP control-transduced cells. (Figure 7b). Additionally, level of plasma total IgM was also significantly higher in the p62<sup>++</sup> group compared to control (Figure 7c) and significantly lower when p62 was knocked out of B1b cells from Id3KO mice (Figure 8) There was no difference in plasma total cholesterol levels ( $p = 0.47$ ) between p62<sup>++</sup> and p62 WT B1 groups (Figure 7d). Despite similar level of cholesterol, Sudan IV en face staining revealed less atherosclerosis in the p62<sup>++</sup> B1 group when compared to the p62WT B1 control group (Figure 7f).

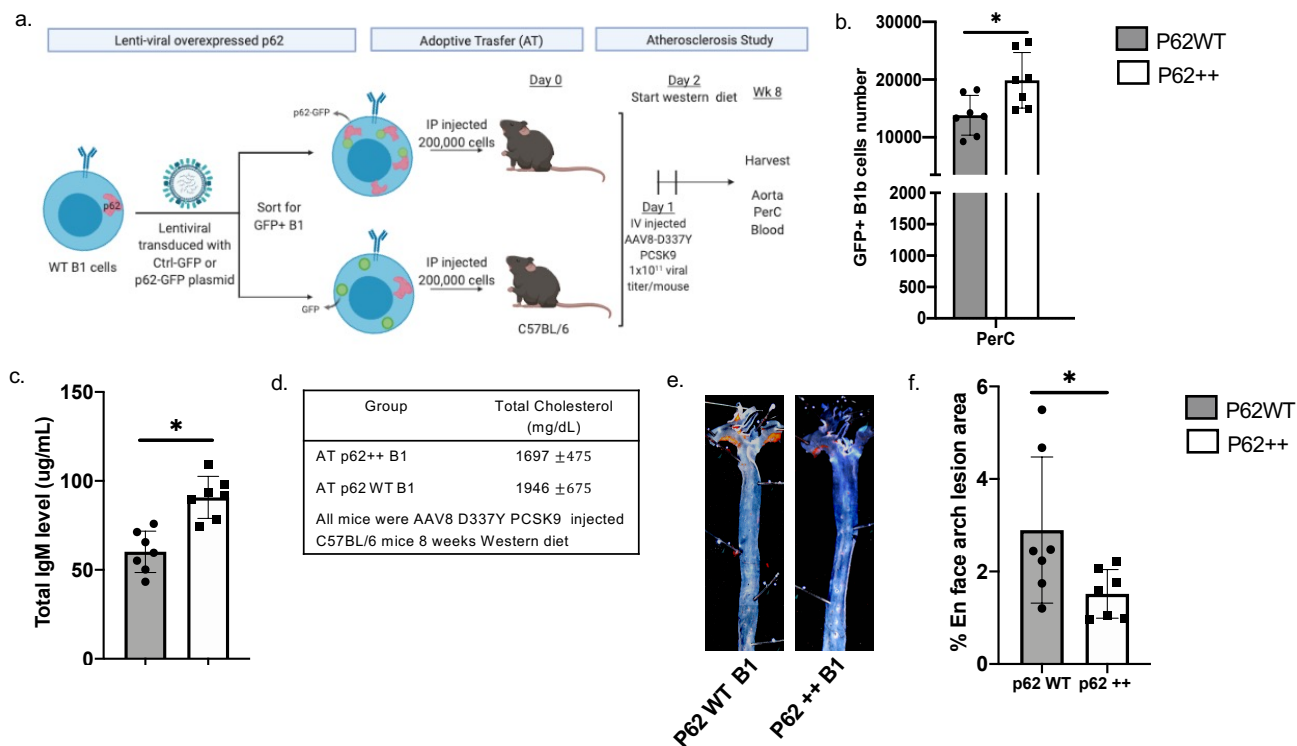


**Figure 7: Overexpression of p62 increased B-1b cell number and plasma IgM levels and reduced diet induced atherosclerosis. (a)** Schematics depicting lentiviral overexpression of p62-eGFP plasmid and GFP plasmid control in murine B cells following FAC sorting for eGFP+ B1 cells and adoptive transfer of p62-eGFP overexpressed B1 (p62++) or eGFP overexpressed B1 (p62 WT) into C57BL/6 host mice to perform diet induced atherosclerosis study. **(b)** Number of recovered GFP+ B1b post atherosclerosis study compared between p62++ and p62 WT groups. **(c)** Plasma total IgM level 8 weeks post-AT compared between p62++ and p62 WT groups measured by ELISA. **(d)** Plasma total cholesterol level compared between p62++ and p62 WT groups after 8 weeks western diet fed. **(e)** Images of en face stained plaque at aortic arch regions in p62++ B1 and p62WT B1 AT groups at the end of 8 weeks western diet fed. **(f)** Quantitative analysis of en face arch lesion area compared among p62++, p62 WT B1 groups. Statistical comparison was performed by using Mann-Whitney test and correlation analysis was performed by using Spearman correlation.

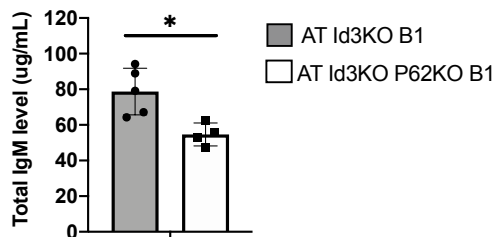


**Figure 8: Plasma total IgM level two weeks post transfer measured by ELISA obtained from AT of Id3KO (grey) and Id3KO p62KO (white) B1 cells into C57BL/6 host mice.**

**Human B1 cells from subjects with an ID3 SNP at rs11574, known to attenuate Id3 function, have increased p62 expression; a finding associated with B1 frequency and plasma IgM to MDA-LDL levels.**

Human missense polymorphism of ID3 rs11574 (A105T) has a reduced ability in dimerizing with its binding partners<sup>40</sup>. This human ID3 rs11574 SNP was also previously shown to be associated with an increased human B1 cell (CD20+CD27+CD43+) frequency and higher level of plasma IgM to MDA-LDL<sup>46</sup>. Here, we measured expression (MFI) of p62 in 58 CAD subjects with the homozygous major (GG, n = 36), heterozygous (AG, n = 17), and homozygous minor allele of ID3 rs11574 SNPs (AA, n = 5) otherwise matched for age, sex, and total cholesterol. Result demonstrated significantly higher p62 expression in human B1 cells (CD20+CD27+CD43+) in subjects with ID3 rs11574 homozygous minor allele when compared to the heterozygous, and homozygous major allele (Figure 9a). In addition, p62 expression directly correlated with the frequency of human B1 cells (Figure 9b) and plasma level of atheroprotective IgM specific to MDA-LDL in 58 CAD subjects (Figure 9c).

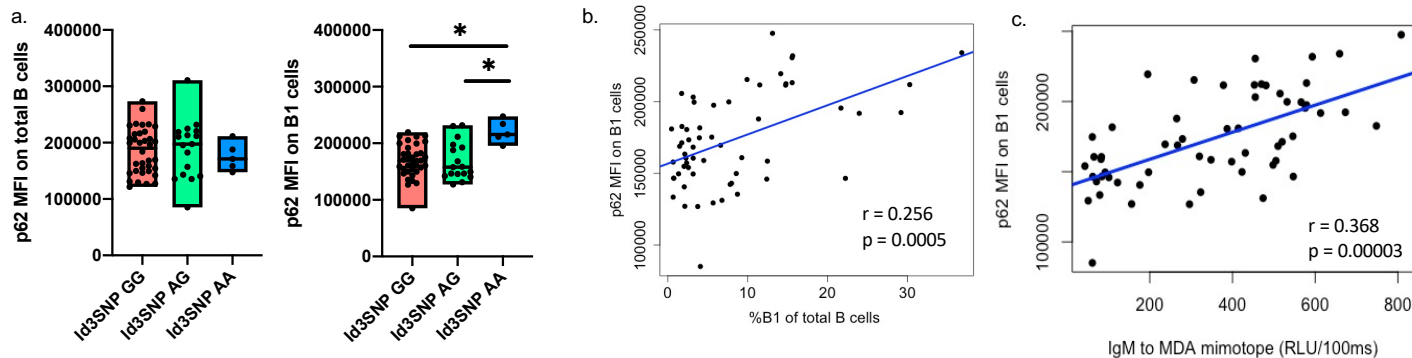


**Figure 9: Human B1 cells from subjects with an ID3 SNP at rs11574, known to attenuate Id3 function, have increased p62 expression; a finding associated with B1 frequency and plasma IgM to MDA-LDL levels. (a)** MFI of p62 within p62+ population in human total B and human B1 (CD27+CD43+) cells across major, heterozygous, and minor allele Id3 rs11574 SNP otherwise age and sex matched. **(b-c)** correlations between human B1 frequency **(b)** and IgM specific to MDL mimotope **(c)** with p62 expression. Statistical comparison was performed by using Mann-Whitney test and correlation analysis was performed by using Spearman correlation.

## Discussion

The B1b subtype of B1 cells has been shown to have unique features compared to B1a cells, allowing for prolonged protection from infection<sup>71</sup> and increased in vivo production of IgM that can block inflammation, protecting from diet-induced atherosclerosis<sup>35,72–75</sup>. Previous study by Rosenfeld et al<sup>46</sup> has demonstrated that loss of helix-loop-helix factor, Id3 in B cells results in an increase in B1b but not in B1a cell number and a reduction in atherosclerosis formation. Yet, the molecular and cellular mechanisms that allow Id3 to uniquely regulate B1b but not B1a cells are poorly understood. The present study provides the first evidence that Id3 is a key regulator of B1b cells self-renewal through a novel BAFF-p62-NFKB signaling pathway.

BAFF signaling is known to regulate self-renewal and development of total B cells through activation of NF $\kappa$ B<sup>76,77</sup>. Yet, whether or not BAFF promotes specifically B1 cells survival and proliferation still remains controversial. Schiemann et al have showed that BAFFR<sup>WT</sup> and BAFFR<sup>KO</sup> mice possess similar number of peritoneal B1 cells as well as B1a/B1b ratio<sup>78</sup>, while others<sup>79,80</sup> have demonstrated that BAFF might regulate B1 cells self-renewal through coupling with toll-like receptor activation. Additionally, Sage et al have utilized bone marrow transplant technique to show that the LDLR<sup>KO</sup> host mice with BAFFR<sup>KO</sup> bone marrow reconstitution has a decrease frequency of B1b and not B1a when compared to the wildtype transplant control suggesting that BAFF mediating B1 cell proliferation might be B1 cell subtype specific<sup>81</sup>. Here, we show that BAFFR is significantly expressed at higher level in B1b compared to B1a cells and BAFF stimulation augmented *in vitro* cell proliferation of B1b but not B1a cells. Interestingly, loss of Id3 also leads to a significant increase BAFFR expression in B1b cells which allows BAFF to drive higher proliferation of Id3<sup>KO</sup> B1b cells compared to Id3<sup>WT</sup> B1b cells. However, future study is still needed to further explore how loss of Id3 leads to an increase in BAFFR expression.

Not only that BAFF signaling is important in driving B1b cell proliferation, our results also suggest that BAFF induced B1b cell proliferation is p62 dependent. p62 is a scaffold and ubiquitination protein that has been widely known in its role in selective autophagy and cancer cell proliferation<sup>82,83</sup>. Prior literatures also have demonstrated that p62 promotes proliferation through binding to TRAF6 and activates NF $\kappa$ B signaling once cells were stimulated with interleukin-1 (IL-1), RANK ligand (RANKL) and nerve growth factor (NGF)<sup>51,52,84</sup>. Here, we are the first to show that BAFF can activate binding between p62 and TRAF6 in B1b cells which further mediate NF $\kappa$ B signaling. NF $\kappa$ B signaling in B cells is known to drive expression of c-myc and subsequent proliferation<sup>85</sup>. We investigate c-myc expression in B1b cells and discover that

BAFF drives expression of c-myc in B1b cells regardless of the presence of Id3, while loss of Id3 augmented C-myc expression. This c-myc expression pattern in B1b cells is also similar to NFkB activation pattern measured by the decrease of IKBa level. These findings altogether suggest that p62 potentially drives B1b cell proliferation through binding with TRAF6, activates NFkB, and enhances pro-proliferative c-myc gene expression.

In addition to identifying a novel role of p62 in mediating BAFF signaling driven B1b cell proliferation, we also discover a regulatory function of Id3 in inhibiting p62 expression. p62 expression has been previously shown to be induced by a bHLH-zipper family transcription factor, TFEB<sup>55,86</sup>. As Id3 and E2A are also bHLH proteins, we evaluate roles of Id3 and E2A in regulating expression of p62. Our results demonstrate that not only TFEB bHLH protein can activate p62 expression, but also E2A bHLH proteins. Overexpression of E2A proteins, E12 and E47, drive endogenous expression of p62 in human B cells as well as Id3 can suppress expression of gene downstream of p62 promoter. This discovery offers a mechanism underlined a relationship between loss of Id3 and an increase in B1b cell number observed by Rosenfeld et al, which potentially through disinhibition of E2A from Id3 deletion allowing E2A to drive p62 expression and further mediates B1b cell proliferation.

As B1b cells are the main producers of atheroprotective IgM *in vivo* and p62 is now demonstrated to mediate B1b cell proliferation, we explore the roles of p62 in mediating atherosclerosis. Sergin et al discovered that p62 facilitates clearance of inclusion body from the macrophage, lowering transformation of macrophage into foam cells, resulting in reduction in plaque burden in mice<sup>50</sup>. Yet, roles of p62 in B cell mediated atherosclerosis have never been explored. Here, we provide the first evidence that overexpression of p62 in B1 cells drove proliferation of peritoneal B1b cells, increased plasma level of IgM, and lower plaque level at

aortic arch region in hyperlipidemic mice. Taken together atheroprotective roles of p62 in both macrophages and B1 cells, p62 is poised to be a promising target for atherosclerosis treatment. However, future studies on roles of p62 in other B cell subtypes such as B2 cells as well as other immune cell types should also be investigated.

To further extrapolate our findings to human, we utilized a human CAD cohort to explore relationships among p62 expression, Id3, B1 cells, and atheroprotective IgM production. While atheroprotective roles of murine B1 cells have been well established, identification of human equivalent B1 cells has been challenging. Griffin et al identified CD20+CD27+CD43+ B cells as putative human B1 cells due to their spontaneous IgM production<sup>87</sup> Here, we demonstrated that humans homozygous for a function-impairing single nucleotide polymorphism (rs11574) in the ID3 gene had increased p62 expression in CD20+CD27+CD43+ B1 cells, and this p62 expression was also associated with B1 cell frequency and circulating levels of IgM to MDA-LDL. This human relationships among p62 expression, Id3 function, B1 cell number, and plasma level of IgM to MDA-LDL are similar to what we discover in murine B1b cells indicating the possibility of human putative B1 to behave more similarly to murine B1b rather than B1a cells. Additionally, this discovery is also in consistent with prior publication indicating increased number of human B1 in subjects with Id3 rs11574 SNP yielding higher IgM to MDA-LDL production<sup>46</sup>.

In summary, this report provides a novel insight on mechanism of how BAFF and p62 regulates cell proliferation in B1b cells as well as unfolds a relationship between Id3 and p62. It also highlights a significance of p62 in atherosclerosis and emphasizes on need of better understanding of p62 in different immune cell subtypes. Our initial findings in human CAD subjects coupled with murine mechanistic study underscore need for a larger study to

investigate a relationship between p62 expression in human putative B1 cells and cardiovascular endpoints.

## **Chapter 4**

**CD24 promotes human B cell CCR6-mediated splenic trafficking and IgM production, limiting vascular inflammation and coronary artery disease severity.**

## Abstract

**Background:** Atherosclerosis is a chronic inflammatory disease and B cells have emerged as important immune cells in modulating atherosclerosis. IgMs that inactivate oxidation specific epitopes (IgM<sup>OSE</sup>) on phospholipids such as low-density lipoprotein (LDL) were shown to confer athero-protection in human. Yet, the subset of human B cells responsible for production of IgM<sup>OSE</sup> as well as mechanisms regulating IgM production remain elusive.

**Methods:** Peripheral blood mononuclear cells (PBMCs) from healthy donors and subjects with coronary artery disease (CAD) undergoing quantitative coronary angiography were used to perform high dimensional analysis, including mass cytometry, bulk RNAseq, and single cell multi-omics sequencing (CITESeq), to identify and characterize human B cell subtype(s) responsible for IgM<sup>OSE</sup> production. *In vitro* and *in vivo* studies using CRISPR/Cas9 genome editing, adoptive transfer, and <sup>18</sup>F-fluorodeoxyglucose-positron emission tomography (FDG-PET) imaging in humanized mice model were performed to investigate mechanisms underlined IgM<sup>OSE</sup> production and their effects on vascular inflammation.

**Results:** CD20<sup>+</sup>CD27<sup>+</sup>IgM<sup>+</sup> cells (B<sup>27+</sup>IgM<sup>+</sup>) spontaneously produced IgM and IgM<sup>MDA-LDL</sup> in response to MDA stimulation when injected into humanized mice; an effect significantly augmented in B<sup>27+</sup>IgM<sup>+</sup> cells with high expression of CD24 (B<sup>27+</sup>IgM<sup>+</sup>CD24<sup>hi</sup>). CD24 expression also enhanced splenic and bone marrow trafficking of B<sup>27+</sup>IgM<sup>+</sup> cells. Blocking CD24 with a mAb reduced CCR6 expression, increased CCL20-induced CCR6 internalization and impaired migration to the spleen leading to lower IgM production. Treatment of CD24 mAb in hyperlipidemic humanized mice reduced number of B<sup>27+</sup>IgM<sup>+</sup>CD24<sup>hi</sup> in the spleen, lowered IgM level, and enhanced vascular inflammation. Lastly, CITESeq of PBMCs from 60 CAD subjects

revealed enhanced CCR6 and IgM signaling in B<sup>27+IgM+CD24<sup>hi</sup></sup> cells in subjects with low compared to high CAD severity.

**Conclusions:** Identification of IgM<sup>OSE</sup>-producing cells and CD24 as a receptor highly regulates IgM production holds promise for a future development of immunotherapy to enhance production of IgM<sup>OSE</sup> and protect against atherosclerosis. Additionally, short-term evaluation of CD24 mAb treatment, a cancer immunotherapy, highlights a potential adverse effect on vascular inflammation.

## Introduction

Oxidized phospholipids (OxPL) and their secondary lipid peroxidation-derived adducts, known as oxidation specific epitopes (OSE), are formed in inflamed tissues, such as atherosclerotic lesions in the artery wall<sup>88-92</sup>, and can mediate further tissue inflammation and damage<sup>6,91,93-95</sup>. B-1 cell-derived IgM that recognize and bind to these OSE can block their pro-inflammatory effects<sup>34,96</sup>. Epidemiological studies in humans clearly demonstrate that levels of IgM to the OSE malondialdehyde-modified low density lipoprotein (MDA-LDL) are inversely associated with coronary artery disease severity and cardiovascular events such as heart attacks and death<sup>16,33,34,36,93,97</sup>. Immunostaining and *in vivo* imaging techniques reveal MDA-LDL as a dominant neoepitope in atherosclerotic plaques<sup>98,99</sup>. In mice, IgM to MDA-LDL (IgM<sup>MDA-LDL</sup>) is produced by both subtypes of atherosclerosis-attenuating B-1 cells (B-1a and B-1b)<sup>46,100</sup>. While a putative human B-1 cell that spontaneously produces IgM has been reported, the cellular source of IgM<sup>MDA-LDL</sup> in humans is unknown.

To identify the human B cell subtype(s) that produce IgM<sup>MDA-LDL</sup>, mass cytometry (CyTOF) using a customized panel containing both established human B cell subtype markers and chemokine

receptors known to regulate murine B-1 IgM<sup>MDA-LDL</sup> production and B cell-mediated atheroprotection<sup>100,101-102</sup> was performed on purified B cells from human subjects with high versus low plasma levels of IgM<sup>MDA-LDL</sup>. This unbiased approach along with further *in vivo* characterization allowed not only identification of human B cell subtypes uniquely marked by CD27 and IgM co-expression as subtypes producing IgM<sup>MDA-LDL</sup>, but also the discovery of a novel role for CD24. Notably, the GPI-anchored sialoglycoprotein, CD24, has emerged as a key treatment for SARS-CoV2 and a target for cancer immunotherapy (Trial NCT04317040, <sup>103</sup>). Yet, anti-inflammatory role of CD24 on B cells nor its effect on cardiovascular disease has never been explored.

## Results

### **CytoTOF clustering identified two subsets of circulating human B cells that are associated with high plasma levels of IgM<sup>MDA-LDL</sup>**

A 24-antibody mass cytometry panel was used to subtype circulating B cells in 28 subjects with high plasma IgM<sup>MDA-LDL</sup> (n=14) and low plasma IgM<sup>MDA-LDL</sup> (n=14), otherwise matched for cardiovascular risk factors (CRF). Results of Self-Organizing Map clustering (FlowSOM)<sup>61</sup> and consensus clustering of CD19+ B cells identified 11 distinct clusters of B cells represented by non-linear embedding space using UMAP (Uniform Manifold Approximation and Projection, Figure 10a). Unexpectedly, cluster frequency analysis revealed one individual with a markedly expanded B cell cluster (CD20+CD27+CD25hi) not seen in any other subject (Figure 10b).

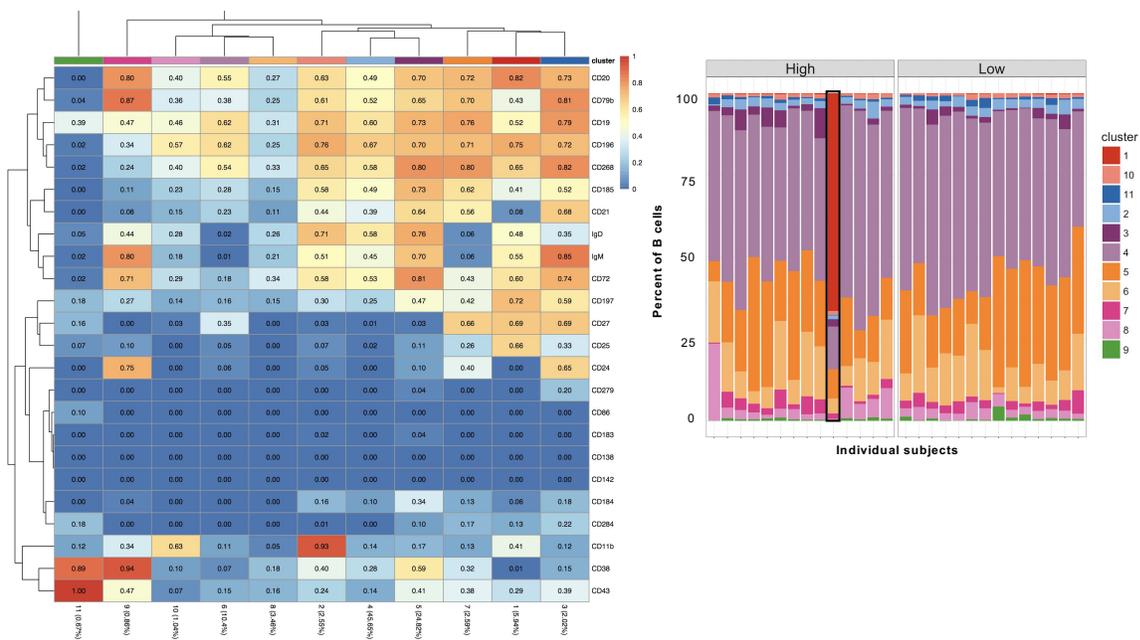


**Figure 10: Unsupervised metalouvain clustering of CD19<sup>+</sup> B cells obtained from 28 subjects with high and low plasma levels of IgM to MDA-LDL (n = 14 high IgM and n = 14 low IgM). Clustering result indicates 11 distinct clusters with a subject from high IgM to MDA-LDL group representing a potential clonal expansion of cluster 1 (CD20<sup>+</sup> CD25<sup>hi</sup> B cells).**

CD20<sup>+</sup>CD27<sup>+</sup>CD25<sup>hi</sup> B cells are a special type of B cell with low capability for immunoglobulin secretion but efficient antigen presentation with potential roles in autoimmune diseases<sup>104,105</sup>.

Due to the clearly aberrant nature of this subject's B cell pool, they were excluded from further analysis. FlowSOM clustering analysis was re-performed on the remaining 27 CRF-matched subjects with high (n=13) and low (n=14) plasma IgM<sup>MDA-LDL</sup> (Figure. 11a). Notably, subjects with high IgM<sup>MDA-LDL</sup> also had significantly more IgM to an MDA-LDL mimotope, phosphoryl choline (PC)-BSA (IgM<sup>PC-BSA</sup>), O<sub>x</sub>CE (IgM<sup>O<sub>x</sub>CE</sup>) (Table 6).

	High IgM <sup>MDA-LDL</sup> group	Low IgM <sup>MDA-LDL</sup> group	p-value
IgM to MDA mimotope	2335 ± 2533.35	537 ± 294.14	0.0238*
IgM to PC-BSA (RLU/mL)	19388 ± 21798	4955 ± 2635	0.006*
IgM to OxCE (RLU/mL)	6672 ± 2481	3075 ± 1357	0.0002*
IgG to PC-BSA (RLU/mL)	7676 ± 3647.26	7943 ± 4418.02	0.868
IgG to MDA-LDL (RLU/mL)	6258 ± 4347	5619 ± 6012	0.49

**Table 6: Differences in IgM and IgG to OSEs between high and low IgM<sup>MDA-LDL</sup> groups.**

Consistent with these findings, levels of plasma IgM<sup>MDA-LDL</sup> significantly correlated with both IgM<sup>PC-BSA</sup> and IgM<sup>OxCE</sup> levels (Figure 12). Measures of IgG to these same epitopes were not different between groups (Table 6). UMAP visualization of this clustering analysis indicates 11 distinct clusters (Figure. 11b). Cluster frequency analysis of these 27 subjects demonstrated comparable frequency of each cluster without marked clonal expansion (Figure. 11c). Each cluster was annotated based on expression of B cell markers represented in the heatmap (Figure. 11d). Of all the clusters, only clusters 1 and 8 had elevated frequency in subjects with high IgM<sup>MDA-LDL</sup> (Figure. 11e).

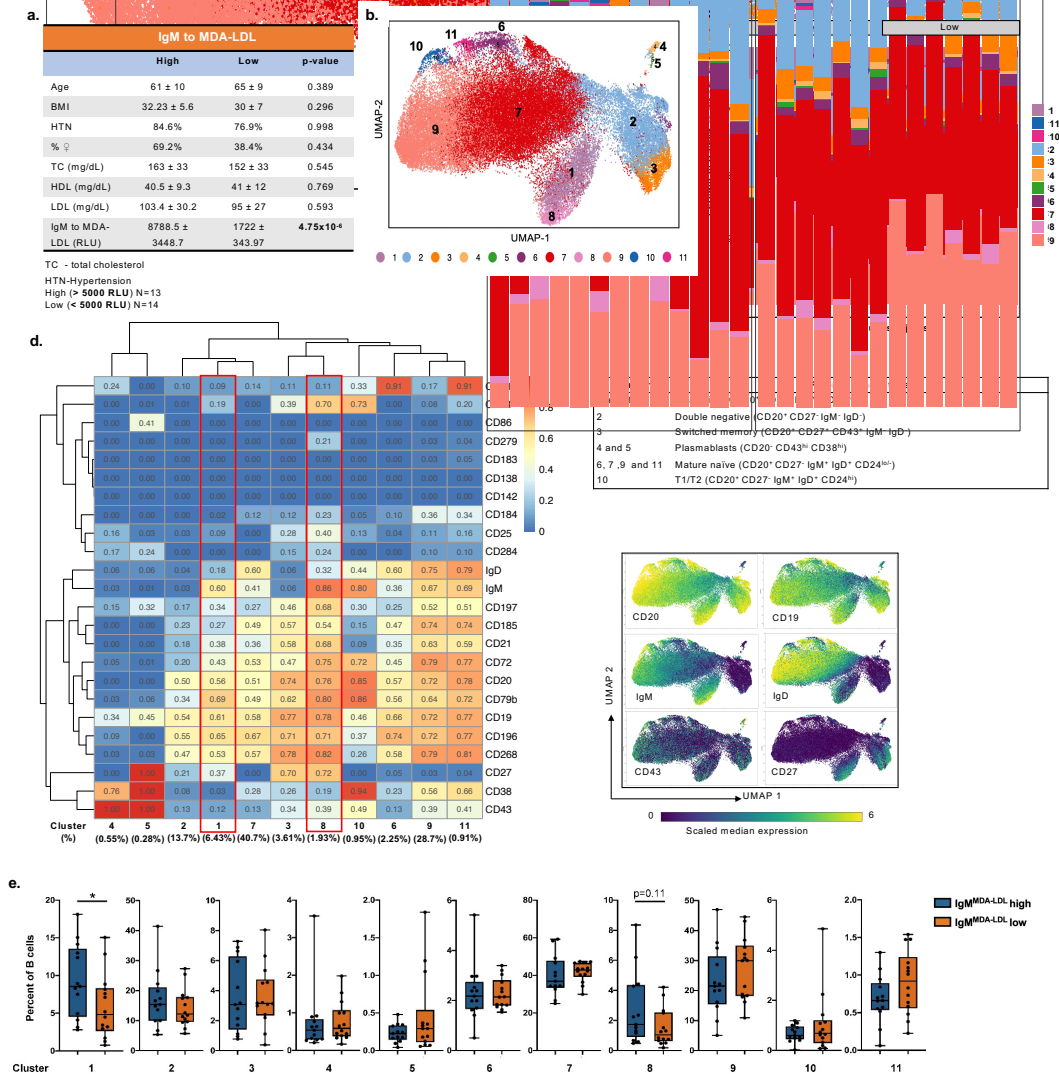


**Figure 11: Clusters 1 and cluster 8 uniquely express CD27<sup>+</sup>IgM<sup>+</sup> (B<sup>27+</sup>IgM<sup>+</sup>) and their frequency as a percentage of total B cells was higher in subjects with high levels of IgM specific to MDA-LDL. (a)** Cohort of 27 subjects with high (IgM to MDA-LDL>5000 RLU, n = 13) and low (IgM to MDA-LDL<5000 RLU, n = 14) IgM specific to MDA-LDL with matched age, BMI, hypertension (HTN), % female, total cholesterol (TC), HDL cholesterol and LDL cholesterol. **(b)** Representative metacluster UMAP showing 11 distinguished B cell subsets by using FlowSOM clustering and representative UMAP plots of distinguishing surface markers used for immunophenotyping B cell subsets. **(c)** Bar chart showing percentage of B cells in all subsets

for all donors colored as in metaclustering UMAP. **(d)** Heatmap showing median expression of 24 surface markers from metaclustering and potential phenotypes 11 B cell subsets. **(e)** Biaxial plots to compare frequency of each cluster as a percentage of total B cells in subjects with high and low IgM MDA-LDL.

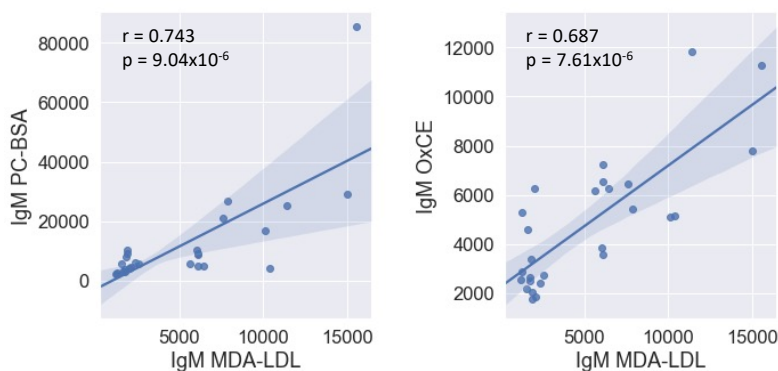


**Figure 12: Plasma level of IgM<sup>MDA-LDL</sup> strongly associates with Plasma level of IgM<sup>PC-BSA</sup> and IgM<sup>OxCE</sup>.**

Rainbow plots revealed that clusters 1 and 8 were the only clusters that were CD27<sup>+</sup>IgM<sup>+</sup>IgD<sup>+</sup>, which is a marker of innate IgM-producing B cells<sup>106</sup>. Clusters 1 and 8 were also CD43<sup>+</sup>, consistent with the human B-1 cell identified by Griffin et al.<sup>107</sup> (CD20<sup>+</sup>CD27<sup>+</sup>CD43<sup>+</sup>). However, high IgM<sup>MDA-LDL</sup> levels were only associated with the percentage of CD43<sup>+</sup> cells in cluster 1, not cluster 8 (Figure 13)

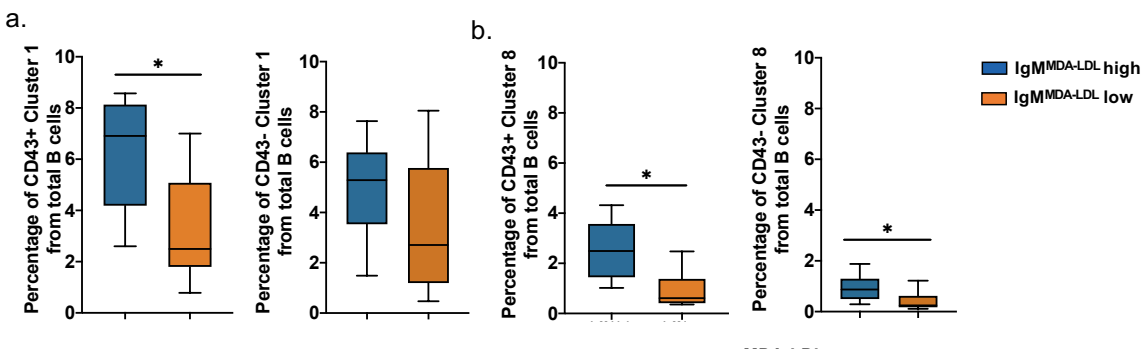


**Figure 13: Subjects with high plasma IgM<sup>MDA-LDL</sup> levels have higher frequencies of CD43+ cluster 1 compared to subjects with low plasma IgM<sup>MDA-LDL</sup> levels. a,** Biaxial plots to compare frequency of CD43+ and CD43- cluster 1 as a percentage of total B cells in subjects with high and low IgM<sup>MDA-LDL</sup>. **b,** Biaxial plots to compare frequency of CD43+ and CD43- cluster 8 as a percentage of total B cells in subjects with high and low IgM<sup>MDA-LDL</sup>.

### CD24 expression of Cluster 1 and 8 positively correlate with IgM<sup>OSE</sup>.

Notably, clusters 1 and 8 had similar surface marker expression with the exception of markedly different CD24 levels (Figure. 11d). Therefore, we compared CD24 expression levels, measured by geometric means (GM), on cluster 1 and 8 cells in subjects with low and high plasma IgM<sup>MDA-LDL</sup>. While levels were lower in cluster 1 than cluster 8, CD24 expression on both clusters were significantly higher in subjects with high compared to low IgM<sup>MDA-LDL</sup> (Figure. 14a). Correlation analysis demonstrated that CD24 expression on clusters 1 and 8 had a significant, direct association with plasma level of IgM<sup>MDA-LDL</sup> (Figure. 14b) and IgM to OxCE (IgM<sup>OxCE</sup>) (Figure. 14c) but not with IgG<sup>MDA-LDL</sup> (Figure 15). Adoptive transfer (AT) via intraperitoneally (IP) injecting equal numbers of vehicle or MDA-mimotope-stimulated human sort-purified B<sup>27+IgM+CD24lo/-</sup> and B<sup>27+IgM+CD24hi</sup> cells into NSG (B, T and functional NK cell-deficient) mice (Figure 14d) revealed

higher total and MDA-specific IgM in the  $B^{27+IgM+CD24hi-}$  compared to the  $B^{27+IgM+CD24lo/-}$ -injected mice (Figure. 14e & f).

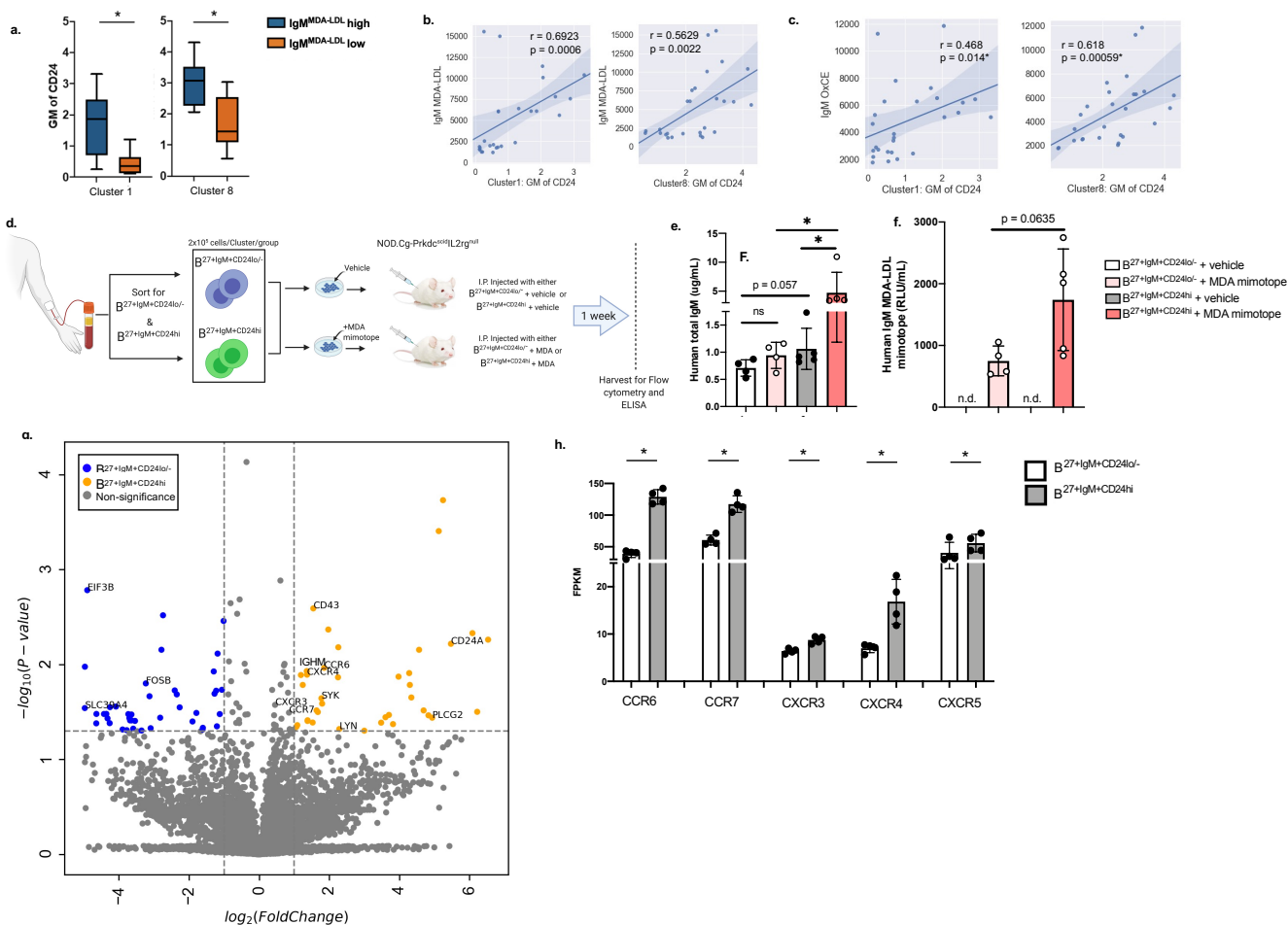


**Figure 14:  $B^{27+IgM+}$  with high CD24 expression produced IgM and  $IgM^{MDA-LDL}$  upon stimulation and has high expression of chemokine receptors. (a) Biaxial plots comparing GM of CD24 between low and high  $IgM^{MDA-LDL}$  groups within clusters 1 and 8. (b-c) Correlation between GM of CD24 on cluster 1 and 8 and the plasma IgM to MDA-LDL level (b) and the plasma IgM to OxCE level (c). (d) Schematics of  $B^{27+IgM+CD24lo/-}$  and  $B^{27+IgM+CD24hi}$  pre-treated with MDA-mimotope or vehicle control then adoptively transferred into humanized mice. (e-f), Plasma level of total human IgM (e) and IgM to MDA-mimotope (f) quantified by ELISA 1 week post transfer of either  $B^{27+IgM+CD24lo/-}$  or  $B^{27+IgM+CD24hi}$  with either MDA mimotope stimulation**

or vehicle control. (g) Volcano plot indicating 117 differentially expressed genes (FDR < 0.05) between  $B^{27+IgM+CD24^{lo/-}}$  (blue) and  $B^{27+IgM+CD24^{hi}}$  (orange) out of 7196 aligned genes ( $n = 4$  per group). (h) Quantitation of RNA expression of specific chemokine receptors comparing  $B^{27+IgM+CD24^{lo/-}}$  and  $B^{27+IgM+CD24^{hi}}$ . Data were analyzed by using Mann-Whitney Wilcoxon test. Values are mean  $\pm$  s.d. \* =  $p < 0.05$ .

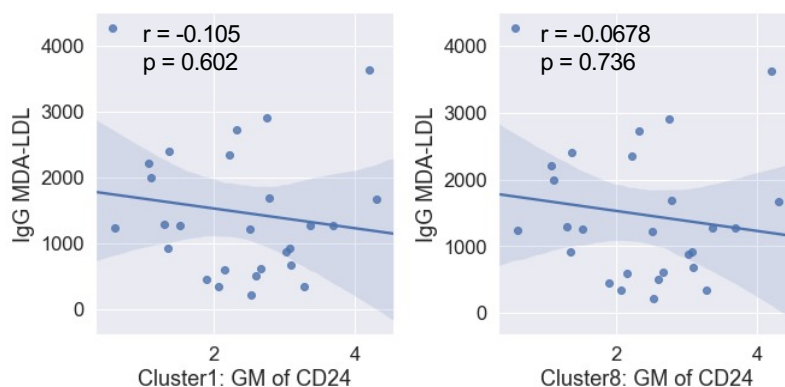


**Figure 15: GM of CD24 on clusters 1 and 8 does not associate with IgG to MDA-LDL.**

**RNA sequencing and pathway analysis comparing  $CD24^{lo/-}$  and  $CD24^{hi}$   $CD20^{+}CD27^{+}IgM^{+}$  ( $B^{27+IgM^{+}}$ ) cells revealed enrichment of pathways involved in migration and IgM production.**

As the CD24 levels on clusters 1 and 8 markedly enhanced their significant association with high levels of  $IgM^{MDA-LDL}$  and  $IgM^{OxCE}$ , we sort-purified the  $B^{27+IgM^{+}}$  cells into  $CD24^{lo}$  ( $B^{27+IgM+CD24^{lo/-}}$ ) and  $CD24^{hi}$  ( $B^{27+IgM+CD24^{hi}}$ ) (Figure 16) and compared the gene expression profiles by bulk RNAseq. Out of 7196 aligned genes, there were 117 genes differentially expressed (DE, FDR < 0.05 and  $\log_2FC > \text{or} < 1$ ) in  $B^{27+IgM+CD24^{hi}}$  compared to  $B^{27+IgM+CD24^{lo/-}}$  cells (Table 7).

**Table 7: DE genes compared between B<sup>27</sup>+IgM+CD24<sup>hi</sup> and B<sup>27</sup>+IgM+CD24<sup>lo/-</sup> cells**

Gene Names	FDR	Log2FC	Gene Names	FDR	Log2FC
HEATR5B	<0.001	-0.360	RPL29	0.034	4.830
ITGA6	<0.001	5.245	SLAMF7	0.036	3.604
ZYX	<0.001	5.123	ATP1A3	0.036	-4.062
IL10RB	0.001	1.607	NDUFC1	0.036	-2.821
EIF3B	0.002	-4.901	PLCG2	0.036	4.936
NAP1L1	0.002	-1.556	MTHFD1	0.037	-3.700
GTF2B	0.002	-1.814	OTULIN	0.037	-4.323
CD43	0.003	1.545	IGHV1-22	0.037	0.637
MAZ	0.003	-0.626	PSTPIP2	0.038	-0.574
ATF6	0.003	-2.741	AKT1	0.039	1.383
SUB1	0.003	-1.014	TFEB	0.039	-3.680
IL10RA	0.004	1.973	GOT2	0.039	-3.639
SQSTM1	0.005	6.084	JARID2	0.039	-3.540
MYL12A	0.005	6.530	IL6ST	0.039	1.380
CD24A	0.006	5.470	SUPT16H	0.040	-1.900
ARFIP2	0.007	2.259	PLRG1	0.041	1.527
RPS24	0.007	-2.786	PDCD1	0.041	3.481
TNFRSF17	0.007	4.562	MAN1A2	0.041	-0.653
ELL2	0.008	-1.184	WRN	0.041	-0.568
CCSER2	0.009	-0.860	LASP1	0.042	-4.262
BLNK	0.010	-0.412	USP7	0.042	-4.644
NFKB1	0.010	0.725	ATP6V0B	0.042	3.819
EIF1B	0.010	0.708	IGHV1-82	0.043	0.424
SLC35E4	0.011	-4.968	TRAF5	0.044	1.089
CCR6	0.011	1.855	CCR9	0.044	0.476
SIGLEC10	0.012	1.360	TLR9	0.045	1.204
HMGB1	0.012	1.294	CD20	0.045	1.062
ELF4	0.012	-0.366	TNFRSF8	0.046	-1.604
CD27	0.012	0.691	UPB1	0.047	-3.094
DUSP6	0.012	4.281	TNFSF2	0.047	0.477
CXCR4	0.013	1.367	PPP1CA	0.047	-3.590
IGHM	0.013	1.192	LYN	0.048	2.287
TUBGCP3	0.013	3.977	IGHV1-72	0.048	0.871
RNU6-811P	0.014	0.786	COX6B1	0.048	-3.894
TGFBI	0.014	2.251	TLR4	0.048	1.610
KLF2	0.015	-0.797	CD21	0.048	0.984
FOSB	0.016	-3.231	CD1C	0.049	1.418
NFKB2	0.016	0.615	CD40	0.049	3.775
ITGAM	0.016	4.299	TRAF2	0.049	0.604
BRIX1	0.016	1.245	CD23	0.050	-3.353
LBR	0.018	-1.062	CNN3	0.050	3.000
CRNKL1	0.019	0.372			
HP1BP3	0.019	-2.406			
STAT3	0.019	1.225			
IGHV1-26	0.020	0.824			
MAPK3	0.020	1.272			
MKRN1	0.021	-2.348			
SETDB2	0.021	-0.879			
NUP188	0.022	-3.126			
PTPN6	0.022	4.342			
SYK	0.023	1.777			
ARL2	0.026	-0.646			
IGHV1-64	0.026	1.797			
CXCR3	0.027	0.455			
PCID2	0.028	-4.082			

\* FC is fold change of B<sup>27</sup>+IgM+CD24<sup>hi</sup> / B<sup>27</sup>+IgM+CD24<sup>lo/-</sup>

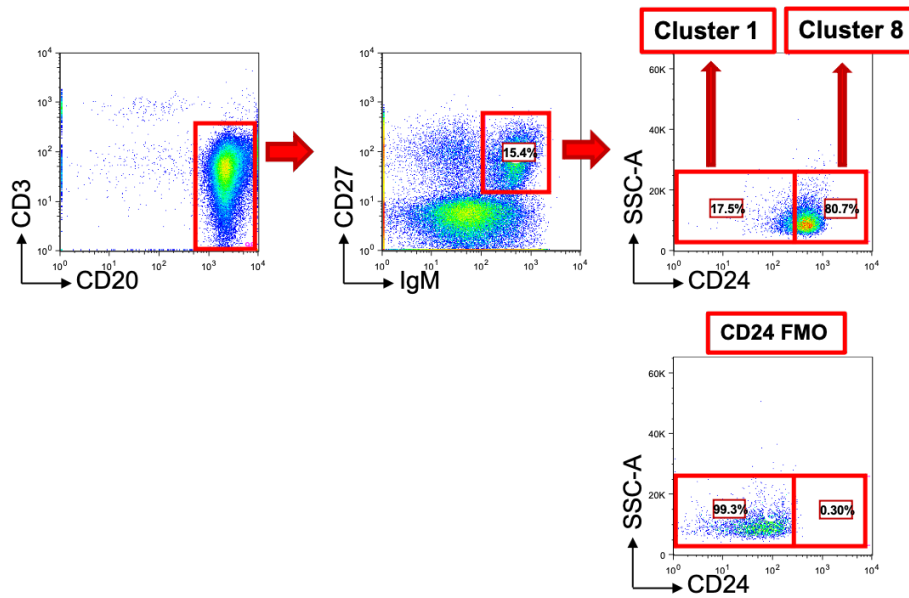


**Figure 16: Sorting strategy for clusters 1 and 8.** Human PBMCs were enriched for B cells and sorted for CD20<sup>+</sup>CD27<sup>+</sup>IgM<sup>+</sup>CD24<sup>lo</sup> for cluster 1 and CD20<sup>+</sup>CD27<sup>+</sup>IgM<sup>+</sup>CD24<sup>hi</sup> for cluster 8.

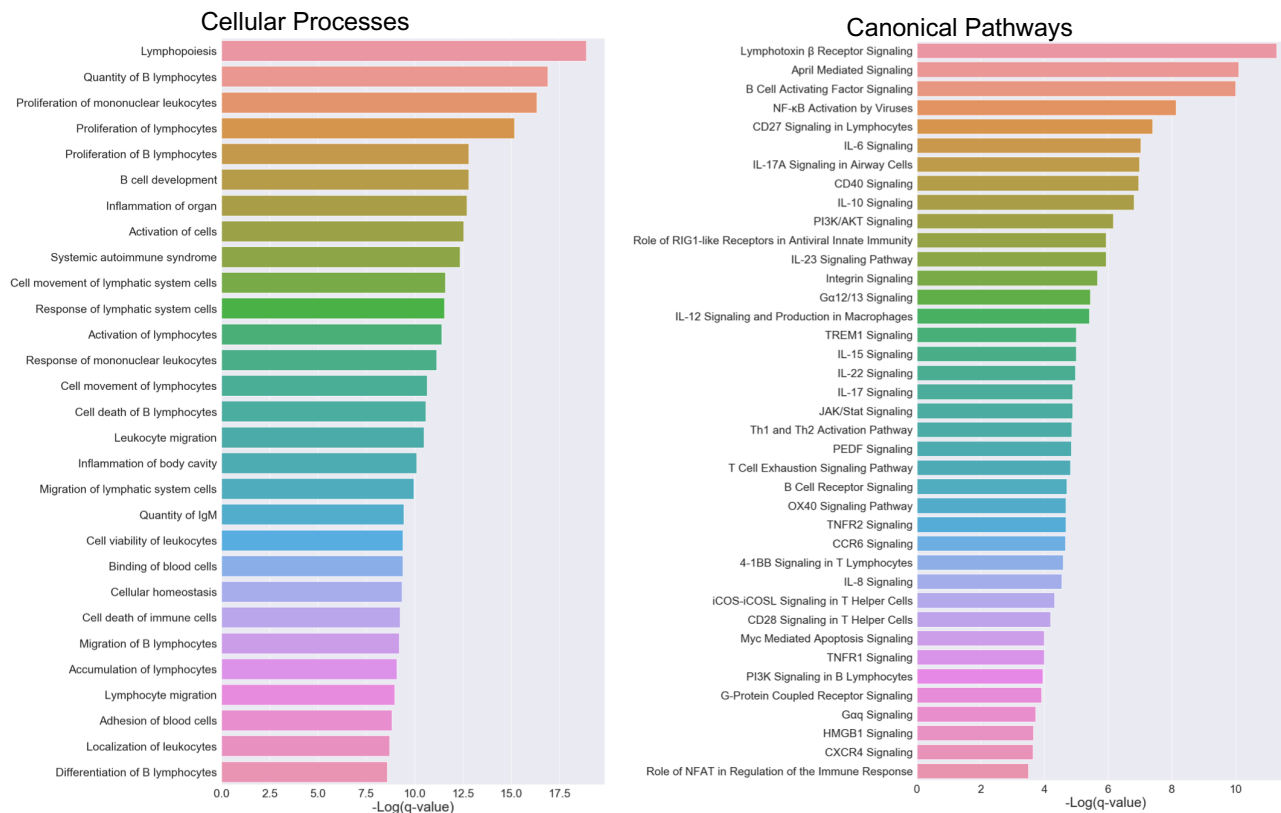


**Figure 17: Pathway analysis to identify upregulated pathways in sort purified  $B^{27+IgM+CD24hi}$ . Top 30 cellular processes (a) and top 40 canonical pathways (b) (ranked by z-score) enriched in  $B^{27+IgM+CD24hi}$  compared to  $B^{27+IgM+CD24lo/-}$ .**

The annotated volcano plot (Figure. 14g) highlights increased expression of chemokine receptors, such as CCR6 and CXCR4, as well as IgM and signals downstream of the BCR (LYN, SYK, PLC $\gamma$ 2) in  $B^{27+IgM+CD24hi}$  compared to  $B^{27+IgM+CD24lo/-}$  cells. Ingenuity Pathway analysis of DE genes identified processes such as lymphocyte survival/proliferation, migration and IgM production (Figure. 17a) and canonical pathways predominated by cytokine, chemokine and BCR signaling (Figure. 17b) as more highly expressed in  $B^{27+IgM+CD24hi}$  compared to  $B^{27+IgM+CD24lo/-}$  cells. Quantified RNA expression of CCR6, CCR7, CXCR3, CXCR4 and CXCR5 showed

elevated expression of these chemokine receptors in  $B^{27+IgM+CD24hi}$  compared to  $B^{27+IgM+CD24lo/-}$  with CCR6 demonstrating the highest fold difference (Figure. 14h).

### $B^{27+IgM+CD24hi}$ cells have characteristics of circulating splenic MZB cells

IP injection of equal numbers of  $B^{27+IgM+CD24lo/-}$  and  $B^{27+IgM+CD24hi}$  cells into NSG mice (Figure. 18a) revealed no significant difference in cell number in the peritoneal cavity (PerC) but significantly more  $B^{27+IgM+CD24hi}$  cells in the spleen and bone marrow compared to  $B^{27+IgM+CD24lo/-}$  cells 7 days later (Figure. 18b). Additionally, a higher percentage of  $B^{27+IgM+CD24hi}$  than  $B^{27+IgM+CD24lo/-}$  cells were induced by MDA-mimotope stimulation to express CD138 (Figure. 18c), suggesting that CD24 promotes antigen-induced plasma cell differentiation. Consistent with these findings, flow cytometry further identified  $B^{27+IgM+CD24hi}$  cells as  $CD21^{mid}CD23^{lo/-}CD1c^+$ , similar to MZB cells<sup>106,108</sup> (Figure. 18d&e).

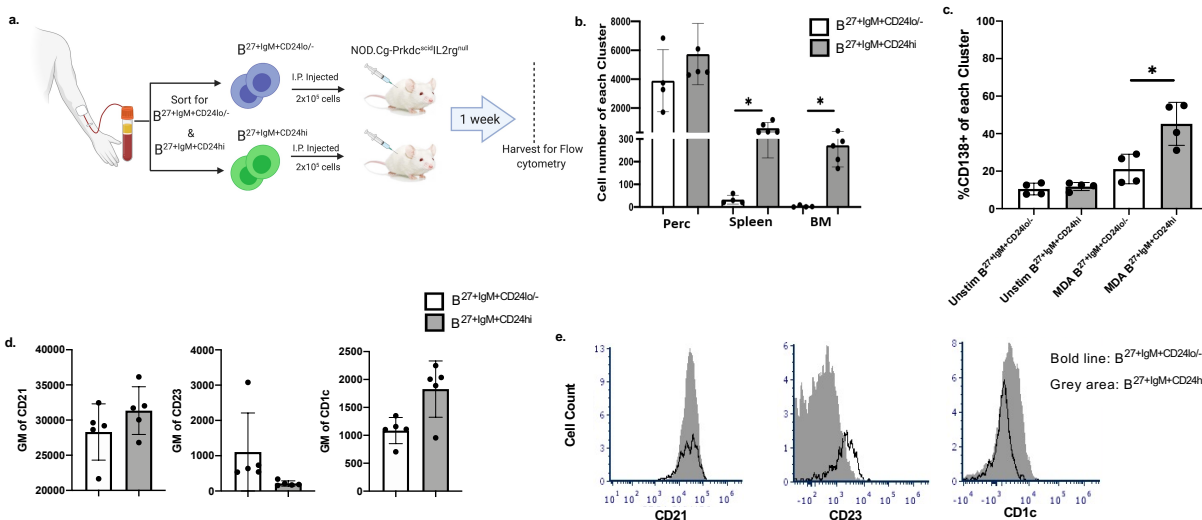


**Figure 18:  $B^{27+IgM+CD24hi}$  cells have characteristics of circulating MZ B cells. (a)** Schematics of adoptive transfer for trafficking studies. **(b)** Cell numbers of transferred  $B^{27+IgM+CD24lo/-}$  and  $B^{27+IgM+CD24hi}$  recovered from peritoneal cavity, spleen and bone marrow 1 week post adoptive

transfer. **(c)** %CD138<sup>+</sup> of B<sup>27+IgM+CD24lo/-</sup> and B<sup>27+IgM+CD24hi</sup> after 24 hrs of unstimulated and MDA-mimotope-stimulated conditions. **(d-e)** GM **(d)** and histogram of one representative healthy donor **(e)** of surface CD21, CD23, and CD1c expression on B<sup>27+IgM+CD24lo/-</sup> and B<sup>27+IgM+CD24hi</sup>. Data were analyzed using Mann-Whitney Wilcoxon test. Values are mean ± s.d.

### **CD24 helps stabilize CCR6 surface expression by inhibiting CCL20-induced CCR6 internalization**

As CCR6 was identified as the most enriched chemokine receptor RNA in B<sup>27+IgM+CD24hi</sup> when compared to B<sup>27+IgM+CD24lo/-</sup> (Figure. 14h), we performed linear regression analysis on our CyTOF data to determine the association between CD24 and specific chemokine receptors on the surface of B<sup>27+IgM+CD24hi</sup>. Of those analyzed, CCR6 was the only chemokine receptor that significantly, directly correlates with CD24 expression (Figure. 19a).

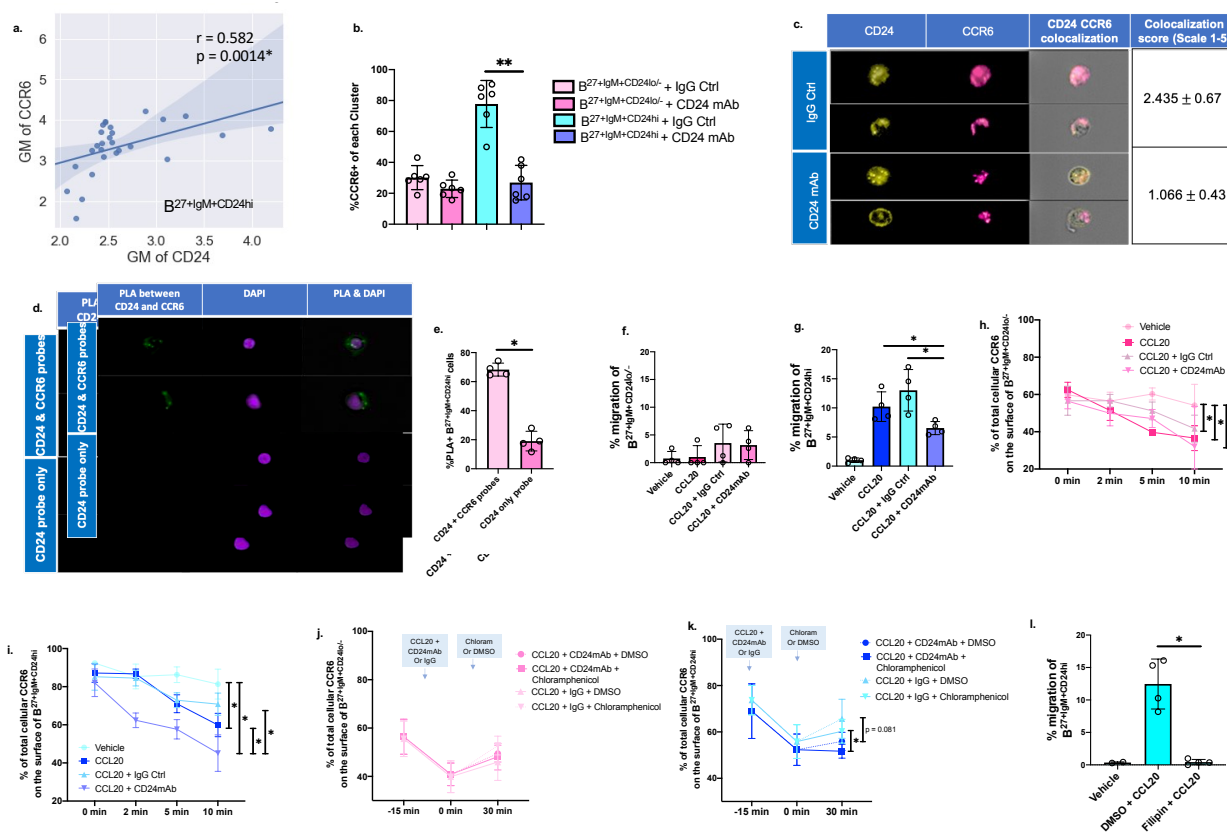


**Figure 19: CD24 reduces CCL20-induced CCR6 internalization and promotes  $B^{27+IgM+CD24hi}$  migration. (a)** Linear regression plots with Spearman correlations between GM of CD24 and GM of CCR6 on  $B^{27+IgM+CD24hi}$  obtained from CyTOF panel. **(b)** Percentage of CCR6+ cells on  $B^{27+IgM+CD24lo/-}$  and  $B^{27+IgM+CD24hi}$  treated with CD24 mAb or IgG isotype control for 12 hrs *in vitro*. **(c)** Visualization and quantitation of CD24 and CCR6 colocalization on  $B^{27+IgM+CD24hi}$  cells by using imaging flow cytometry after 1 hr treatment with either CD24 mAb or IgG isotype control. **(d)** Representative images of CD24 and CCR6 protein interaction on  $B^{27+IgM+CD24hi}$  cells using PLA assay visualized by imaging flow cytometry. **(e)** Quantitative analysis of CD24 and CCR6 interaction on  $B^{27+IgM+CD24hi}$  cells measured by %PLA+ cells of total  $B^{27+IgM+CD24hi}$  cells. **(f-g)** Percent of *in vitro* migration of  $B^{27+IgM+CD24lo}$  (f) and  $B^{27+IgM+CD24hi}$  (g) towards CCL20 after treating for 24 hrs with CD24 mAb or IgG isotype control. **(h-i)** Percentage of total cellular CCR6 on the

surface (GM of surface CCR6 / GM of surface CCR6 + GM of intracellular) of B<sup>27+IgM+CD24lo/-</sup> (h) and B<sup>27+IgM+CD24hi</sup> (i) after treatment with CCL20 along with CD24 mAb or IgG isotype control. (j-k) Percentage of total cellular CCR6 on the surface of B<sup>27+IgM+CD24lo/-</sup> (j) and B<sup>27+IgM+CD24hi</sup> (k) after treatment with CCL20 along with CD24 mAb or IgG isotype control with and without chloramphenicol protein synthesis inhibitor. (l) Percentage of *in vitro* migration of live B<sup>27+IgM+CD24hi</sup> towards CCL20 after 24 hrs with and without Filipin treatment. Data were analyzed by using Mann-Whitney Wilcoxon test. Values are mean  $\pm$  s.d.

Interestingly, there was an inverse correlation between CD24 and CXCR4 expression but no correlation with CCR7, CXCR3 or CXCR5 (Figure 20). The inverse relationship between CD24 and CXCR4 expression aligns with a previously published report demonstrating that CD24 reduces CXCR4 localization in lipid rafts, thereby leading to lower CXCR4 signaling in pre-B cells<sup>109</sup>.

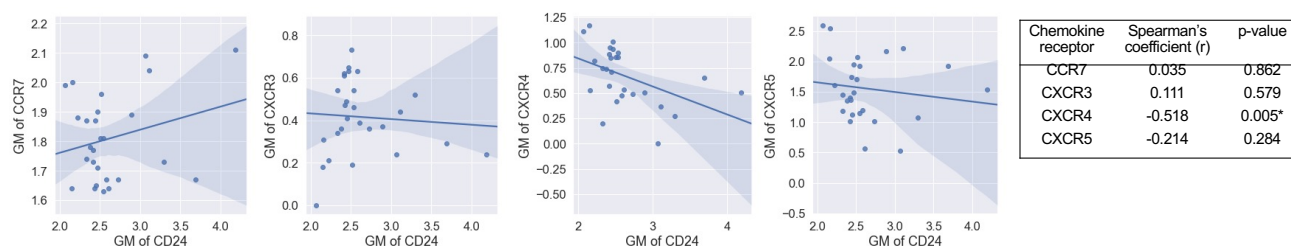


**Figure 20: GM of CD24 on B<sup>27+IgM+CD24hi</sup> does not associate with GM of CCR7, CXCR3, CXCR4, CXCR5 chemokine receptors.**

To determine potential mechanisms for the association between CD24 and CCR6 on B<sup>27+IgM+CD24hi</sup> cells, cultured human sort-purified B<sup>27+IgM+CD24lo/-</sup> and B<sup>27+IgM+CD24hi</sup> cells were incubated for 24 hours with either a CD24 neutralizing monoclonal antibody (mAb, clone SN3) or an IgG isotype control. Flow cytometry for CCR6 revealed that the CD24 blocking mAb

significantly reduced CCR6 expression on  $B^{27+IgM+CD24hi}$  but not  $B^{27+IgM+CD24lo/-}$  (Figure. 19b). Imaging flow cytometry on  $B^{27+IgM+CD24hi}$  cells incubated with either the CD24 mAb or IgG control suggested that CD24 and CCR6 may co-localize, an effect abrogated with the CD24 blocking mAb (Figure. 19c). Proximity ligation assay (PLA) was used to analyze protein interaction between CD24 and CCR6. Imaging flow cytometry on  $B^{27+IgM+CD24hi}$  cells indicated presence of PLA+ cells (Figure. 19d, 19e) suggesting direct protein interaction between CD24 and CCR6. *In vitro* transwell migration assay revealed no significant  $B^{27+IgM+CD24lo/-}$  cell migration towards CCL20 and that CD24mAb treatment had no effect on migration (Figure. 19f). In contrast, CCL20 induced a significant increase in  $B^{27+IgM+CD24hi}$  cell migration, an effect significantly reduced by the CD24mAb (Figure. 19g).

To determine if CD24 blocked CCL20-induced internalization, an effect known to limit CCR6 signaling<sup>110</sup>,  $B^{27+IgM+CD24hi}$  and  $B^{27+IgM+CD24lo/-}$  cells were treated *in vitro* with CD24mAb or IgG control, and flow cytometry for surface and intracellular CCR6 was performed to calculate the CCR6 percentage on the surface (GM of surface CCR6 / GM of surface CCR6 + GM of intracellular CCR6). Consistent with our prior data (Figure. 19b), there was more CCR6 on  $B^{27+IgM+CD24hi}$  compared to  $B^{27+IgM+CD24lo/-}$  cells at baseline. Within 10 minutes, CCL20 significantly induced CCR6 internalization on  $B^{27+IgM+CD24lo/-}$ , and neither CD24mAb nor IgG control treatment further changed CCR6 internalization (Figure. 19h). In contrast, CD24 mAb significantly enhanced CCL20-induced internalization of CCR6 in  $B^{27+IgM+CD24hi}$  cells compared to IgG isotype control and vehicle groups (Figure. 19i). The reduced CCR6 surface expression was not due to a change in CCR6 protein synthesis, as CCR6 surface expression levels were similar between Chloramphenicol-treated and DMSO control groups for both  $B^{27+IgM+CD24lo/-}$  (Figure. 19j) and  $B^{27+IgM+CD24hi}$  (Figure. 19k) cells. The CD24mAb reduced the CCR6 percentage on the surface of  $B^{27+IgM+CD24hi}$  cells in both Chloramphenicol-treated (at a significant level) or DMSO control (at a

trending significant level) (Figure. 19k). Results support our hypothesis that CD24 helps lower CCL20-induced CCR6 internalization, thus leaving CCR6 on the surface for continued CCL20-induced migration. As CD24 is a known GPI-anchored protein and resides in lipid raft, CD24 mediates CCL20/CCR6 induced migration was tested whether it is lipid raft dependent. CCL20 stimulations of live  $B^{27+IgM+CD24hi}$  cells treated with Filipin, an antifungal drug known to disintegrate lipid rafts, showed significantly abrogated CCL20-induced migration compared to cells treated with DMSO control (Figure. 19l).

### **CD24 promotes CCR6-mediated trafficking of $B^{27+IgM+CD24hi}$ cells to spleen**

CD24mAb treatment of sort-purified  $B^{27+IgM+CD24hi}$  cells (Figure. 21a) led to reduced CCR6 surface expression in PerC and spleen after IP injection (Figure. 21b), decreased numbers of  $B^{27+IgM+CD24hi}$  cells in the spleen (Figure. 21c) and lower plasma levels of IgM (Figure. 21d) compared to IgG control. To further validate that higher  $B^{27+IgM+CD24hi}$  cell trafficking to the spleen is CCR6 dependent, CCR6 was knocked out of  $B^{27+IgM+CD24hi}$  cells by nucleotransfecting Cas9/CCR6-targeted gRNA and IP injecting it into NSG mice (Figure. 21e). The results showed fewer CCR6 knockout  $B^{27+IgM+CD24hi}$  cells (CCR6KO  $B^{27+IgM+CD24hi}$ ) recovered from the spleen compared to CCR6+ wildtype  $B^{27+IgM+CD24hi}$  cells (CCR6WT  $B^{27+IgM+CD24hi}$ ) IP injection (Figure. 21f).

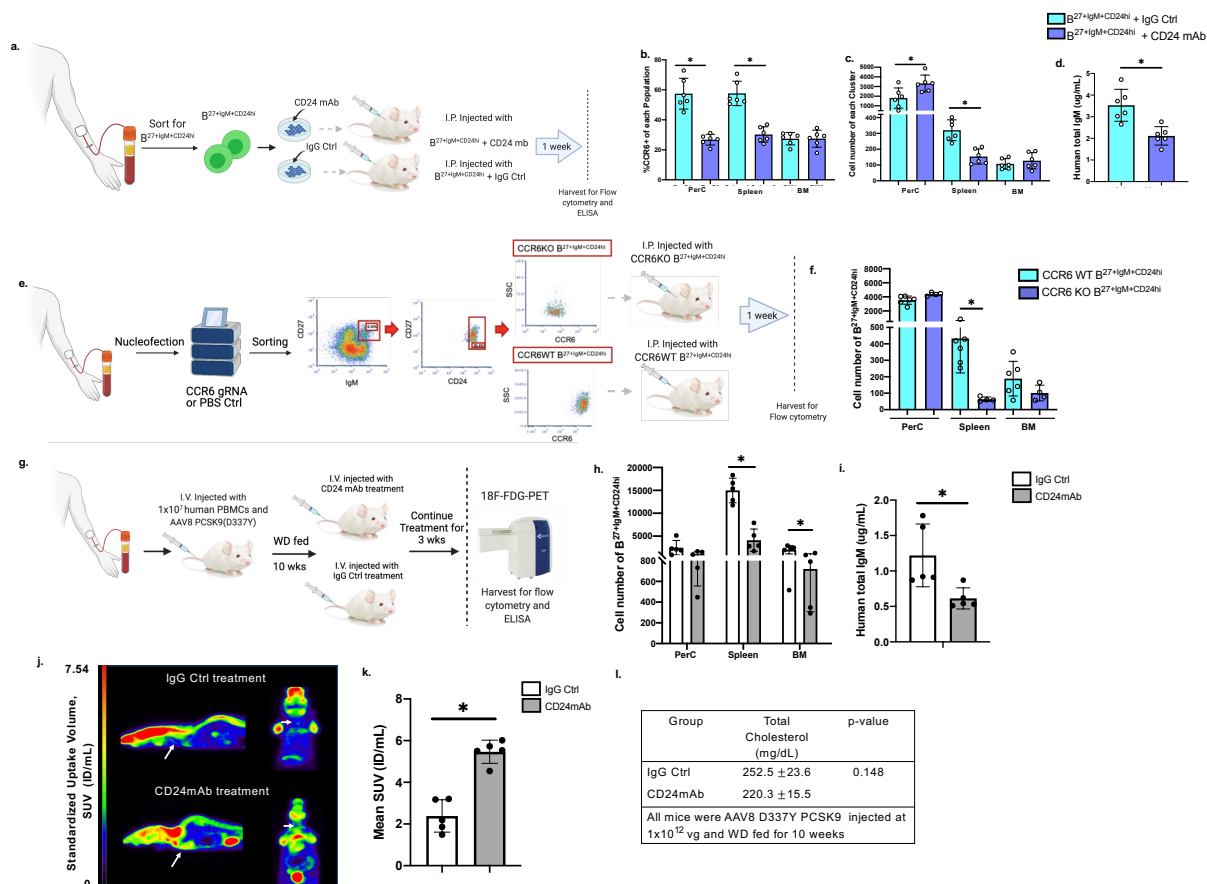


**Figure 21: CD24 inhibition reduces surface CCR6 expression, splenic trafficking, IgM production and increased diet induced vascular inflammation *in vivo*.** (a) Schematics of  $B^{27+}IgM^{+}CD24^{hi}$  adoptive transfer into humanized mice pre-treated with CD24mAb or IgG isotype control. (b-d) Percentage of CCR6+  $B^{27+}IgM^{+}CD24^{hi}$  cells (b), number of  $B^{27+}IgM^{+}CD24^{hi}$  cells recovered from peritoneal cavity, spleen or bone marrow (c) and human plasma total IgM measured by ELISA (d) 1 week post transfer. (e) Experimental scheme for adoptive transfer of CCR6KO and CCR6WT  $B^{27+}IgM^{+}CD24^{hi}$  cells into humanized mice. (f) Number of CCR6KO and CCR6WT  $B^{27+}IgM^{+}CD24^{hi}$  cells recovered from peritoneal cavity, spleen or bone marrow. (g), Schematics of hyperlipidemic humanized mice treated with 200ug of CD24mAb or IgG isotype control 2 times/week for 3 weeks. (h-i), Number of  $B^{27+}IgM^{+}CD24^{hi}$  recovered from peritoneal cavity, spleen or bone marrow (h), and human plasma total IgM measured by ELISA (i) after 3 weeks

of CD24mAb or IgG isotype control treatment. (j-k), Representative images (j) and mean standardized uptake volume (SUV) obtained from FDG-PET (k) to evaluate aortic vascular inflammation of hyperlipidemic humanized mice treated with CD24mAb or IgG isotype control treatment. (i) plasma total cholesterol in hyperlipidemic humanized mice after 10 weeks WD fed and either CD24mAb or IgG isotype control treatment. Data were analyzed by using Mann-Whitney Wilcoxon test. Values are mean  $\pm$  s.d..

### **CD24 protects against diet induced vascular inflammation**

NSG mice were engrafted with human PBMCs and AAV8-PCSK9 with 10 weeks Western diet was used to induce hyperlipidemia condition similarly to study conducted by Proto et al<sup>111</sup>. These hyperlipidemic NSG mice were treated with CD24mAb or IgG isotype control for 3 weeks via intravascular injection (Figure. 21g). CD24mAb treatment led to a significantly lower  $B^{27+IgM+CD24hi}$  cells recovered from spleen and bone marrow (Figure. 21h) as well as lower plasma level of total human IgM (Figure. 21i). <sup>18</sup>F-Fluorodeoxyglucose PET (FDG-PET) imaging was used to evaluate vascular inflammation. The imaging result indicated that CD24mAb treatment led to a higher FDG uptake in the aorta area (Figure. 21j+21k) despite similar plasma total cholesterol level in both IgG isotype control and CD24mAb treatment groups (Figure. 21l).

### **CITEseq revealed enhanced expression of genes encoding CCR6, IgM, and their downstream signaling intermediates in the $B^{27+IgM+CD24hi}$ cells of subjects with less severe CAD**

Subjects in our study had their CAD severity assessed by quantitative coronary angiography (QCA) at the time of their blood draw, and CAD severity was measured by the well-established Gensini scoring system<sup>112</sup> (Figure 22)

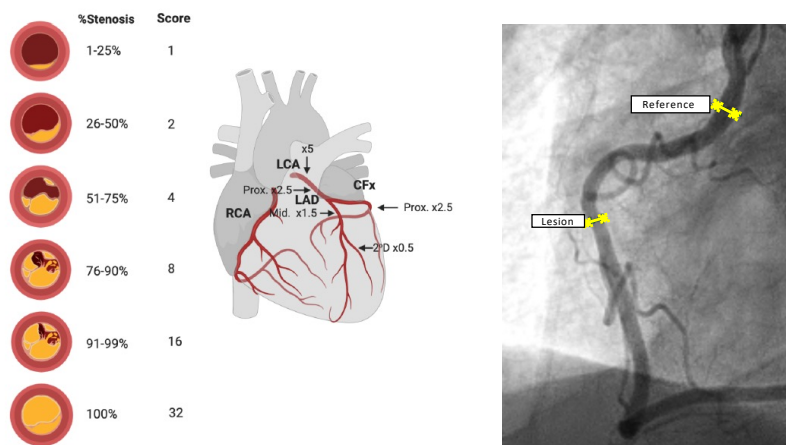


**Figure 22: Schematics demonstrating Genisini scoring system to evaluate CAD severity.**

A 26-antibody CITEseq panel was used to subtype circulating B cells in a cohort of CRF-matched subjects divided by high ( $\geq 32$ ,  $n=30$ ) and low ( $< 6$ ,  $n=30$ ) Genisini severity score (Figure. 23a). Results of CD19+ B cell metalouvain clustering revealed 10 distinct B cell clusters (Figure. 23b). Potential phenotypes for each cluster were based on expression of distinguishing B cell markers as represented in the heatmap (Figure.23c-d). Consistent with our CyTOF findings (Figure. 11), two B cell clusters identified as CD27<sup>+</sup> IgM<sup>+</sup> with low to moderate IgD expression (clusters 6 and 9) could be distinguished by CD24; cluster 6 had higher CD24 levels (B<sup>27+</sup>IgM<sup>+</sup>CD24<sup>hi</sup>) and cluster 9 had lower CD24 levels (B<sup>27+</sup>IgM<sup>+</sup>CD24<sup>lo/-</sup>). Cluster frequency analysis of these 60 subjects indicated an increase in cluster 6's frequency in subjects with low CAD severity while other clusters demonstrated comparable frequency between high and low CAD severity subjects (Figure. 23e). The associative analysis indicated enrichment of CD24 expression on cluster 6 (a surrogate of B<sup>27+</sup>IgM<sup>+</sup>CD24<sup>hi</sup>) in low CAD severity subjects (Figure. 23f).

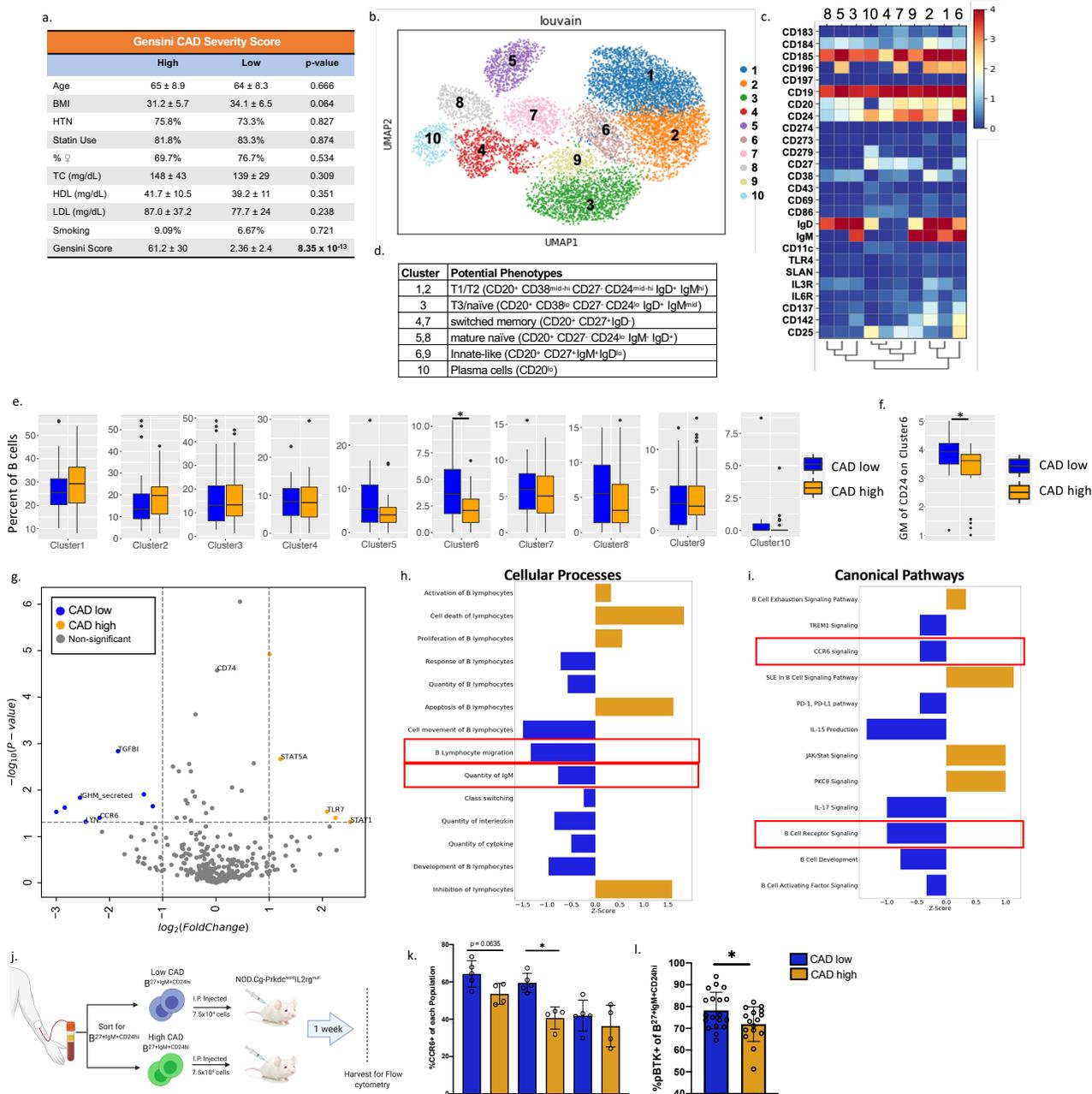


**Figure 23: CITEseq demonstrated increased in Cluster 6 (a surrogate of B<sup>27+</sup>IgM+CD24<sup>hi</sup>) frequency and CD24 expression as well as enhanced CCR6 signaling, BCR signaling, and IgM production in low CAD severity subjects. (a) Cohort of 60 subjects with high (Gensini score  $\geq 32$ , n = 30) and low (Gensini score  $< 6$ , n = 30) CAD severity with matched age, BMI,**

hypertension (HTN), %Statin Use, % female, total cholesterol (TC), HDL cholesterol, LDL cholesterol, and smoking status. **(b)** Representative metacluster UMAP showing 10 distinct B cell subsets by using louvain clustering **(c)**, heatmap showing median expression of surface markers from metaclustering **(d)**, table showing potential phenotypes of each B cell subset resulting from unsupervised clustering. **(e)**, Biaxial plots to compare frequency of each cluster as a percentage of total B cells in subjects with high and low CAD severity. **(f)** Biaxial plots to compare CD24 expression on cluster 6 in subjects with high and low CAD severity. **(g)** Volcano plot of 488 gene array demonstrating DE genes of cluster 8 when compared between CAD low (blue) and high (orange). **(h-i)** Significant cellular processes **(h)** and canonical pathways **(i)** enriched in CAD low (blue) and CAD high (orange) in cluster 8 cells. **(j)** Schematics of  $B^{27+IgM+CD24hi}$  obtained from high- and low-CAD severity subjects adoptively transfer into humanized mice. **(l-k)** Percentage of  $CCR6+ B^{27+IgM+CD24hi}$  cells **(k)**, number of  $B^{27+IgM+CD24hi}$  cells recovered from peritoneal cavity, spleen or bone marrow **(l)**, and human plasma total IgM measured by ELISA **(m)** 1 week post-transfer. **(n)** Percentage of  $p-BTK+ B^{27+IgM+CD24hi}$  cells from high- and low-CAD severity subjects. Data were analyzed by using Mann-Whitney Wilcoxon test. Values are mean  $\pm$  s.d..

Using the CITEseq 488 genes array to analyze differentially expressed genes and pathways in cluster 6 (surrogate of  $B^{27+IgM+CD24hi}$ ) and cluster 9 (surrogate of  $B^{27+IgM+CD24lo}$ ) cells from subjects with low and high CAD severity revealed 13 and 18 DE genes, respectively (Table 8 and 9).

Gene Names	FDR	Log <sub>2</sub> FC
LTB	<0.001	1.009
TGFBI	0.001	-1.836
STAT5A	0.002	1.214
TCL1A	0.013	-1.350
sIGHM	0.015	-2.549
CD14	0.022	-1.183
KLRB1	0.024	-2.837
TLR7	0.029	2.090
CD5	0.030	-2.995
CCR6	0.040	-2.181
CD4	0.040	2.251
LYN	0.048	-2.444
STAT1	0.049	2.526

\* FC is fold change of high-CAD/ low-CAD subjects

**Table 8: DE genes compared between high- versus low-CAD subjects obtained from**

**B<sup>27</sup>+IgM+CD24<sup>hi</sup> cells**

Gene Names	FDR	Log <sub>2</sub> FC
CD79B	<0.001	1.012
TCL1A	<0.001	-1.882
IGHA1_secreted	<0.001	1.076
TGFBI	0.001	-1.870
SYNE2	0.001	-1.817
CD70	0.002	2.027
YBX3	0.002	-1.014
PDIA4	0.003	-3.210
LAP3	0.005	-1.483
GNG11	0.007	1.309
RGS1	0.009	1.013
ITGAM	0.015	-1.033
SORL1	0.018	-2.519
IL32	0.031	-1.003
NKG7	0.034	1.205
CBLB	0.034	-1.200
VCAN	0.040	1.532
CLEC4E	0.049	-2.332

\* FC is fold change of high-CAD/ low-CAD subjects

**Table 9: DE genes compared between high- versus low-CAD subjects obtained from**

**B<sup>27</sup>+IgM+CD24<sup>lo/-</sup> cells**

Volcano plots of DE genes (FDR < 0.05 and log<sub>2</sub>FC > or < 1) and differentially regulated pathways of cluster 9 cells showed that TGF $\beta$  and genes involved in lymphocyte migration were enriched in patients with less severe CAD (Figure 24).

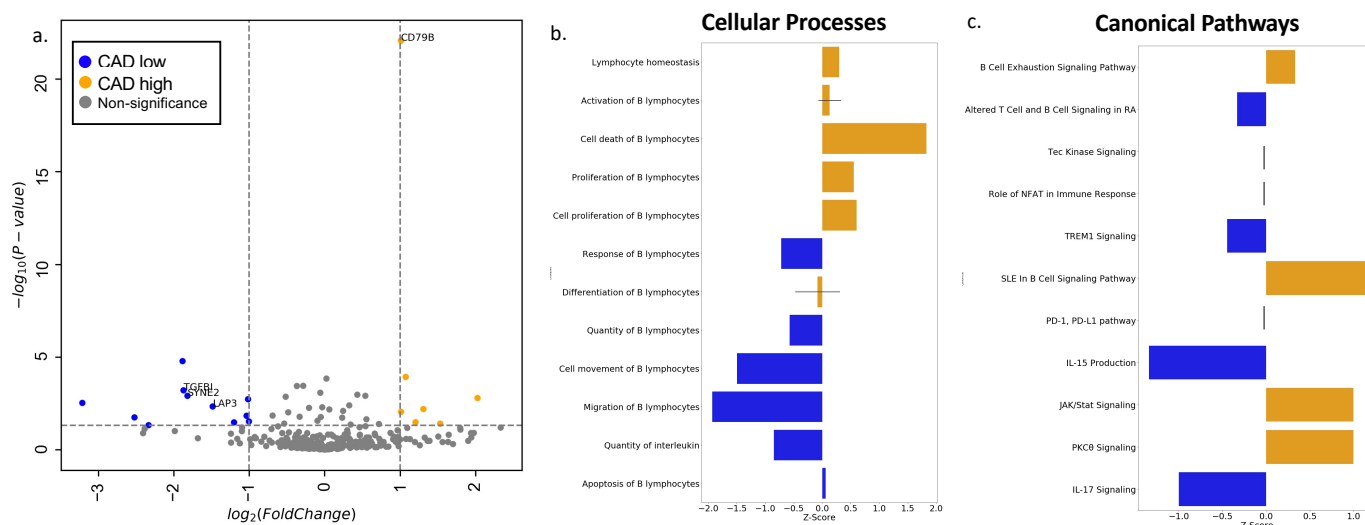


**Figure 24: Differential gene expression and pathway analysis of cluster 9 (surrogate of B27+IgM+CD24<sup>lo</sup>).** Volcano plot of 488 gene array demonstrating DE genes of cluster 8 when compared between CAD low (blue) and high (orange) (a). Significant cellular processes (b) and canonical pathways (c) enriched in CAD low (blue) and CAD high (orange) in cluster 9 cells.

Notably, volcano plots of DE genes in cluster 6 cells from subjects with less severe CAD (Figure. 23g) demonstrated the same TGF $\beta$  enrichment but also elevated CCR6, secreted IgM, and the intracellular intermediate of BCR activation LYN kinase. Consistent with these DE genes, subjects with low CAD severity were enriched for genes involved in B lymphocyte migration, IgM cellular process quantity (Figure. 23h) and canonical CCR6 and BCR signaling pathways (Figure. 23i). Lastly, B27+IgM+CD24<sup>hi</sup> cells sort-purified from CRF-matched subjects with high (Gensini > 32, n =4) and low (Gensini < 6, n = 5) CAD severity were transferred via IP injection into NSG mice (Figure. 23j). The low-severity CAD group had higher CCR6 expression

on B<sup>27+IgM+CD24hi</sup> cells migrated to the spleen than the high-severity CAD group 7 days post injection (Figure. 23k). Lastly, phosphor-BTK (a downstream BCR signaling of LYN kinase) was enriched in B<sup>27+IgM+CD24hi</sup> cells in low CAD severity subjects after polyclonal B cells activation (Figure. 23l). These results altogether further indicate that CD24 plays a role in atheroprotection, Splenic trafficking of B<sup>27+IgM+CD24hi</sup> cells mediated by CCR6-CCL20, IgM production as well as BCR activation in B<sup>27+IgM+CD24hi</sup> are also atheroprotective.

## Discussion

There is clear evidence that IgM<sup>OSE</sup> limits inflammation in pre-clinical models of inflammatory diseases including atherosclerosis<sup>96,113–118</sup>. The main source of IgM<sup>OSE</sup> in mice is B-1 cells<sup>117,119,120</sup>, a cell type known to limit diet-induced inflammation and inflammation-related diseases such as insulin resistance and atherosclerosis<sup>29,32,46,118,121</sup>. Yet, the cellular source of IgM to OSE in humans remains elusive. Oxidation of cellular membranes, lipids and proteins can produce a wide range of OSE, but aldehyde adducts on LDL such as malondialdehyde (MDA) are prominent OSE in atherosclerotic plaques<sup>99</sup>. A wealth of epidemiological data demonstrates that subjects with advanced atherosclerotic disease and major adverse cardiac events (MACE) have low levels of IgM<sup>MDA-LDL</sup>.<sup>1-6</sup> The importance of identification of the cellular source of IgM<sup>MDA-LDL</sup> is highlighted by these findings and the likelihood that this same cell produces IgM<sup>OSE</sup> of other specificities such as MAA, ApoB100, OxCE, PC<sup>122,74</sup>. Indeed, our findings demonstrate a strong correlation between IgM<sup>MDA-LDL</sup>, IgM<sup>PC-BSA</sup> and IgM<sup>OxCE</sup> in humans (Figure 12), and the amount of CD24 on B<sup>27+IgM+</sup> cells was significantly associated with both IgM<sup>MDA-LDL</sup> and IgM<sup>OxCE</sup>. As such, identification of the cellular source of IgM<sup>MDA-LDL</sup>-producing cells in humans has the potential to allow for the development of therapeutics aimed at cellular targeting that may allow for enhancing production of IgM to the many OSE produced during inflammatory states such as atherosclerosis.

Here, we utilize CyTOF of human B cells coupled with *in vitro* and *in vivo* studies to identify circulating B<sup>27+IgM+</sup> cells as producers of IgM<sup>OSE</sup> in humans. We confirm a B<sup>27+IgM+</sup> cell subtype for which the association with IgM<sup>OSE</sup> plasma levels depends on CD43 expression, a result consistent with the work of Griffin et al.<sup>107</sup>. Moreover, we provide the first evidence that CD24 expression divides B<sup>27+IgM+</sup> cells into two subtypes with unique expression of chemokine receptors and different capacities for splenic trafficking and IgM<sup>OSE</sup> production. Additional flow cytometry suggests that these B<sup>27+IgM+CD24hi</sup> may be circulating MZB cells as opposed to B-1 cells, which are the IgM<sup>MDA-LDL</sup> producing cells in mice. Like B-1 cells, human MZB cells are innate-like B cells that produce natural IgM<sup>123</sup> in response to innate stimuli (e.g. OxPL and OSE)<sup>72,124–126</sup>. However, in humans MZB cells may be found in circulation, whereas murine MZB cells are confined to the spleen, which may underline these differences in functionality between species. Our B<sup>27+IgM+CD24hi</sup> cells do in fact express markers traditionally used to identify human circulating splenic MZB (CD21<sup>mid</sup>CD23-CD1C<sup>+</sup>, Figure. 4c)<sup>108,127,128</sup>. They also differentiate into antibody-producing cells/plasma cells, migrate to the spleen, produce IgM in a T cell-independent manner and increase total and MDA-specific IgM production in response to MDA antigen stimulation, which is indicative of human MZB cell functionality<sup>123,125,128,129</sup>. As such, we provide the first evidence that circulating human MZB cells produce atheroprotective IgM and that these cells occur more frequently in patients with less severe CAD.

In addition to identifying human B<sup>27+IgM+CD24hi</sup> cells as the main producers of IgM<sup>OSE</sup>, we provide the first evidence for a novel role for CD24 in regulating human IgM<sup>MDA-LDL</sup> producing B cells. CD24, a GPI-anchored sialoglycoprotein present in lipid rafts, has known anti-inflammatory roles in dendritic cells mainly through binding with Siglec-G/10 to encounter Toll-like receptor dependent pro-inflammatory response<sup>130</sup>. These anti-inflammatory properties have led to the

development of important CD24 targeted agents such as the CD24Fc recombinant Fc fusion protein being tested in severe COVID-19 induced pneumonia (NCT04317040). Our study highlights a novel anti-inflammatory mechanism in cardiovascular disease whereby CD24 on B<sup>27+IgM+CD24hi</sup> cells (MZB-like cells) stabilizes CCR6 in lipid rafts, protects the cell from ligand-induced internalization of the chemokine receptor CCR6 and promotes CCL20-induced splenic trafficking and anti-inflammatory IgM production.

In addition to regulating CCR6-mediated splenic trafficking of B<sup>27+IgM+</sup> cells, CD24 also likely mediates atheroprotection through governing BCR localization, signaling, and function as BCR activation is essential for antibody production. A striking result from our RNAseq DE gene and pathway analysis of sort-purified B<sup>27+IgM+CD24hi</sup> and B<sup>27+IgM+CD24lo/-</sup> cells also demonstrated that the canonical BCR pathway and the expression of specific BCR-activation signals such as Lyn kinase, SYK and PLCG2 are enriched in B<sup>27+IgM+CD24hi</sup> cells as compared to B<sup>27+IgM+CD24lo/-</sup> cells, thereby suggesting greater BCR-mediated activation. CITEseq on CAD subjects also showed canonical CCR6 and BCR signaling pathways elevation in addition to enriched B lymphocyte migration and IgM quantity in subjects with low-severity CAD, which further supports the role of these factors in human cardiovascular diseases.

Finally, given the robust anti-inflammatory impact of CD24, we also explored the role of CD24 in mediating vascular inflammation. Immune-modulatory agents have a prominent role in the treatment of cancers (e.g. anti-PD1/PD-L1, anti-CTLA4, anti-CD47) and blocking the “don’t eat me” signal of CD24 mAb is amongst one of the more recent immunotherapy regimens being tested in trials. However, despite efficacy of cancer immunotherapy there are clear associations with cardiovascular toxicities that are not surprising given that immune cells also underlie pathogenesis of cardiovascular diseases. So far, anti-PD1 as well as anti-CTLA-4 were shown

to increase arterial inflammation<sup>131</sup>, while anti-CD47 suppressed vascular inflammation<sup>132</sup> in cancer patients. For the first time, we show that CD24mAb aggravate diet induced vascular inflammation.

In summary, the present study is the first to identify B<sup>27+IgM+</sup> cells as IgM<sup>MDA-LDL</sup>-producing B cells in humans. Characterizing the B<sup>27+IgM+CD24hi</sup> cells ascertained human circulating MZB cells that were highly regulated by CD24 and CCR6 and could be more robustly induced to produce atheroprotective IgM<sup>MDA-LDL</sup> by specific antigen stimulation. These two features hold promise for modulating this subtype to bolster innate immune protection from OSE in atherosclerosis and other inflammatory diseases. In addition, as anti-CD24 is now under development as a cancer immunotherapy, this present study assessed a short-term effect of CD24 inhibition and highlighted an important adverse effect of increasing vascular inflammation. Therefore, long-term effects of CD24 inhibition on subclinical and clinical cardiovascular events as well as effects on other OSE-related diseases should be considered.

## **Chapter 5**

### **Discussion and Future Directions**

Atherosclerotic cardiovascular disease is a leading cause of death worldwide. Therefore, understanding of inflammatory processes underpinning its pathology is critical. B cells have been implicated as a key immune cell regulating atherosclerosis. However, whether B cells are atheroprotective or atherogenic is subtypes dependent. In murine B cells, innate-like B cells including B1 cells and marginal zone B cells are shown to be atheroprotective, while B2 cells are atherogenic. Despite plethora studies of murine B cells and atherosclerosis, it is near impossible to directly translate the findings to humans. The major issues contributing to this limitation include differences in surface markers and immune responses in immune cells between mice and human. Not only that understanding of human B cells and atherosclerosis remains unclear, various immunotherapies have been recently developed to treat cancers as well as autoimmune diseases but impacts of these therapies on B cells and cardiovascular disease were also limitedly explored.

In Chapter 3, we presented the evidences that p62 mediates BAFF signaling to promote B1b cell proliferation, and bHLH-transcription factor, TCF3 or E2A, drives p62 expression through activating its promoter while Id3 dimerizes with E2A to inhibit p62 promoter activation. More importantly, we discovered that through promoting B1b cell proliferation by overexpressing p62, we can increase plasma IgM and reduce atherosclerotic plaque formation in mice. In human, expression level of p62 in putative human CD20<sup>+</sup>CD27<sup>+</sup>CD43<sup>+</sup> B1 cells was observed to be higher in CAD subjects with Id3 functionally reduced rs11574 SNP, and the expression also directly associates with higher level of IgM to OSE. Several questions arise from this work, including 1) As TCF3/E2A activates p62 promoter, are there any mutations on TCF3 that change p62 expression and associate with CAD severity? 2) As p62 is known to regulate autophagy and cell survival, what is the impact of p62 on B1 cell autophagy/survival and 3) what is the potential role of p62 in B2 cells and how it might affect atherosclerosis?

In chapter 4, we identified IgM to OSE producing human B cells marked by CD27+IgM+ and CD24 high expression ( $B^{27+IgMCD24hi}$ ) and CD24 as a regulator of IgM to OSE production through enhancing CCR6 mediated splenic trafficking. Functional studies and deeper phenotyping show that these  $B^{27+IgMCD24hi}$  cells are potentially human circulating MZB cells. MZB cells are innate-like B cells similar to B1 cells that can spontaneously produce IgM. The major difference is that MZB cells can also produce IgM upon antigen stimulation through direct interaction with the antigen or through T cells help<sup>125</sup>. Interestingly, Rosenfeld et al previously demonstrated that B1b cells can also produce IgM to OSE *in vivo* following OSE antigen stimulation<sup>46</sup> which is not a typical B1 cell characteristics but more of characteristics of MZB cells. Additionally, CD24 was not only the marker to help identify IgM-producing human B cells, but also a novel target for both COVID-19 treatment and cancer therapies. In B cells, CD24 regulates BCR activation and differentiation<sup>133</sup>, while CD24 exerts its anti-inflammatory effect through interacting with siglec-10 to block TLR activation on macrophages and dendritic cells. Our study demonstrated for the first time that CD24 blocking antibody used in cancer therapies can potentially aggravate vascular inflammation, an early sign of atherosclerosis. This study raises some important questions, 1) does IgM to OSE production from  $B^{27+IgMCD24hi}$  cells alone offer atheroprotection or CD24 from other immune cell type plays a more important role in mediating atheroprotection? 2) how does a well-known interaction between CD24 and Siglec10 might impact atherosclerosis? And 3) how does CD24 might play a role in B cell survival and development?

**TCF3 mutations associates with reduced p62 expression in human IgM producing B cells and an increase in CAD severity**

Id3 rs11574 functionally reduced SNP has been shown as a predictor of atherosclerosis burden as well as CAD severity<sup>134,135</sup>. As Id3 is a binding partner of E2A or TCF3, question arises whether there exists TCF3 mutations that change binding affinity to Id3 or E-box sequences of

the promoters leading to change in expression of downstream gene and impacts atherosclerosis.

In B cells, TCF3 has been known to control early B cell development allowing lymphoid progenitors to commit to the B cell lineage<sup>136</sup>. It is also essential in VDJ recombination and class-switching to IgG isotypes<sup>137</sup> through activating *Aicda* gene and differentiation to plasma cells<sup>138</sup>. However, roles of TCF3 in mature B cells have been limitedly explored.

Clonal hematopoiesis of indeterminate potential (CHIP) refers to somatic mutations that arise in mature blood or immune cells leading to clonal expansion derived from the cells that gained the mutations. Oftentimes, frequency of CHIP increases with age. However, these CHIP mutations do not meet criteria of hematologic neoplasia<sup>139</sup>. CHIP has been recently discovered to associate with an increase risk cardiovascular disease, especially large clone CHIPs such as TET2, DNMT3A<sup>140</sup>. Here, we explored the roles of TCF3 somatic mutations in driving clonal expansion of lymphoid cells and determine potential of these mutations in cardiovascular disease.

PBMCs of 87 CAD subjects over the age of 60 were sequenced of targeted genes mutations. These subjects also had coronary imaging obtained and CAD severity was quantified using Gensini scoring system. Out of 87 CAD subjects, 19 subjects were presented with TCF3 mutations (Allele frequency < 0.3 was used to classify somatic mutations). Within these 87 CAD subjects, CAD severity score was compared between subjects with and without of TCF3 somatic mutations otherwise matched for cardiac risk factors. CAD severity was found to be higher in subjects with presence of TCF3 mutations (Figure 25).

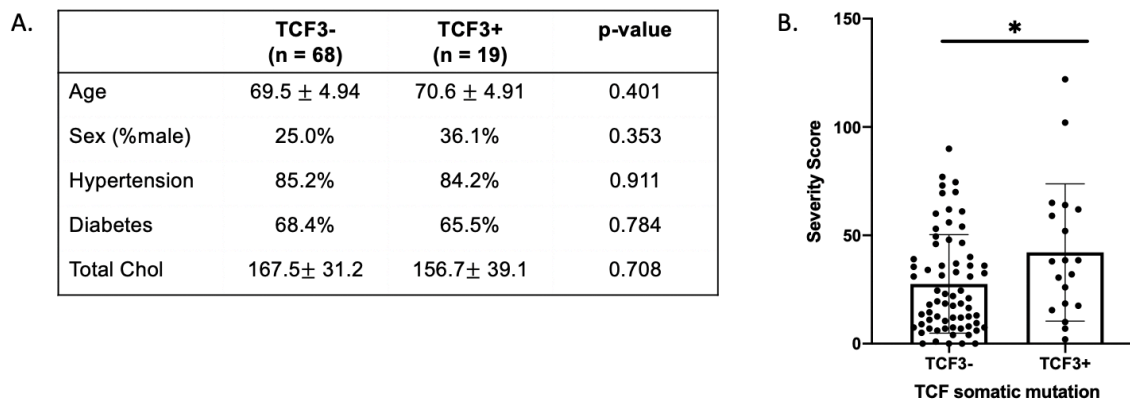


**Figure 25: Presence of TCF3 somatic mutations associates with higher coronary artery disease.** (A) Cardiac risk factors characteristics of coronary artery disease subjects with (n =19) and without TCF3 mutations (n = 68). (B) Coronary artery disease severity score measured by Gensini scoring system comparing between subjects with and without TCF3 mutations.

This finding and the fact that TCF3 plays a major role in B cell survival and class-switching led us to speculate that these TCF3 somatic mutations might increase CAD severity through change in B cell class-switching. Therefore, we explored TCF3 mutations that might be enriched in CD27+IgM+, B cell subtype we previously reported in chapter 4 as IgM producing B cells in human.

We identified mutations at Chr19 position 1622418 and 1622422, which are located in a splice region (Figure 26) to be enriched in subjects with high CAD severity. Interestingly, our result also indicated that these two mutations were enriched at higher allele frequency in CD27+IgM+ B cells (Figure 26). However, functional assay is needed to verify that these two mutations at the splice region might lead to loss of function TCF3. The importance of these mutations should also be validated in a larger sample human study and *in vivo* functional studies showing these two TCF3 mutations in CD27+IgM+ actually mediate atherosclerosis also needs to be performed.

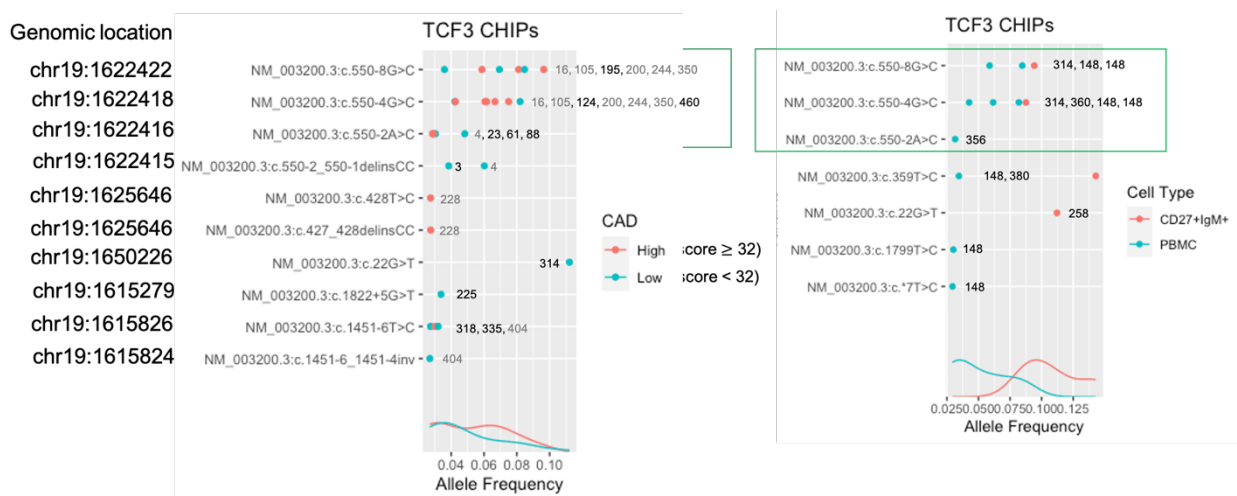


**Figure 26: TCF3 somatic mutations are potentially enriched in subjects with high CAD severity and in CD27+IgM+ B cells.**

As we previously discovered that TCF3 or E2A protein can activate p62 promoter and p62 can drive proliferation of murine B1b cells through NF $\kappa$ B activation, we investigated relationship among TCF3 somatic mutations, frequency of B cell subtypes, p62 expression, and p-NF $\kappa$ B level in B cell subtypes using flow cytometry. We found that CAD subjects with TCF3 somatic mutation (n = 11) has a decrease in frequency of CD27+IgM+CD24<sup>lo</sup> and CD27+IgM+CD24<sup>hi</sup> B cells, but an increase in double negative (CD27-IgD<sup>-</sup>) B cells when compared to CAD subjects

without TCF3 mutation (n = 57) (Figure 27). Additionally, p62 expression as well as intracellular signaling molecules including p-mTOR and p-NFKB were found to be enriched in CD27+IgM+CD24hi B cells in subjects with TCF3 somatic mutations (Figure 28). Taken these together, we speculate that these TCF3 mutations might be loss of function mutations leading to a decrease in p62 expression resulting in lower NFKB activation and reduced proliferation of CD27+IgM+CD24hi B cells which are the main producer of atheroprotective IgM to MDA-LDL.

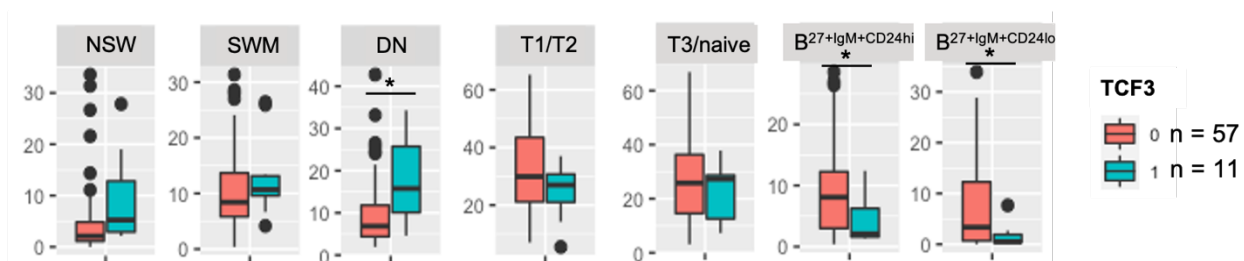


**Figure 27: Subjects with TCF3 somatic mutations have decreased frequency of**

**B<sup>27+IgM+CD24hi</sup> and B<sup>27+IgM+CD24lo/-</sup>.**

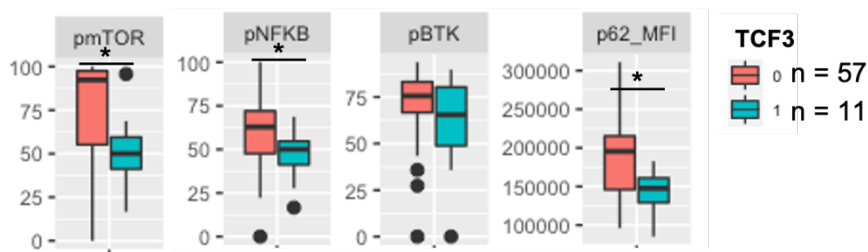


**Figure 28: Subjects with TCF3 somatic mutations have decreased mTOR, NFKB activation and p62 expression.**

Further investigation to validate this speculation is still required and can possibly be done through knocking out of TCF3 or performed a mutagenesis on TCF3 overexpression plasmid. These genome editing approaches will facilitate causal functional assays to validate that TCF3 somatic mutations are the key for CD27+IgM+CD24hi cells proliferation and mediate atherosclerosis.

### **P62, autophagy and B cell survival**

As briefly mentioned earlier in chapter 3, p62 has been long known in its role as a classical receptor of autophagy. It mediates cell survival both in normal and stress conditions mainly through delivering ubiquitinated proteins for degradation at proteasomes<sup>141</sup>. p62 is a multifunctional protein consisting of various binding domains, including a Phox-BEM1 domain (PB1), a zing finger domain, a TRAF6-binding (TB) domain, a nuclear localization signal (NLS), an export motif (NES), an LC3-interacting region (LIR), a Keap-1 interacting region (KIR), and a ubiquitin-associated domain (UBA). We previously focused on an interaction between p62 and TRAF6 through TB domain and its downstream activation of NF $\kappa$ B mediating B1b cell proliferation. However, some other pathways promoting cell survival might also contribute to an increase in B1b cell number when p62 was overexpressed in B1 cells. LIR and KIR domains of p62 play major roles in mediating autophagy. LC3 binds directly to p62 LIR domain to facilitate protein ubiquitination and degradation<sup>142</sup> while KIR domain is involving in Keap1-Nrf2 pathway<sup>141</sup>. At resting state, Keap1 binds to Nrf2 which leads to degradation Nrf2. However, once p62 level is increased, p62 can bind and ubiquitinate Keap1 allowing Nrf2 to be activated<sup>143</sup>.

Taken these together, we explored levels of Nrf2 in B1a and B1b with Id3WT and t Id3KO. The result indicated that Nrf2 level is increased in both B1a and B1b with loss of Id3 and BAFF stimulation does not affect Nrf2 level (Figure 29). However, downstream signaling and changes

in these B1 cells homeostasis or their capabilities in producing IgM still await future investigation.

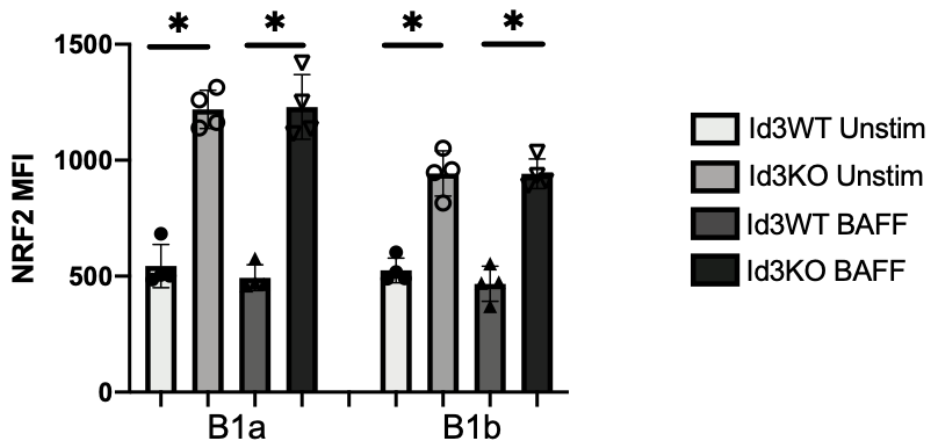


**Figure 29: Loss of Id3 in both B1a and B1b lead to an increase in NRF2 expression.**

This finding is consistent with a concept that B1a B cells require autophagy for metabolic homeostasis to maintain their self-renewal capabilities<sup>144</sup>. Yet, roles of Nrf2-p62 in maintaining B1 self-renewal and homeostasis as well as whether the self-renewal capacity remains through life and across tissue compartments are aspects that have never been explored. More importantly, whether this discovery can be translated into human putative B1 or CD27+IgM+CD24hi IgM producing B cells still requires further investigation.

### **Roles of p62 in B2 B cells**

B2 cells are atherogenic while B1 cells are atheroprotective. These opposite consequences on atherosclerosis of the two B cell subsets are the major obstacle why targeted B cell therapies always have controversial cardiovascular disease side effects<sup>145</sup>. Therefore, to enable use of p62 overexpression in B cells as a targeted immune-modulatory therapy for atherosclerosis, the effect of p62 on B2 cells should be evaluated.

We explored level of p62 in B2 cells compared to B1b cells as well as proliferation of these cells. The results indicated that p62 expressed higher in B2 compared to B1b, while BAFF stimulation did not drive B2 proliferation as much as B1b cells (Figure 30). These results allow us to hypothesize that p62 might not play a major role in BAFF induced cell proliferation in B2 cells. However, whether p62 involves in cell survival of B2 or other cell proliferation pathways (eg. BCR activation, CD40 driven proliferation) still remains unknown.

CD40 mediated cell proliferation and survival is one of promising pathways that should be further explored in regard of p62. p62 is known to bind to TRAF6<sup>52</sup>, and CD40 has been known to activate B cell differentiation and proliferation via TRAF6 signaling<sup>146</sup> and associates with increased macrophages induced atherosclerosis<sup>69</sup>. These prior findings allow us to hypothesize that p62 might play a role in CD40 mediating B cell proliferation. Evaluation of roles of p62 in B2 cells is important as knocking down of p62 in B2 or inhibiting CD40 driven p62-TRAF6 signaling axis can potentially be an alternative therapy of atherosclerosis

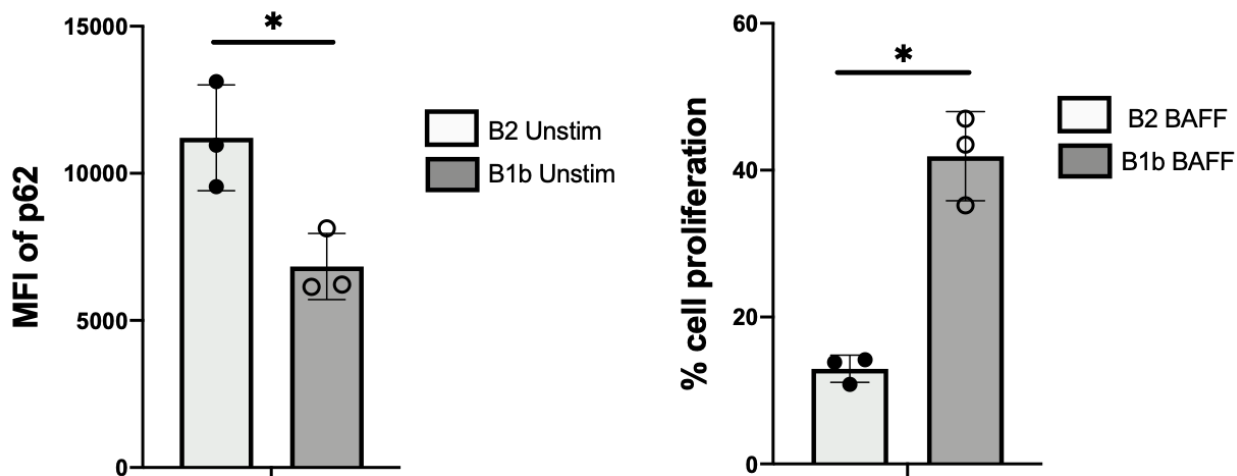


**Figure 30: Higher expression of p62 but lower BAFF induced cell proliferation in B2 cells than B1b cells.**

### P62 as a target for B cell modulatory therapy to treat atherosclerosis

In addition to evaluating the roles of p62 in both B1 and B2 cells, it is also important to perform an atherosclerosis study in a transgenic mice model with B cell specific overexpression of p62 or B cell specific knock out of p62. The atherosclerosis study will allow us to assess the direct effect of p62 overexpression/knockout of total B cells on atherosclerotic plaque formation. Further investigation of plasma total IgG and IgM levels, IgG and IgM specific to OSEs as well as pro- and anti-inflammatory cytokines will also unveil whether p62 also mediates immunoglobulin and cytokine productions in addition to mediating B cell proliferation and survival. A transgenic mice model with B cell specific overexpression of p62 will also facilitate discovery of potential side effects such as development of B cell lymphoma as p62 was previously shown to play a role in cancer cell proliferation in various cancer types<sup>53</sup>.

Another alternative strategy of targeted therapy of p62 for atherosclerosis is to only overexpress p62 in B1 cells. However, this strategy is less feasible in human as identification of human B1 cells still remains elusive. Chapter 4 provides some clues that overexpression of p62 in B<sup>27+IgM+CD24hi</sup>, an IgM producing human B cells, might be a potential alternative. However, use of bispecific antibodies gene delivery platform to target in B<sup>27+IgM+CD24hi</sup> cells can still be challenging as CD27 also expresses on T cells and the bispecific antibodies might lead to an undesired B and T cell reaction.

### **IgM to oxidation specific epitopes and atheroprotection**

In chapter 4, we have previously shown that human B cells marked by CD27+ and IgM+ are the producers of IgM to MDA-LDL, the major IgM to OSE in humans, and CD24 augments the IgM production. However, whether these cells alone produce sufficient amount of IgM to OSE to

protect against diet induced atherosclerosis, where these cells produce the antibodies, or which immunoglobulin repertoires were utilized by these cells still remain unknown.

We previously demonstrated CD24 blocking mAb enhanced vascular inflammation and reduced plasma level of IgM. However, we have never shown whether lower amount of plasma IgM alone was the only or a main cause of aggravation in vascular inflammation. To seek for the answers to these questions, it is important to perform an adoptive transfer experiment of  $B^{27+IgM+CD24hi}$  cells into hyperlipidemic humanized mice model and evaluate vascular inflammation post-adoptive transfer. However, there is also possibility that  $B^{27+IgM+CD24hi}$  cells adoptively transferred into humanized mice might not produce enough of IgM to OSE to prevent vascular inflammation. Therefore, multiple adoptive transfer might be required. This investigation will allow us to evaluate how feasible it is to utilize  $B^{27+IgM+CD24hi}$  cell therapy as a potential therapeutic for atherosclerosis.

In the case that an adoptive transfer of  $B^{27+IgM+CD24hi}$  cells is insufficient for atherosclerosis protection, the alternative is that we can inject an IgM cocktail that binds to OSEs instead of injecting a high number of rare  $B^{27+IgM+CD24hi}$  cells which is unlikely to be feasible and scalable. However, to do this, IgM repertoires utilized by  $B^{27+IgM+CD24hi}$  cells have to be first identified. Upadhye et al demonstrated earlier that IgM repertoires utilized by B cells are B cell subtypes as well as tissue compartments specific<sup>100</sup>. Therefore, it is important to sequence B cell receptors of  $B^{27+IgM+CD24hi}$  cells that reside in antibody producing niches (eg. spleen and bone marrow). Identification of IgM repertoires will allow in vitro/ ex vivo assays to synthesize the IgM cocktails. Another possibility is through hybridoma production fusing with  $B^{27+IgM+CD24hi}$  cells. This technique will allow a mass production of IgM that is potentially atheroprotective.

As previously mentioned, IgM repertoires are tissue compartments specific. It is important to identify where  $B^{27+IgM+CD24hi}$  cells produce IgM. In Chapter 4, we concluded that circulating

$B^{27+IgM+CD24hi}$  cells are potentially marginal zone B cell precursors. Therefore, the main niche of these cells' antibody producing site can potentially be spleen. However, prior publications from the lab also indicated other antibody producing sites such as bone marrow, omental fat, and perivascular adipose tissue<sup>16</sup>. Investigating these other sites can also answer the questions whether IgM repertoires utilized by  $B^{27+IgM+CD24hi}$  cells differ across compartments in human.

### **CD24 and Siglec10**

Role of CD24 and Siglec 10 has been well elucidated in cancer. Barkal et al reported that CD24/Siglec 10 is a non-conventional “don't eat me” signal<sup>147</sup> in addition to a conventional “don't eat me” CD47/SIRPa signal. This report led us to hypothesize that our discovery of higher number of  $B^{27+IgM+CD24hi}$  cells recovered in the spleen compared to number of  $B^{27+IgM+CD24lo}$  cells might also result from a higher survival of  $B^{27+IgM+CD24hi}$  cells resulting from a reduction in macrophage uptake of CD24hi B cell subtype. To answer this question, we developed a preliminary model using human PBMCs engraftment in humanized mice following with adoptive transfer of human B cells loaded with celltrace-violet. The pilot model showed a detection of cell-trace violet+ B cells inside human resident macrophages (Figure 31). This model can be used to further investigate whether  $B^{27+IgM+CD24hi}$  cells will be engulfed at a lower level than  $B^{27+IgM+CD24lo}$  cells into Siglec10+ macrophages.

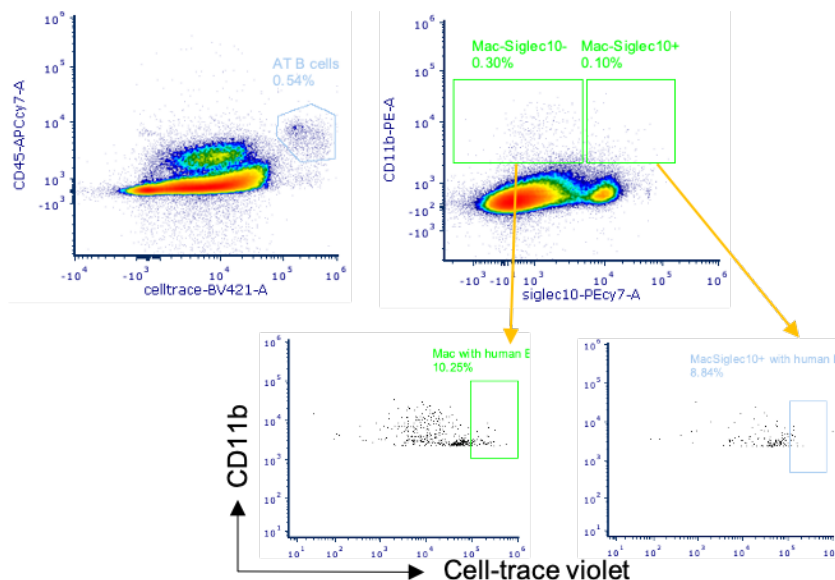


**Figure 31: Humanized mice model for in vivo macrophage engulfment of B cells.**

Furthermore, CD24 has also been known to reduce tissue damage resulting from danger associated molecular-patterns (DAMPs) through inhibition of Siglec-10 and lowering NF $\kappa$ B activation in dendritic cells<sup>58</sup>. Oxidation specific epitopes are DAMPs<sup>148</sup>. This connection allows us to speculate that CD24 might also inhibit Siglec-10 on the macrophags and lowering macrophage activation by oxidation specific epitopes. To investigate this concept, we can utilize hyperlipidemic humanized model introduced in chapter 4 and test whether CD24 blocking mAb treatment reduces the level of NF $\kappa$ B activation in the resident macrophages.

Siglec10 is not only important in dendritic cells and macrophages. Jellusova et al demonstrated that Siglec G, a mouse homolog of human Siglec 10, suppresses BCR signaling in mouse B1 cells<sup>149</sup>. Siglec $g^{-/-}$  B1a were shown to have a lower level of spontaneous apoptosis and a prolonged life span<sup>149</sup>. As CD24 is known to inhibit Siglec10, this allows us to hypothesize that B<sup>27+IgM+CD24<sup>hi</sup></sup> cells might have a longer life span than B<sup>27+IgM+CD24<sup>lo</sup></sup> cells. This prolonged life span and potential higher self-renewal aspect of B<sup>27+IgM+CD24<sup>hi</sup></sup> cells should be evaluated as CD24 mAb is a potential therapy for cancer. If these B<sup>27+IgM+CD24<sup>hi</sup></sup> cells are self-renewed, then the reduction

of  $B^{27+IgM+CD24hi}$  cell number from CD24 mAb treatment leading to higher vascular inflammation can be a short-term effect and CD24 mAb might not have a long-term adverse effect in increasing risk of developing coronary artery disease.

### **CD24, B cell proliferation, and antibody/cytokine production**

CD24 is a well-known immature B cells marker, and plays a major role in B cell differentiation and development. Previous publication also found that CD24 expression on transitional B cells is decreased once B cells reach germinal center in the spleen and become activated B cells. CD24 promotes antigen dependent proliferation of B cells while preventing their terminal differentiation into antibody forming cells (AFCs). Majority of antibody forming cells are plasma cells which mainly produce IgG antibody. Therefore, the facts that CD24 is preventing differentiation into AFCs and  $B^{27+IgM+CD24hi}$  cells are producing IgM imply that CD24 on these  $B^{27+IgM+CD24hi}$  cells might prevent differentiation into IgG producing B cells and increases capacity of self-renewal. However, further investigations are still required to prove this hypothesis.

In addition to the significance of CD24 in IgM production, CD24hi CD27+ cells also have a characteristics of regulatory B cells through production of IL-10<sup>150</sup>. IL-10 has been known as an anti-inflammatory cytokine through downregulating Th1 immune responses and their inflammatory reactions to limit atherosclerosis<sup>151</sup>. Therefore, there is also a possibility that  $B^{27+IgM+CD24hi}$  cells might be atheroprotective through their production of IL-10 in addition to their capability of producing atheroprotective IgM.

## Literature cited

1. Arnett DK, Blumenthal RS, Albert MA, et al. 2019 ACC/AHA Guideline on the Primary Prevention of Cardiovascular Disease: A Report of the American College of Cardiology/American Heart Association Task Force on Clinical Practice Guidelines. *Circulation*. 2019;140(11):e596-e646. doi:10.1161/CIR.0000000000000678
2. Benjamin EJ, Virani SS, Callaway CW, et al. *Heart Disease and Stroke Statistics - 2018 Update: A Report from the American Heart Association*. Vol 137.; 2018. doi:10.1161/CIR.0000000000000558
3. Ross R. The pathogenesis of atherosclerosis--an update. *N Engl J Med*. 1986;314(8):488-500. doi:10.1056/NEJM198602203140806
4. GERLIS LM. The significance of adventitial infiltrations in coronary atherosclerosis. *Br Heart J*. 1956;18(2):166-172. doi:10.1136/hrt.18.2.166
5. SCHWARTZ CJ, MITCHELL JR. Cellular infiltration of the human arterial adventitia associated with atheromatous plaques. *Circulation*. 1962;26:73-78. doi:10.1161/01.cir.26.1.73
6. Ross BM, Mamalias N, Moszczynska A, Rajput AH, Kish SJ. Elevated activity of phospholipid biosynthetic enzymes in substantia nigra of patients with Parkinson's disease. *Neuroscience*. 2001;102(4):899-904. doi:10.1016/S0306-4522(00)00501-7
7. Libby P. Inflammation in atherosclerosis. *Arterioscler Thromb Vasc Biol*. 2012;32(9):2045-2051. doi:10.1161/ATVBAHA.108.179705
8. Libby P, Lichtman AH, Hansson GK. Immune effector mechanisms implicated in atherosclerosis: from mice to humans. *Immunity*. 2013;38(6):1092-1104. doi:10.1016/j.immuni.2013.06.009
9. Libby P, Loscalzo J, Ridker PM, et al. Inflammation, Immunity, and Infection in

- Atherothrombosis: JACC Review Topic of the Week. *J Am Coll Cardiol.* 2018;72(17):2071-2081. doi:10.1016/j.jacc.2018.08.1043
10. Tabas I, Lichtman AH. Monocyte-Macrophages and T Cells in Atherosclerosis. *Immunity.* 2017;47(4):621-634. doi:10.1016/j.immuni.2017.09.008
  11. Saigusa R, Winkels H, Ley K. T cell subsets and functions in atherosclerosis. *Nat Rev Cardiol.* 2020;3050:1-15. doi:10.1038/s41569-020-0352-5
  12. Steinberg D, Witztum JL. Oxidized low-density lipoprotein and atherosclerosis. *Arterioscler Thromb Vasc Biol.* 2010;30(12):2311-2316. doi:10.1161/ATVBAHA.108.179697
  13. Doran AC, Yurdagul A, Tabas I. Efferocytosis in health and disease. *Nat Rev Immunol.* 2020;20(4):254-267. doi:10.1038/s41577-019-0240-6
  14. Winkels H, Ehinger E, Vassallo M, et al. Atlas of the immune cell repertoire in mouse atherosclerosis defined by single-cell RNA-sequencing and mass cytometry. *Circ Res.* 2018;122(12):1675-1688. doi:10.1161/CIRCRESAHA.117.312513
  15. Zernecke A, Winkels H, Cochain C, et al. Meta-Analysis of Leukocyte Diversity in Atherosclerotic Mouse Aortas. *Circ Res.* 2020;127(3):402-426. doi:10.1161/CIRCRESAHA.120.316903
  16. Srikakulapu P, Upadhye A, Rosenfeld SM, et al. Perivascular adipose tissue harbors atheroprotective IgM-producing B cells. *Front Physiol.* 2017;8(SEP):719. doi:10.3389/fphys.2017.00719
  17. Srikakulapu P, Upadhye A, Rosenfeld SM, et al. Perivascular adipose tissue harbors atheroprotective IgM-producing B cells. *Front Physiol.* 2017;8(SEP):719. doi:10.3389/fphys.2017.00719
  18. Cooper MD. The early history of B cells. *Nat Rev Immunol.* 2015;15(3):191-197. doi:10.1038/nri3801

19. Kantor AB, Herzenberg LA. Origin of murine B cell lineages. *Annu Rev Immunol.* 1993;11:501-538. doi:10.1146/annurev.iy.11.040193.002441
20. Alugupalli KR, Gerstein RM. Divide and conquer: Division of labor by B-1 B cells. *Immunity.* 2005;23(1):1-2. doi:10.1016/j.immuni.2005.07.001
21. Baumgarth N. B-1 cell heterogeneity and the regulation of natural and antigen-induced IgM production. *Front Immunol.* 2016;7(SEP):324. doi:10.3389/fimmu.2016.00324
22. Ghosn EEB, Yamamoto R, Hamanaka S, et al. Distinct B-cell lineage commitment distinguishes adult bone marrow hematopoietic stem cells. *Proc Natl Acad Sci U S A.* 2012;109(14):5394-5398. doi:10.1073/pnas.1121632109
23. Tung JW, Mrazek MD, Yang Y, Herzenberg LA, Herzenberg LA. Phenotypically distinct B cell development pathways map to the three B cell lineages in the mouse. *Proc Natl Acad Sci U S A.* 2006;103(16):6293-6298. doi:10.1073/pnas.0511305103
24. Srikakulapu P, McNamara CA. B cells and atherosclerosis. *Am J Physiol - Hear Circ Physiol.* 2017;312(5):H1060-H1067. doi:10.1152/ajpheart.00859.2016
25. Upadhye A, Sturek JM, McNamara CA. 2019 Russell Ross Memorial Lecture in Vascular Biology: B Lymphocyte-Mediated Protective Immunity in Atherosclerosis. *Arterioscler Thromb Vasc Biol.* 2020;40(2):309-322. doi:10.1161/ATVBAHA.119.313064
26. Caligiuri G, Nicoletti A, Poirier B, Hansson GK. Protective immunity against atherosclerosis carried by B cells of hypercholesterolemic mice. *J Clin Invest.* 2002;109(6):745-753. doi:10.1172/JCI7272
27. Major AS, Fazio S, Linton MF. B-lymphocyte deficiency increases atherosclerosis in LDL receptor-null mice. *Arterioscler Thromb Vasc Biol.* 2002;22(11):1892-1898. doi:10.1161/01.atv.0000039169.47943.ee
28. Kyaw T, Tay C, Hosseini H, et al. Depletion of b2 but not b1a b cells in baff receptor-deficient apoe -/- mice attenuates atherosclerosis by potently ameliorating arterial

- inflammation. *PLoS One*. 2012;7(1):1-10. doi:10.1371/journal.pone.0029371
29. Kyaw T, Tay C, Krishnamurthi S, et al. B1a B lymphocytes are atheroprotective by secreting natural IgM that increases IgM deposits and reduces necrotic cores in atherosclerotic lesions. *Circ Res*. 2011;109(8):830-840.  
doi:10.1161/CIRCRESAHA.111.248542
  30. Kyaw T, Tay C, Khan A, et al. Conventional B2 B Cell Depletion Ameliorates whereas Its Adoptive Transfer Aggravates Atherosclerosis. *J Immunol*. 2010;185(7):4410-4419.  
doi:10.4049/jimmunol.1000033
  31. Covens K, Verbinnen B, Geukens N, et al. Characterization of proposed human B-1 cells reveals pre-plasmablast phenotype. *Blood*. 2013;121(6):5176-5183. doi:10.1182/blood-2012-12-471953
  32. Upadhye A, Sriakulapu P, Gonen A, et al. Diversification and CXCR4-Dependent Establishment of the Bone Marrow B-1a Cell Pool Governs Atheroprotective IgM Production Linked to Human Coronary Atherosclerosis. *Circ Res*. 2019;125(10):e55-e70.  
doi:10.1161/CIRCRESAHA.119.315786
  33. Tsimikas S, Willeit P, Willeit J, et al. Oxidation-specific biomarkers, prospective 15-year cardiovascular and stroke outcomes, and net reclassification of cardiovascular events. *J Am Coll Cardiol*. 2012;60(21):2218-2229. doi:10.1016/j.jacc.2012.08.979
  34. Ravandi A, Boekholdt SM, Mallat Z, et al. Relationship of IgG and IgM autoantibodies and immune complexes to oxidized LDL with markers of oxidation and inflammation and cardiovascular events: Results from the EPIC-norfolk study. *J Lipid Res*. 2011;52(10):1829-1836. doi:10.1194/jlr.M015776
  35. Prasad A, Clopton P, Ayers C, et al. Relationship of Autoantibodies to MDA-LDL and ApoB-Immune Complexes to Sex, Ethnicity, Subclinical Atherosclerosis, and Cardiovascular Events. *Arterioscler Thromb Vasc Biol*. 2017;37(6):1213-1221.

- doi:10.1161/ATVBAHA.117.309101
36. van den Berg VJ, Haskard DO, Fedorowski A, et al. TEMPORARY REMOVAL: IgM anti-malondialdehyde low density lipoprotein antibody levels indicate coronary heart disease and necrotic core characteristics in the Nordic Diltiazem (NORDIL) study and the Integrated Imaging and Biomarker Study 3 (IBIS-3). *EBioMedicine*. 2018;36:63-72.  
doi:10.1016/j.ebiom.2018.08.023
  37. Murre C. Helix-loop-helix proteins and lymphocyte development. *Nat Immunol*. 2005;6(11):1079-1086. doi:10.1038/ni1260
  38. Kumar MS, Hendrix J, Johnson AD, Owens GK. The smooth muscle alpha-actin gene requires two Eboxes for proper expression in vivo and is a target of class I basic HLH proteins. *Circ Res*. 2003;92:840-847.
  39. Doran AC, Meller N, Cutchins A, et al. The Helix–Loop–Helix Factors Id3 and E47 Are Novel Regulators of Adiponectin. *Circ Res*. 2008;103(6):624-634.  
doi:10.1161/CIRCRESAHA.108.175893
  40. Doran AC, Lehtinen AB, Meller N, et al. Id3 Is a novel atheroprotective factor containing a functionally significant single-nucleotide polymorphism associated with intima-media thickness in humans. *Circ Res*. 2010;106(7):1303-1311.  
doi:10.1161/CIRCRESAHA.109.210294
  41. Lipinski MJ, Campbell KA, Duong SQ, et al. Loss of Id3 increases VCAM-1 expression, macrophage accumulation, and atherogenesis in Ldlr<sup>-/-</sup> mice. *Arterioscler Thromb Vasc Biol*. 2012;32(12):2855-2861. doi:10.1161/ATVBAHA.112.300352
  42. Doran AC, Lipinski MJ, Oldham SN, Garmey JC, Campbell KA. B cell Aortic Homing and Atheroprotection Depend on Id3. 110(1):e1-e12. doi:10.1371/journal.pone.0178059
  43. Engel I, Murre C. The function of E- and id proteins in lymphocyte development. *Nat Rev Immunol*. 2001;1(3):193-199. doi:10.1038/35105060

44. Pan L, Sato S, Frederick JP, Sun XH, Zhuang Y. Impaired immune responses and B-cell proliferation in mice lacking the Id3 gene. *Mol Cell Biol.* 1999;19(9):5969-5980.  
doi:10.1128/MCB.19.9.5969
45. Kee BL, Rivera RR, Murre C. Id3 inhibits B lymphocyte progenitor growth and survival in response to TGF- $\beta$ . *Nat Immunol.* 2001;2(3):242-247. doi:10.1038/85303
46. Rosenfeld SM, Perry HM, Gonen A, et al. B-1b Cells Secrete Atheroprotective IgM and Attenuate Atherosclerosis. *Circ Res.* 2015;117(3):e28-39.  
doi:10.1161/CIRCRESAHA.117.306044
47. Jiang G, Liang X, Huang Y, et al. P62 promotes proliferation, apoptosis-resistance and invasion of prostate cancer cells through the Keap1/Nrf2/ARE axis. *Oncol Rep.* 2020;43(5):1547-1557. doi:10.3892/or.2020.7527
48. Calvo-Garrido J, Maffezzini C, Schober FA, et al. SQSTM1/p62-Directed Metabolic Reprogramming Is Essential for Normal Neurodifferentiation. *Stem Cell Reports.* 2019;12(4):696-711. doi:10.1016/j.stemcr.2019.01.023
49. Serrano M, Leitges M, Flores JM, et al. The Atypical PKC-Interacting Protein p62 Is an Important Mediator of RANK-Activated Osteoclastogenesis. 2004;6:303-309.
50. Sergin I, Bhattacharya S, Emanuel R, et al. atherosclerosis. 2016;9(409).  
doi:10.1126/scisignal.aad5614.p62-enriched
51. Linares JF, Duran A, Yajima T, Pasparakis M, Moscat J, Diaz-Meco MT. K63 polyubiquitination and activation of mTOR by the p62-TRAF6 complex in nutrient-activated cells. *Mol Cell.* 2013;51(3):283-296. doi:10.1016/j.molcel.2013.06.020
52. Wooten MW, Geetha T, Seibenhener ML, Babu JR, Diaz-Meco MT, Moscat J. The p62 scaffold regulates nerve growth factor-induced NF- $\kappa$ B activation by influencing TRAF6 polyubiquitination. *J Biol Chem.* 2005;280(42):35625-35629.  
doi:10.1074/jbc.C500237200

53. Moscat J, Karin M, Diaz-Meco MT. p62 in Cancer: Signaling Adaptor Beyond Autophagy. *Cell*. 2016;167(3):606-609. doi:10.1016/j.cell.2016.09.030
54. Ning H, Liu D, Yu X, Guan X. Oxidized low-density lipoprotein-induced p62/SQSTM1 accumulation in THP-1-derived macrophages promotes IL-18 secretion and cell death. *Exp Ther Med*. 2017;14(6):5417-5423. doi:10.3892/etm.2017.5221
55. Sergin I, Evans TD, Zhang X, et al. Exploiting macrophage autophagy-lysosomal biogenesis as a therapy for atherosclerosis. *Nat Commun*. 2017;8. doi:10.1038/ncomms15750
56. Altevogt P, Sammar M, Hüser L, Kristiansen G. Novel insights into the function of CD24: A driving force in cancer. *Int J Cancer*. 2021;148(3):546-559. doi:https://doi.org/10.1002/ijc.33249
57. Valente M, Resende TP, Nascimento DS, et al. Mouse HSA+ immature cardiomyocytes persist in the adult heart and expand after ischemic injury. *PLoS Biol*. 2019;17(6):e3000335. doi:10.1371/journal.pbio.3000335
58. Chen GY, Tang J, Zheng P, Liu Y. CD24 and siglec-10 selectively repress tissue damage - Induced immune responses. *Science (80- )*. 2009;323(5922):1722-1725. doi:10.1126/science.1168988
59. Howell KW, Meng X, Fullerton DA, Jin C, Reece TB, Cleveland JCJ. Toll-like receptor 4 mediates oxidized LDL-induced macrophage differentiation to foam cells. *J Surg Res*. 2011;171(1):e27-31. doi:10.1016/j.jss.2011.06.033
60. Jiao J, Lu Y-Z, Xia N, et al. Defective Circulating Regulatory B Cells in Patients with Dilated Cardiomyopathy. *Cell Physiol Biochem*. 2018;46(1):23-35. doi:10.1159/000488405
61. Van Gassen S, Callebaut B, Van Helden MJ, et al. FlowSOM: Using self-organizing maps for visualization and interpretation of cytometry data. *Cytometry A*. 2015;87(7):636-645.

- doi:10.1002/cyto.a.22625
62. Wilkerson MD, Hayes DN. ConsensusClusterPlus: a class discovery tool with confidence assessments and item tracking. *Bioinformatics*. 2010;26(12):1572-1573.  
doi:10.1093/bioinformatics/btq170
  63. Shultz LD, Lyons BL, Burzenski LM, et al. Human Lymphoid and Myeloid Cell Development in NOD/LtSz- scid IL2R  $\gamma$  null Mice Engrafted with Mobilized Human Hemopoietic Stem Cells . *J Immunol*. 2005;174(10):6477-6489.  
doi:10.4049/jimmunol.174.10.6477
  64. Vallejo J, Saigusa R, Gulati R, et al. Combined protein and transcript single cell RNA sequencing reveals cardiovascular disease and HIV signatures. *bioRxiv*. January 2020:2020.09.10.292086. doi:10.1101/2020.09.10.292086
  65. Pattarabanjird T, Li C, McNamara C. B Cells in Atherosclerosis: Mechanisms and Potential Clinical Applications. *JACC Basic to Transl Sci*. 2021;6(6):546-563.  
doi:10.1016/J.JACBTS.2021.01.006
  66. Berland R, Wortis HH. Origins and functions of B-1 cells with notes on the role of CD5. *Annu Rev Immunol*. 2002;20:253-300. doi:10.1146/annurev.immunol.20.100301.064833
  67. Roschger C, Cabrele C. The Id-protein family in developmental and cancer-associated pathways. *Cell Commun Signal*. 2017;15(1):7. doi:10.1186/s12964-016-0161-y
  68. Schneider P, MacKay F, Steiner V, et al. BAFF, a novel ligand of the tumor necrosis factor family, stimulates B cell growth. *J Exp Med*. 1999;189(11):1747-1756.  
doi:10.1084/jem.189.11.1747
  69. Seijkens TTP, van Tiel CM, Kusters PJH, et al. Targeting CD40-Induced TRAF6 Signaling in Macrophages Reduces Atherosclerosis. *J Am Coll Cardiol*. 2018;71(5):527-542. doi:10.1016/j.jacc.2017.11.055
  70. Vozenilek AE, Blackburn CMR, Schilke RM, et al. AAV8-mediated overexpression of

- mPCSK9 in liver differs between male and female mice. *Atherosclerosis*. 2018;278:66-72.  
doi:10.1016/j.atherosclerosis.2018.09.005
71. Haas KM, Poe JC, Steeber DA, Tedder TF. B-1a and B-1b Cells Exhibit Distinct Developmental Requirements and Have Unique Functional Roles in Innate and Adaptive Immunity to *S. pneumoniae*. *Immunity*. 2005;23(1):7-18.  
doi:10.1016/J.IMMUNI.2005.04.011
72. Shaw PX, Goodyear CS, Chang M-K, Witztum JL, Silverman GJ. The autoreactivity of anti-phosphorylcholine antibodies for atherosclerosis-associated neo-antigens and apoptotic cells. *J Immunol*. 2003;170(12):6151-6157. doi:10.4049/jimmunol.170.12.6151
73. Choi SH, Sviridov D, Miller YI. Oxidized cholesteryl esters and inflammation. *Biochim Biophys Acta - Mol Cell Biol Lipids*. 2017;1862(4):393-397.  
doi:10.1016/j.bbalip.2016.06.020
74. Gonen A, Hansen LF, Turner WW, et al. Atheroprotective immunization with malondialdehyde-modified LDL is hapten specific and dependent on advanced MDA adducts: Implications for development of an atheroprotective vaccine. *J Lipid Res*. 2014;55(10):2137-2155. doi:10.1194/jlr.M053256
75. Sriakulapu P, McNamara CA. B cells and atherosclerosis. *Am J Physiol - Hear Circ Physiol*. 2017;312(5):H1060-H1067. doi:10.1152/ajpheart.00859.2016
76. Yoshimura LC, Tamayo AT, Lin-Lee Y-C, Pham L V., Fu L, Ford RJ. BAFF-R promotes cell proliferation and survival through interaction with IKK $\beta$  and NF- $\kappa$ B/c-Rel in the nucleus of normal and neoplastic B-lymphoid cells. *Blood*. 2009;113(19):4627-4636.  
doi:10.1182/blood-2008-10-183467
77. Smulski CR, Eibel H. BAFF and BAFF-Receptor in B Cell Selection and Survival. *Front Immunol*. 2018;9(OCT):2285. doi:10.3389/FIMMU.2018.02285
78. Schiemann B, Gommerman JL, Vora K, et al. An Essential Role for BAFF in the Normal

- Development of B Cells Through a BCMA-Independent Pathway. *Science* (80- ). 2001;293(5537):2111-2114. doi:10.1126/SCIENCE.1061964
79. Ng LG, Ng C-H, Woehl B, et al. BAFF costimulation of Toll-like receptor-activated B-1 cells. *Eur J Immunol*. 2006;36(7):1837-1846. doi:10.1002/eji.200635956
80. Amezcua Vesely MC, Schwartz M, Bermejo DA, et al. FcγRIIb and BAFF Differentially Regulate Peritoneal B1 Cell Survival. *J Immunol*. 2012;188(10):4792 LP - 4800. doi:10.4049/jimmunol.1102070
81. Sage AP, Tsiantoulas D, Baker L, et al. BAFF receptor deficiency reduces the development of atherosclerosis in mice--brief report. *Arterioscler Thromb Vasc Biol*. 2012;32(7):1573-1576. doi:10.1161/ATVBAHA.111.244731
82. Umemura A, He F, Taniguchi K, et al. p62, Upregulated during Preneoplasia, Induces Hepatocellular Carcinogenesis by Maintaining Survival of Stressed HCC-Initiating Cells. *Cancer Cell*. 2016;29(6):935-948. doi:10.1016/j.ccell.2016.04.006
83. Valencia T, Kim JY, Abu-Baker S, et al. Metabolic Reprogramming of Stromal Fibroblasts through p62-mTORC1 Signaling Promotes Inflammation and Tumorigenesis. *Cancer Cell*. 2014;26(1):121-135. doi:https://doi.org/10.1016/j.ccr.2014.05.004
84. Sanz L, Diaz-Meco MT, Nakano H, Moscat J. The atypical PKC-interacting protein p62 channels NF-kappaB activation by the IL-1-TRAF6 pathway. *EMBO J*. 2000;19(7):1576-1586. doi:10.1093/emboj/19.7.1576
85. Duyao MP, Buckler AJ, Sonenshein GE. Interaction of an NF-kappa B-like factor with a site upstream of the c-myc promoter. *Proc Natl Acad Sci U S A*. 1990;87(12):4727-4731. doi:10.1073/pnas.87.12.4727
86. Pan B, Li J, Parajuli N, et al. The Calcineurin-TFEB-p62 Pathway Mediates the Activation of Cardiac Macroautophagy by Proteasomal Malfunction. *Circ Res*. 2020;127(4):502-518. doi:10.1161/CIRCRESAHA.119.316007

87. Griffin DO, Rothstein TL. Human B1 Cell Frequency: Isolation and Analysis of Human B1 Cells. *Front Immunol.* 2012;3(MAY):122. doi:10.3389/fimmu.2012.00122
88. Ikura Y, Ohsawa M, Suekane T, et al. Localization of oxidized phosphatidylcholine in nonalcoholic fatty liver disease: Impact on disease progression. *Hepatology.* 2006;43(3):506-514. doi:10.1002/hep.21070
89. Bossola M, Tazza L, Merki E, et al. Oxidized low-density lipoprotein biomarkers in patients with end-stage renal failure: Acute effects of hemodialysis. *Blood Purif.* 2008;25(5-6):457-465. doi:10.1159/000112465
90. Birukova AA, Fu P, Chatchavalvanich S, et al. Polar head groups are important for barrier-protective effects of oxidized phospholipids on pulmonary endothelium. *Am J Physiol - Lung Cell Mol Physiol.* 2007;292(4). doi:10.1152/ajplung.00395.2006
91. Tsimikas S, Witztum JL. The role of oxidized phospholipids in mediating lipoprotein(a) atherogenicity. *Curr Opin Lipidol.* 2008;19(4):369-377. doi:10.1097/MOL.0b013e328308b622
92. Sottero B, Rossin D, Poli G, Biasi F. Lipid Oxidation Products in the Pathogenesis of Inflammation-related Gut Diseases. *Curr Med Chem.* 2017;25(11):1311-1326. doi:10.2174/0929867324666170619104105
93. Fraley AE, Schwartz GG, Olsson AG, et al. Relationship of Oxidized Phospholipids and Biomarkers of Oxidized Low-Density Lipoprotein With Cardiovascular Risk Factors, Inflammatory Biomarkers, and Effect of Statin Therapy in Patients With Acute Coronary Syndromes. Results From the MIRACL (Myocardial Ischemia Reduction With Aggressive Cholesterol Lowering) Trial. *J Am Coll Cardiol.* 2009;53(23):2186-2196. doi:10.1016/j.jacc.2009.02.041
94. Feng X, Li H, Rumbin AA, et al. ApoE<sup>-/-</sup>Fas<sup>-/-</sup> C57BL/6 mice: A novel murine model simultaneously exhibits lupus nephritis, atherosclerosis, and osteopenia. *J Lipid Res.*

- 2007;48(4):794-805. doi:10.1194/jlr.M600512-JLR200
95. Qin J, Goswami R, Balabanov R, Dawson G. Oxidized phosphatidylcholine is a marker for neuroinflammation in multiple sclerosis brain. *J Neurosci Res.* 2007;85(5):977-984. doi:10.1002/jnr.21206
  96. Que X, Hung MY, Yeang C, et al. Oxidized phospholipids are proinflammatory and proatherogenic in hypercholesterolaemic mice. *Nature.* 2018;558(7709):301-306. doi:10.1038/s41586-018-0198-8
  97. Tsimikas S, Brilakis ES, Lennon RJ, et al. Relationship of IgG and IgM autoantibodies to oxidized low density lipoprotein with coronary artery disease and cardiovascular events. *J Lipid Res.* 2007;48(2):425-433. doi:10.1194/jlr.M600361-JLR200
  98. Rosenfeld ME, Palinski W, Ylä-Herttuaia S, Butler S, Witztum JL. Distribution of oxidation specific lipid-protein adducts and apolipoprotein B in atherosclerotic lesions of varying severity from WHHL rabbits. *Arterioscler Thromb Vasc Biol.* 1990;10(3):336-349. doi:10.1161/01.ATV.10.3.336
  99. Senders ML, Que X, Cho YS, et al. PET/MR Imaging of Malondialdehyde-Acetaldehyde Epitopes With a Human Antibody Detects Clinically Relevant Atherothrombosis. *J Am Coll Cardiol.* 2018;71(3):321-335. doi:10.1016/j.jacc.2017.11.036
  100. Upadhye A, Srikakulapu P, Gonen A, et al. Diversification and CXCR4-Dependent Establishment of the Bone Marrow B-1a Cell Pool Governs Atheroprotective IgM Production Linked to Human Coronary Atherosclerosis. *Circ Res.* 2019;125(10):e55-e70. doi:10.1161/CIRCRESAHA.119.315786
  101. Döring Y, Jansen Y, Cimen I, et al. B-cell-specific CXCR4 protects against atherosclerosis development and increases plasma IgM levels. *Circ Res.* 2020;126(6):787-788. doi:10.1161/CIRCRESAHA.119.316142
  102. Doran AC, Lipinski MJ, Oldham SN, et al. B-cell aortic homing and atheroprotection

- depend on Id3. *Circ Res.* 2012;110(1):e1. doi:10.1161/CIRCRESAHA.111.256438
103. Barkal AA, Brewer RE, Markovic M, et al. CD24 signalling through macrophage Siglec-10 is a target for cancer immunotherapy. *Nature.* 2019;572(7769):392-396.  
doi:10.1038/s41586-019-1456-0
104. Amu S, Tarkowski A, Dörner T, Bokarewa M, Brisslert M. The Human Immunomodulatory CD25 + B Cell Population belongs to the Memory B Cell Pool. *Scand J Immunol.* 2007;66(1):77-86. doi:10.1111/j.1365-3083.2007.01946.x
105. Brisslert M, Bokarewa M, Larsson P, Wing K, Collins LV, Tarkowski A. Phenotypic and functional characterization of human CD25+ B cells. *Immunology.* 2006;117(4):548-557.  
doi:10.1111/j.1365-2567.2006.02331.x
106. Kaminski DA, Wei C, Qian Y, Rosenberg AF, Sanz I. Advances in human B cell phenotypic profiling. *Front Immunol.* 2012;3(OCT). doi:10.3389/fimmu.2012.00302
107. Griffin DO, Holodick NE, Rothstein TL. Human B1 cells in umbilical cord and adult peripheral blood express the novel phenotype CD20+CD27+CD43+CD70-. *J Exp Med.* 2011;208(1):67-80. doi:10.1084/jem.20101499
108. Weller S, Braun MC, Tan BK, et al. Human blood IgM “memory” B cells are circulating splenic marginal zone B cells harboring a prediversified immunoglobulin repertoire. *Blood.* 2004;104(12):3647-3654. doi:10.1182/blood-2004-01-0346
109. Schabath H, Runz S, Joumaa S, Altevogt P. CD24 affects CXCR4 function in pre-B lymphocytes and breast carcinoma cells. *J Cell Sci.* 2006;119(2):314-325.  
doi:10.1242/jcs.02741
110. Lu MY, Lu SS, Chang SL, Liao F. The phosphorylation of CCR6 on distinct Ser/Thr residues in the carboxyl terminus differentially regulates biological function. *Front Immunol.* 2018;9(MAR):415. doi:10.3389/fimmu.2018.00415
111. Proto JD, Doran AC, Subramanian M, et al. Hypercholesterolemia induces T cell

- expansion in humanized immune mice. *J Clin Invest*. 2018;128(6):2370-2375.  
doi:10.1172/JCI97785
112. Rampidis GP, Benetos G, Benz DC, Giannopoulos AA, Buechel RR. A guide for Gensini Score calculation. *Atherosclerosis*. 2019;287:181-183.  
doi:10.1016/j.atherosclerosis.2019.05.012
113. Binder CJ, Hökkö S, Dewan A, et al. Pneumococcal vaccination decreases atherosclerotic lesion formation: molecular mimicry between *Streptococcus pneumoniae* and oxidized LDL. *Nat Med*. 2003;9(6):736-743. doi:10.1038/nm876
114. Shaw PX, Hökkö S, Chang MK, et al. Natural antibodies with the T15 idiotype may act in atherosclerosis, apoptotic clearance, and protective immunity. *J Clin Invest*. 2000;105(12):1731-1740. doi:10.1172/JCI8472
115. Palinski W, Miller E, Witztum JL. Immunization of low density lipoprotein (LDL) receptor-deficient rabbits with homologous malondialdehyde-modified LDL reduces atherogenesis. *Proc Natl Acad Sci U S A*. 1995;92(3):821-825.  
doi:10.1073/pnas.92.3.821
116. Faria-Neto JR, Chyu K-Y, Li X, et al. Passive immunization with monoclonal IgM antibodies against phosphorylcholine reduces accelerated vein graft atherosclerosis in apolipoprotein E-null mice. *Atherosclerosis*. 2006;189(1):83-90.  
doi:10.1016/j.atherosclerosis.2005.11.033
117. Chou M-Y, Fogelstrand L, Hartvigsen K, et al. Oxidation-specific epitopes are dominant targets of innate natural antibodies in mice and humans. *J Clin Invest*. 2009;119(5):1335-1349. doi:10.1172/JCI36800
118. Harmon DB, Srikakulapu P, Kaplan JL, et al. Protective Role for B-1b B Cells and IgM in Obesity-Associated Inflammation, Glucose Intolerance, and Insulin Resistance. *Arterioscler Thromb Vasc Biol*. 2016;36(4):682-691. doi:10.1161/ATVBAHA.116.307166

119. Masmoudi H, Mota-Santos T, Huetz F, Coutinho A, Cazenave PA. All T15 Id-positive antibodies (but not the majority of VHT15+ antibodies) are produced by peritoneal CD5+ B lymphocytes. *Int Immunol*. 1990;2(6):515-520. doi:10.1093/intimm/2.6.515
120. Tsiantoulas D, Gruber S, Binder CJ. B-1 cell immunoglobulin directed against oxidation-specific epitopes. *Front Immunol*. 2012;3:415. doi:10.3389/fimmu.2012.00415
121. Shen L, Chng MHY, Alonso MN, Yuan R, Winer DA, Engleman EG. B-1a Lymphocytes Attenuate Insulin Resistance. *Diabetes*. 2015;64(2):593 LP - 603. doi:10.2337/db14-0554
122. Björkbacka H, Alm R, Persson M, Hedblad B, Nilsson J, Fredrikson GN. Low Levels of Apolipoprotein B-100 Autoantibodies Are Associated with Increased Risk of Coronary Events. *Arterioscler Thromb Vasc Biol*. 2016;36(4):765-771. doi:10.1161/ATVBAHA.115.306938
123. Cerutti A, Cols M, Puga I. Marginal zone B cells: virtues of innate-like antibody-producing lymphocytes. *Nat Rev Immunol*. 2013;13(2):118-132. doi:10.1038/nri3383
124. Palm A-KE, Kleinau S. Marginal zone B cells: From housekeeping function to autoimmunity? *J Autoimmun*. 2021;119:102627. doi:https://doi.org/10.1016/j.jaut.2021.102627
125. Martin F, Oliver AM, Kearney JF. Marginal zone and B1 B cells unite in the early response against T-independent blood-borne particulate antigens. *Immunity*. 2001;14(5):617-629. doi:10.1016/S1074-7613(01)00129-7
126. Grasset EK, Duhlin A, Agardh HE, et al. Sterile inflammation in the spleen during atherosclerosis provides oxidation-specific epitopes that induce a protective B-cell response. *Proc Natl Acad Sci*. 2015;112(16):E2030-E2038. doi:10.1073/PNAS.1421227112
127. Appelgren D, Eriksson P, Ernerudh J, Segelmark M. Marginal-Zone B-Cells Are Main Producers of IgM in Humans, and Are Reduced in Patients With Autoimmune Vasculitis

- . *Front Immunol* . 2018;9:2242.  
<https://www.frontiersin.org/article/10.3389/fimmu.2018.02242>.
128. Steiniger B, Timphus EM, Barth PJ. The splenic marginal zone in humans and rodents: an enigmatic compartment and its inhabitants. *Histochem Cell Biol*. 2006;126(6):641-648. doi:10.1007/s00418-006-0210-5
  129. Balázs M, Martin F, Zhou T, Kearney J. Blood dendritic cells interact with splenic marginal zone B cells to initiate T-independent immune responses. *Immunity*. 2002;17(3):341-352. doi:10.1016/s1074-7613(02)00389-8
  130. Chen GY, Tang J, Zheng P, Liu Y. CD24 and siglec-10 selectively repress tissue damage - Induced immune responses. *Science (80- )*. 2009;323(5922):1722-1725.  
doi:10.1126/science.1168988
  131. Calabretta R, Hoeller C, Pichler V, et al. Immune Checkpoint Inhibitor Therapy Induces Inflammatory Activity in Large Arteries. *Circulation*. 2020;142(24):2396-2398.  
doi:10.1161/CIRCULATIONAHA.120.048708
  132. Jarr K-U, Ye J, Kojima Y, et al. 18F-Fluorodeoxyglucose-Positron Emission Tomography Imaging Detects Response to Therapeutic Intervention and Plaque Vulnerability in a Murine Model of Advanced Atherosclerotic Disease—Brief Report. *Arterioscler Thromb Vasc Biol*. 2020;40:2821-2828. doi:10.1161/ATVBAHA.120.315239
  133. Ayre DC, Christian SL. CD24: A Rheostat That Modulates Cell Surface Receptor Signaling of Diverse Receptors. *Front Cell Dev Biol*. 2016;4(DEC):146.  
doi:10.3389/fcell.2016.00146
  134. Manichaikul A, Rich SS, Perry H, et al. A functionally significant polymorphism in ID3 is associated with human coronary pathology. *PLoS One*. 2014;9(3):1-7.  
doi:10.1371/journal.pone.0090222
  135. Pattarabanjird T, Cress C, Nguyen A, Taylor A, Bekiranov S, McNamara C. A Machine

- Learning Model Utilizing a Novel SNP Shows Enhanced Prediction of Coronary Artery Disease Severity. *Genes*. 2020;11(12). doi:10.3390/genes11121446
136. Bain G, Maandag EC, Izon DJ, et al. E2A proteins are required for proper B cell development and initiation of immunoglobulin gene rearrangements. *Cell*. 1994;79(5):885-892. doi:10.1016/0092-8674(94)90077-9
137. Quong MW, Harris DP, Swain SL, Murre C. E2A activity is induced during B-cell activation to promote immunoglobulin class switch recombination. *EMBO J*. 1999;18(22):6307-6318. doi:10.1093/emboj/18.22.6307
138. Kwon K, Hutter C, Sun Q, et al. Instructive Role of the Transcription Factor E2A in Early B Lymphopoiesis and Germinal Center B Cell Development. *Immunity*. 2008;28(6):751-762. doi:https://doi.org/10.1016/j.immuni.2008.04.014
139. Libby P, Sidlow R, Lin AE, et al. Clonal Hematopoiesis: Crossroads of Aging, Cardiovascular Disease, and Cancer: JACC Review Topic of the Week. *J Am Coll Cardiol*. 2019;74(4):567-577. doi:10.1016/j.jacc.2019.06.007
140. Jaiswal S, Natarajan P, Silver AJ, et al. Clonal Hematopoiesis and Risk of Atherosclerotic Cardiovascular Disease. *N Engl J Med*. 2017;377(2):111-121. doi:10.1056/NEJMoa1701719
141. Liu WJ, Ye L, Huang WF, et al. p62 links the autophagy pathway and the ubiquitin–proteasome system upon ubiquitinated protein degradation. *Cell Mol Biol Lett*. 2016;21(1):29. doi:10.1186/s11658-016-0031-z
142. Pankiv S, Clausen TH, Lamark T, et al. p62/SQSTM1 binds directly to Atg8/LC3 to facilitate degradation of ubiquitinated protein aggregates by autophagy. *J Biol Chem*. 2007;282(33):24131-24145. doi:10.1074/jbc.M702824200
143. Katsuragi Y, Ichimura Y, Komatsu M. Regulation of the Keap1–Nrf2 pathway by p62/SQSTM1. *Curr Opin Toxicol*. 2016;1:54-61.

- doi:<https://doi.org/10.1016/j.cotox.2016.09.005>
144. Clarke AJ, Riffelmacher T, Braas D, Cornall RJ, Simon AK. B1a B cells require autophagy for metabolic homeostasis and self-renewal. *J Exp Med*. 2018;215(2):399-413. doi:10.1084/jem.20170771
  145. Novikova DS, Popkova T V, Lukina G V, et al. The Effects of Rituximab on Lipids, Arterial Stiffness and Carotid Intima-Media Thickness in Rheumatoid Arthritis. *J Korean Med Sci*. 2016;31(2):202-207. doi:10.3346/jkms.2016.31.2.202
  146. Kobayashi T, Kim TS, Jacob A, et al. TRAF6 is required for generation of the B-1a B cell compartment as well as T cell-dependent and -independent humoral immune responses. *PLoS One*. 2009;4(3):e4736. doi:10.1371/journal.pone.0004736
  147. Barkal AA, Brewer RE, Markovic M, et al. CD24 signalling through macrophage Siglec-10 is a target for cancer immunotherapy. *Nature*. doi:10.1038/s41586-019-1456-0
  148. Tsimikas S, I. Miller Y. Oxidative Modification of Lipoproteins: Mechanisms, Role in Inflammation and Potential Clinical Applications in Cardiovascular Disease. *Curr Pharm Des*. 2011;17(1):27-37. doi:10.2174/138161211795049831
  149. Jellusova J, Düber S, Gückel E, et al. Siglec-G regulates B1 cell survival and selection. *J Immunol*. 2010;185(6):3277-3284. doi:10.4049/jimmunol.1001792
  150. de Masson A, Bouaziz J-D, Le Buanec H, et al. CD24<sup>hi</sup>CD27<sup>+</sup> and plasmablast-like regulatory B cells in human chronic graft-versus-host disease. *Blood*. 2015;125(11):1830-1839. doi:10.1182/blood-2014-09-599159
  151. Terkeltaub RA. IL-10: An “Immunologic Scalpel” for Atherosclerosis? *Arterioscler Thromb Vasc Biol*. 1999;19(12):2823-2825. doi:10.1161/01.ATV.19.12.2823